8-2019

A Cumulative Summation Nonparametric Multiple Stream Process Control Chart Based on the Extended Median Test

Austin R. Brown

UNIVERSITY OF NORTHERN COLORADO

Greeley, Colorado

The Graduate School

A CUMULATIVE SUMMATION NONPARAMETRIC MULTIPLE STREAM PROCESS CONTROL CHART BASED ON THE EXTENDED MEDIAN TEST

A Dissertation Submitted in Partial Fulfillment
of the Requirements for the Degree of
Doctor of Philosophy

Austin R. Brown

College of Education and Behavioral Sciences
Department of Applied Statistics and Research Methods

August 2019

This Dissertation by: Austin R. Brown

Entitled: *A Cumulative Summation Nonparametric Multiple Stream Process Control Chart Based on the Extended Median Test*

has been approved as meeting the requirement for the Degree of Doctor of Philosophy in College of Education and Behavioral Sciences in Department of Applied Statistics and Research Methods.

Accepted by the Doctoral Committee

Trent Lalonde, Ph.D., Research Advisor

Khalil Shafie, Ph.D., Committee Member

Han Yu, Ph.D., Committee Member

Rutilio Martinez, Ph.D., Faculty Representative

Date of Dissertation Defense

Accepted by the Graduate School

Linda L. Black, Ed.D.
Associate Provost and Dean
Graduate School and International Admissions
Research and Sponsored Projects

ABSTRACT

Brown, Austin R. *A Cumulative Summation Nonparametric Multiple Stream Process Control Chart Based on the Extended Median Test.* Published Doctor of Philosophy dissertation, University of Northern Colorado, 2019.

In statistical process control applications, situations may arise in which several presumably identical processes or "streams" are desired to be simultaneously monitored. Such a monitoring scenario is commonly referred to as a "Multiple Stream Process (MSP)." Charts which have been designed to monitor an MSP typically monitor the means of the streams through collecting samples from each stream and calculating some function of the sample means. The resulting statistic is then iteratively compared to control limits to determine if a single stream or subset of streams may have shifted away from a specified target value. Traditional MSP charting techniques rely on the assumption of normality, which may or may not be met in practice. Thus, a cumulative summation nonparametric MSP control charting technique, based on a modification of the classical extended median test was developed and is referred to as the "Nonparametric Extended Median Test – Cumulative Summation (NEMT-CUSUM) chart." The development of control limits and estimation of statistical power are given. Through simulation, the NEMT-CUSUM is shown to perform consistently in the presence of normal and non-normal data. Moreover, it is shown to perform more optimally than parametric alternatives in certain circumstances. Results suggest the NEMT-CUSUM may be an attractive alternative to existing parametric MSP monitoring

techniques in the case when distributional assumptions about the underlying monitored process cannot reasonably be made.

ACKNOWLEDGEMENTS

First and foremost, I would like to thank my Mom and Dad, Carlene and Jeff Brown, for their endless love, encouragement, support (and mangos) not just during my graduate school journey, but throughout my life. I consider them living saints, and am humbled that such genuine, kind, and selfless people would choose to walk this beautiful journey with me. Truth be told, I would be in a very different situation in life if it were not for a conversation with my Dad one October day in 2014 over lunch at Dairy Queen in Fort Morgan. I was working at a local bank, which was a great job, but I had always had aspirations of pursuing a Ph.D. He told me that if I even had the tiniest inclination to pursue a Ph.D., that I needed to do it as soon as I could, before life might prevent me from doing so. If he had not said anything that day, I absolutely would not have done this. It's very beautiful to look back and see all the dominos falling to lead me to now. I could write pages about how much my parents mean to me and how much they have helped me. I love you both very much and am so grateful for you.

In a very close second, I would like to thank my sisters, Keeley, Whitney and Lainey, and my brothers, Dallas and Tad. There is no group of people more loving, more loyal, or more hilarious than these goons. Each of them is such a sincerely great person and I couldn't be more proud of their incredible accomplishments, and more importantly, the quality of their character. I know not everyone is not so fortunate to have super close relationships with their siblings, so I certainly do not take the wonderful relationships we have for granted. And you guys know what's funnier than 24? 25.

Another incredibly important person to whom I am greatly indebted to who has been instrumental not only in the creation of this manuscript, but also in my development as an academic, an educator, a cautiously optimistic Rockies fan, and a person is my mentor and first advisor, Dr. Jay Schaffer, or as he is commonly referred to, Dr. J. During the Fall 2016 semester, I was enrolled in the process control class which Dr. J taught and really fell in love with the subject. I knew at that point that process control was going to be the subject of my dissertation and be one of my main research areas. In the Spring 2017 semester, when Dr. J was on sabbatical, I reached out to him to see if we could kick the tires on a few ideas, and he enthusiastically agreed. However, despite being my first semester technically enrolled in the Ph.D. program, it was without a doubt my most academically rigorous. My stress and anxiety levels were so high at the end of that semester that I was seriously considering leaving the program (my parents and close friends can attest). Over the course of that summer, I reached out to Dr. J and apologized for not being more engaged with him over the summer, and just hinted that I was trying to find ways to remove stress from my life after coming off of such a difficult semester. He responded with one of the kindest messages I have ever received. He encouraged me to persist because of the potential he saw in me. If I had not received such a response, I would not be at the point I am today. And that's when I truly learned why so many people respect Dr. J: he doesn't just care about students getting through coursework, his priority is care for students as people. I can't thank him enough for doing that for me.

After having taken linear models with Dr. Shafie, nonparametric statistics with Dr. J, and then taking my written comps, I realized how fragile the assumptions of traditional testing procedures and traditional control charting techniques really are. I

brought this up with Dr. J and that I wanted to work on this for my dissertation, and he said something to the effect of "start reading." I initially came up with an idea to use Friedman's test in a Shewhart-style framework for the case where several subject is monitored at several time points, like a repeated measures ANOVA with the time points being the within subject effect and the subjects serving as their own blocking effect. I brought this to him, and he asked if anyone had developed a nonparametric chart which first examined a multiple stream process. From what I found, there hadn't been. He said to tuck the Friedman's test idea in my back pocket and "build a bridge" of publications out to it. He told me first, scrap the Shewhart chart and go with CUSUM, and start with the least complex nonparametric test for comparing multiple groups, the Extended Median Test, and work your way up to Kruskal-Wallis. At first, I was a little disappointed because I really liked the Friedman's test idea. But then he told me that a dissertation isn't a final destination, it's a launching pad. Start here and you'll get to where you want to be. I am very grateful for his advice and helping me put things in perspective. He helped me refine my academic writing from something that read like a sports column to something more scientific. He helped me go through proofs and papers to ensure that what I was proposing was sound. He also, in an Ernest Hemmingway-esque way, told me that a sentence should be simple and convey one point instead of 50 points. "I don't want to read War and Peace," as he would sometimes jokingly say. Suffice it to say, I owe a lot to Dr. J. He has been a profoundly important part of my journey here at UNC and will continue to be as I go out into the academy. Thank you Dr. J. I am very grateful for your presence in my life.

I would also like to sincerely thank my second dissertation chair, Dr. Trent Lalonde, for all of his help and advice throughout my academic career, and especially as I have been in the final stages of my doctoral journey. During the summer of 2017 when I was considering leaving, I also reached out to Dr. Lalonde to ask if he had any advice on remaining balanced and persisting as I couldn't mentally or physically handle a semester like I had just endured. He also gave me a lot of encouragement and told me to persist because of the potential he also saw in me. He asked me to come by his office and chat, so I did. I thought I needed to be doing a lot more outside research and things of that nature if I wanted a chance at a tenure-track job, as I observed one particular (who will know who they are if they read this) more senior student doing. He told me that learning to say no, especially in our discipline, is an important skill to develop. I had never realized saying no was even an option, but it changed the trajectory of my academic career and gave me a lot more confidence in the path I was on. I am very grateful for that.

Because of the way things worked out with various faculty taking sabbatical, the person I was instructed most by, besides Dr. J, has been Dr. Khalil Shafie. Dr. Shafie has been profoundly kind and encouraging to me during my journey through coursework, the master's comps, more coursework, the written comps, and especially as my dissertation has been wrapping up. He has always been more than happy to help me and has been so accommodating to me. Between him, Dr. J, and Dr. Lalonde, they have created a departmental culture that is supportive, collaborative, and compassionate. I couldn't have succeeded if it were not for them.

I am also very grateful for the guidance of Dr. Han Yu, who has been incredibly gracious and accommodating to me throughout this somewhat unique dissertation

journey. And lastly, to my first statistics professor at UNC, Dr. Rutilio Martinez, I am so very thankful for your advice, insight, and willingness to see me through to the finish. I can't thank you enough for that.

I would also like to thank my friend and mentor Dr. David Thomas. Dr. Thomas has been guiding me throughout my post-undergraduate career. He helped me decide to go to CSU. He helped me choose between statistics and business for a Ph.D. He has written me numerous letters of recommendation. He edited my cover letter, teaching statement, and research statement as I was applying for academic jobs. And he has been nothing short of an encouraging, empowering force in my life. Thanks for helping the quiet kid in your entrepreneurship class find a path in this world.

There are many, many others who have also been part of this journey. My partner in crime, who has eaten so many subs with me from the UC, Bryce, has become one of my very closest friends during my time here. We have worked together through a lot of tough classes, tough situations, and presentations (hopefully a publication here soon). He's always been willing to grab a beer and just talk though the ups and downs of the graduate journey. I'm thankful for you man. I am also very thankful for my other two very close friends I have made at UNC, Kofi Wagya and Hend Aljobaily, who have listened to me talk in thousands of circles about process control, programming, and life in general. I really appreciate you both. And to all of my friends and colleagues at UNC, thank you. You've given me a lot of joy. Like I always say, once a Bear, always a Bear.

Finally, I am thankful to the Universe for the perfect way in which all effortlessly occurs and for teaching me to never hurry, but always be present. That is, to Be Here Now.

TABLE OF CONTENTS

LIST OF TABLES

LIST OF FIGURES

CHAPTER I

INTRODUCTION

Over the course of the 20th century and into the 21st century, statistical process control (SPC) and quality management and their myriad of benefits have become more highly emphasized in many types of organizations ("History of Total Quality Management," n.d.). From Henry Ford's assembly lines in the early 1900s, to Walter Shewhart's formal development of a control chart at Bell Laboratories in 1924, to the founding of groups focused upon quality in more modern times, practitioners and academics over the last century have worked together to identify sources of variability in business processes in order to provide quality products and services to customers (Montgomery, 2013). The principle of using statistical information to improve the quality of processes and products was brought to notoriety by Dr. W. Edwards Deming who, in the 1950s, gave a series of lectures to Japanese executives who were attempting to economically recover and rebuild from World War II (Delavigne & Robertson, 1994). Deming's principles ran contrary to the classical and, at the time, ubiquitous management style brought to prominence during the Industrial Revolution by Fredrick Taylor (Delavigne & Robertson, 1994). In Taylor's view, processes and procedures could be optimized such that the only source of variability is user error, thus implying processes are entirely deterministic. Deming's insight was that processes have two sources of variability, one due to assignable cause and one due to random chance, as is the case in traditional statistical hypothesis testing (Delavigne & Robertson, 1994). Therefore, if

assignable causes can be quickly identified and corrected, overall quality would improve. That is, as variability decreases, quality increases (Montgomery, 2013). Deming informed the Japanese executives that if they would implement his quality and management philosophy of continuous monitoring and improvement through utilization of statistical techniques, that they would "capture the world," (Delavigne & Robertson, 1994; Neave, 1990). The executives heeded his advice and grew companies such as Mitsubishi and Toyota into the large, powerful, and profitable modern global organizations they are today (Delavigne & Robertson, 1994).

While not as widely adopted as early, American companies began implementing statistical techniques for ensuring quality during and after World War II, and the American Society for Quality (ASQ) was founded in 1946 ("History of Total Quality Management," n.d.). However, it was not until nearly 40 years later that the Deming philosophy was even widely known in the United States when NBC famously aired a television documentary named, "If Japan Can…Why Can't We?" (Walton, 1991). This documentary was followed closely by an article authored by Deming explaining the benefits of his methods (Deming, 1981). Business executives from across the country and globe became highly interested in these principles and further developed the field of quality management through concepts such as Motorola's "Six Sigma" initiative, the founding of the International Organization for Standardization (ISO), and Lean Manufacturing (Montgomery, 2013). Walton (1991) gave several anecdotes of American organizations implementing Deming's philosophy and enjoying great successes.

Some of the primary principles Deming presented to the executives in 1950s (referred to as Deming's 14 Points) Japan and promoted for the remainder of his life are:

(1) The role of business is to innovate and improve; (2) All of the organization must fully and closely adhere to the philosophy of continuous improvement; (3) "Require statistical evidence of built-in quality;" (4) Do not only consider supplier price in awarding contracts; (5) Never cease in the improvement of all processes; (6) Continually train employees; (7) Ensure leadership empowers workers to take ownership of the work; (8) "Drive out fear" of asking questions or making improvement recommendations to leadership; (9) Remove departmental partitions to allow cross-organizational collaboration; (10) Eliminate managerial slogans and "exhortations;" (11) Do not set unrealistic, arbitrary quotas; (12) Provide workers with the encouragement to perform good work; (13) "Encourage Education;" (14) Top management commitment to the quality program (Neave, 1990; Walton, 1991). While much of the Deming method is rooted in a qualitative organizational paradigm shift, the concrete ways this shift occurs is through allowing empirical data, visualized as to aid in understanding, to drive decisions (Walton, 1991). Walton (1991) outlined seven "helpful charts" for this purpose: (1) the cause-and-effect diagram; (2) the flow chart; (3) the Pareto chart; (4) the runs or trend chart; (5) the histogram; (6) the scatterplot; and (7) the control chart. Of these charts, the control chart is of particular interest to statisticians.

Statistical Process Control Charts

The control chart is a popular tool in quality management as they have been shown to improve productivity, prevent the manufacturing of defective products, minimize the frequency of process adjustments, give "diagnostic information" about a process, and give information about the capability of a process (Montgomery, 2013). The general idea, originally developed by Walter Shewhart in Bell Laboratories in 1924, is to

determine if an observable process has substantially or significantly changed (Shewhart, 1924). In his charting scheme, which bears his name, there are three main components: a specified mean target value, say μ_0, which the process ideally meets, and two control limits, one upper control limit (referred to as UCL) and one lower control limit (referred to as LCL). Future sample observations of size n, where $n \geq 1$, usually taken at equal time intervals, are compared to the UCL and LCL (Shewhart, 1924; Montgomery, 2013). When the process is performing as expected, referred to as an "in-control process," future sample observations taken should deviate minimally from the target value μ_0. However, when a sample observation falls beyond either the UCL or LCL, this signals to the process operator that the process mean may have deviated from μ_0. That is, evidence exists that the process may be "out-of-control," and that an investigation to determine if an assignable cause for this possible shift can be found is warranted. The concept described here is referred to as a "charting scheme" or "charting technique." The UCL, LCL, and μ_0 are typically plotted as horizontal lines on a graph and the future sample observations are plotted against these values, typically from left to right with the rightmost observation being the most recently observed (Montgomery, 2013). The basic construction, plotting the deviations of empirical observations from its target value and comparing those deviations to a control limit or limits, is the foundation of all control charting techniques. The style of chart chosen depends upon what is desired to be monitored, the nature of the process being monitored, and the magnitude of deviation from target to be protected against (i.e., desired sensitivity to shifts from target), which is often quantified in terms of the process' standard deviation, σ.

The Shewhart-style chart can be used for variables, such as the $\bar{X}$-chart, to directly monitor a process' mean (Montgomery, 2013). It can also be used for the monitoring of attributes, such as the number of nonconformities, average number of nonconformities per unit inspected, or the fraction of units in a sample having some nonconformity (Montgomery, 2013). Moreover, the Shewhart-style chart can be used to monitor a process' variability, such as the R-chart or the s-chart (Montgomery, 2013).

However, there exist other many other charting techniques which can be used when the nature of the process does not lend itself well to the Shewhart-style chart, such as in the case when the sample size from the monitored process is $n = 1$, or when the magnitude of the shift desired to protect against is small. In both cases, the Shewhart-style chart is known to be ineffective (Montgomery, 2013). Page (1954) developed a control chart where cumulative summations of deviations from target, in both the positive and negative direction, of sequential observations are plotted against a control limit. This type of technique is referred to as a "CUSUM" (an acronym for "cumulative summation") chart, is commonly used to monitor a process' mean, and can be used when future samples are of size $n = 1$ (Montgomery, 2013). The CUSUM method, unlike Shewhart-style charts, takes into consideration the entire sequence of observations rather than only the latest observation (Montgomery, 2013). Roberts (1959) developed a control chart based upon the geometric series. In his charting scheme, the current plotted point is the weighted mean of the current observation and the previous observations, which is plotted against an upper and lower control limit. This technique, referred to as the "Exponentially Weighted Moving Average (EWMA)" chart, is similar to the CUSUM

technique in that it considers the entire sequence of observations in addition to being effective when the sample size is $n = 1$.

The aforementioned charting techniques are univariate, that is, they monitor a single process. Multivariate charts, which jointly monitor multiple processes, have also been developed. These techniques are advantageous in the case when it is desired to simultaneously monitor several different processes with possibly differing target values as they take into consideration the correlation structure between the processes. In 1947, Harold Hotelling developed a multivariate analogue to the Shewhart $\bar{X}$-chart referred to as Hotelling's-T^2 chart (Montgomery, 2013). Lowry, Woodall, Champ, & Rigdon (1992) developed a multivariate extension of the EWMA chart. Pignatiello & Runger (1990) presented two multivariate extensions of the CUSUM charting technique. Bersimis, Psarakis, & Panaretos (2007) gave a comprehensive overview of modern multivariate control charting schemes. Woodall & Montgomery (2014) also discussed advances in multivariate control charting schemes as well as a variety of other schemes, including those designed for time-to-event data, autocorrelated data, and functional data.

As is the case in many classical statistical models, many control charts are dependent upon the assumption of the underlying process following a normal distribution. While several charting schemes, including those mentioned previously, are robust to small departures from normality, extreme non-normality can lead to the deterioration of the performance of a particular charting technique (Montgomery, 2013). Montgomery (2013) outlines several studies which examine the effects of non-normality on various control charts. One issue, however, is that it is often difficult if not impossible to ascertain the distribution of a process, especially when the quality control program is

in its relative infancy. Because of this practical consideration, attention has been given to the creation of nonparametric control charting schemes (Chakraborti, Van Der Laan, & Bakir, 2001). Nonparametric statistical methods are not dependent upon the variables of interest following any particular distribution and are still valid even in the case when the measurement scale is less than interval (Conover, 1999). Bakir & Reynolds (1979) developed a CUSUM chart which utilizes the one sample nonparametric Wilcoxon Signed Rank Test. Amin, Reynolds, & Bakir (1995) proposed several control charts based on the one sample nonparametric sign test. Wang, Zhang, & Xiong (2017) developed a univariate CUSUM chart based on the Mann-Whitney test statistic.

Statement of the Problem

As mentioned, the type of control chart chosen for practical implementation should be related to the nature of what is to be monitored. For instance, there may be cases where there are several presumably identical processes with identical target values. Such processes are referred to as "multiple-stream" processes (MSP), and when in-control, can be conceptualized as a one-way analysis of variance (ANOVA) model under the null hypothesis (Montgomery, 2013). Boyd (1950) initially proposed a Shewhart-style control charting scheme to monitor a MSP's mean and variation by calculating the sample mean and range for each stream and taking the minimum and maximum as the plotting statistic. Mortell & Runger (1995) point out the inefficiency which can arise in Boyd's chart and propose two charting schemes: one to monitor variability among the streams which uses a variant of the Shewhart-style $\bar{\bar{X}}$-chart, and one to monitor the variability of one stream with respect to the others using Shewhart, EWMA, and CUSUM-style frameworks to monitor the maximum range of all the stream sample

means at a given sample. Montgomery (2013) concludes that if all the streams are highly correlated, that only one stream needs to be monitored. Meneces, Olivera, Saccone & Tessore (2008) suggest utilizing a Shewhart chart for each stream as this technique is a more effective use of information. Vicentin, Silva, Piccirillo, Bueno & Oprime (2018) proposed considering an MSP as mixture of multiple related distributions, which come from the same parametric family, but may possibly have different parameters. The authors developed a Shewhart-style charting scheme for their proposed MSP conceptualization. Jirasettapong & Rojanarowan (2011) discussed several competing MSP charts and when their respective use is most appropriate. However, they conclude that there exists "no perfect MSP chart that is better than the others in all aspects," (Jirasettapong & Rojanarowan, 2011). Additionally, since many of these charting schemes, and specifically those of Boyd, Mortell and Runger, and Meneces, use the Shewhart-style $\bar{X}$-chart, their ability to quickly detect shifts from target may possibly deteriorate in the presence of non-normal data since normality is an assumption for the use of the $\bar{X}$-chart (Montgomery, 2013).

Purpose of the Study

There are two primary purposes of this study. After the body of literature was reviewed for nonparametric control charts and for MSP control charts independently in Chapter II, this study assessed the performance via Monte Carlo simulation of the Boyd, Mortell and Runger, and Meneces MSP control charting techniques in non-normal data situations, such as light-tailed data, heavy-tailed data, and skewed data, to determine their in-control and out-of-control performance, as generally measured by the average number of samples required to detect a shift of a particular magnitude. The measure is referred to

as "Average Run Length (ARL)" and is denoted in the in-control case as "ARL_0," and as "ARL_1," in the out-of-control case (Montgomery, 2013). Second, this study developed and proposed a new nonparametric MSP control charting technique using the Extended Median Test (EMT) which uses the CUSUM framework. Its in-control and out-of-control performance is compared to the Boyd, Mortell and Runger, and Meneces MSP charting schemes in normal, light-tailed, heavy-tailed, and skewed data situations. In Chapter III, the mathematical foundations and recommended operation of this study's proposed charting technique was given. The new chart is referred to as the "Nonparametric Extended Median Test CUSUM (NEMT-CUSUM)" chart.

Research Questions

The research questions guiding this study are as follows:

Q1 What values of the parameter δ of the NEMT-CUSUM chart yield the commonly desired ARL_0 values of 200, 370, and 500 which correspond to Type I error rates of $\alpha = 0.005, 0.0027,$ and 0.002?

Q2 For a specified value of ARL_0, what is the statistical power yielded when a subset of the C monitored streams has shifted away from target, considering different magnitude shifts, number of monitored streams, and sample sizes of the streams?

Q3 How does the performance of the NEMT-CUSUM chart, in terms of ARL_1, compare to the performance of the Boyd, Mortell and Runger, and Meneces MSP charts in the presence of data coming from normal, light-tailed, heavy-tailed, and skewed distributions when half of the monitored streams shift from the target median of magnitudes ranging from 0 to 3 in increments of 0.25 have occurred?

Limitations of Study

As is the case in most all research, there exist limitations. It is important to clearly state these limitations for the sake of other researchers who may wish to replicate or expand upon these analyses as well as for practitioners who may wish to implement the

newly proposed techniques in a practical setting. One primary limitation is with respect to the ARL_1 performance assessment in comparing the new charting scheme to existing charting schemes. As Monte Carlo computer simulations in the statistical software package *R* were used for the sake of time, this implies that the data used in analysis came from known, well-defined distributions. In practice, this may not necessarily be the case, and it may difficult to determine from what distribution observed data come. Because of this, results are only valid for the distributions used. Moreover, while 12 different shifts away from target will be considered for both ARL_0 and ARL_1 assessment, this analysis does not consider shifts of small increments or shifts of larger than 3σ, which may be desired to be known in practice. Third, as the NEMT-CUSUM relies upon an application of a χ^2 Goodness of Fit test under independent binomial sampling, its practical application for MSP monitoring is limited to the assumptions of that test. Specifically, it is assumed: (1) the streams are independent of each other; (2) under the null hypothesis, all streams have the same median; (3) the sample sizes taken from each stream are sufficiently large such that the asymptotic properties of the χ^2 test statistic can be used; and (3) each cell's expectation must be ≥ 5 (Conover, 1999; Agresti, 2007). Fourth, it is also assumed that random samples taken between at each time point are independent of the samples taken at all other time points for a given stream. In a practical setting, autocorrelation may be present and may impact the performance of the proposed charting scheme. Fifth, it is also assumed that if chart operators do not have a specified target median value, $\tilde{\mu}_0$, then they have a good estimate of what it is. In practice, this may not necessarily be the case.

To summarize, the various existing statistical process control charts were designed to efficiently monitor a particular process exhibiting particular characteristics. Classically, these charts were designed to monitor a univariate process, such as a single product being manufactured on a single assembly line. However, sometimes the process desired to be monitored is comprised of several presumably identical processes, or "streams." Such a process is referred to as a "Multiple Stream Process (MSP)" and charting techniques have been developed for this circumstance. However, existing MSP charting techniques depend on the underlying process following a normal distribution, which may or may not necessarily be the case in practice. A comprehensive review of the literature uncovered an apparent gap where, to the best of the author's knowledge, no chart had been developed for monitoring an MSP which was also nonparametric in nature. Thus, the purpose of this dissertation was to fill this gap by developing a nonparametric MSP chart.

CHAPTER II

LITERATURE REVIEW

In this chapter, a review of relevant existing literature regarding univariate charting techniques is given. Specifically, this chapter reviews traditional parametric charting techniques used for detecting shifts in a process' mean, including the Shewhart $\bar{X}$-chart, EWMA and CUSUM charts, as well as MSP charts. Additionally, a review of nonparametric statistical tests for comparing location parameters of multiple independent groups and nonparametric charting schemes are also given.

Review of Univariate Control Charts

As mentioned in Chapter I, the Shewhart-style control chart, first developed in 1924, is a commonly used technique to monitor a process' mean (Shewhart, 1924; Montgomery, 2013). When the Shewhart-style chart is used to monitor a process' mean, it is referred to as the "$\bar{X}$-chart," as the sample statistic used to estimate the process' mean is the sample mean, $\bar{X}$. The $\bar{X}$-chart's effectiveness is most evident in detecting large mean shifts away from a target value often referred to as μ_0 (Montgomery, 2013). "Large" contextually means two or more standard deviations, both in the positive and negative direction, where a process' true standard deviation is denoted as σ. To use the $\bar{X}$-chart, let $x_1 \ldots x_n$ denote a random sample of size n from a normally distributed random variable with mean, μ_0, and standard deviation, σ, both of which may or may not be known, and may possibly need to be estimated. Then, sample means for each future

sample taken are calculated and plotted against the UCL and LCL. The UCL and the LCL, in the case where μ_0 and σ are known, are calculated by:

$$\begin{aligned} UCL &= \mu_0 + L\sigma \\ LCL &= \mu_0 - L\sigma. \end{aligned} \tag{1}$$

Here, "L" represents the number of standard deviations in the positive and negative direction the control limits are from the target value, μ_0, and is sometimes referred to as the "half-width" (Meneces et al., 2008). Generally, this value is taken to be 3, which is synonymous with having a probability of observing a point exceeding either control limit when the process is in-control (a "false alarm" or "Type I Error" from hypothesis testing) of $\alpha = 0.0027$ (Montgomery, 2013). Such a chart construction yields $ARL_0 = 370$ (Montgomery, 2013). However, in practice, it may be unreasonable to assume either μ_0 or σ are known, and therefore they both need to be estimated using historical observations. In such cases, Montgomery (2013) recommended taking approximately 20-25 samples of size n to estimate both μ_0 and σ. When $4 \leq n \leq 6$, it is common practice to use the sample relative range as an estimate of σ, where the relative range is defined as $W = R/\sigma$ (Montgomery, 2013). Thus, the estimates for μ_0 and σ are given by:

$$\begin{aligned} \hat{\mu}_0 &= \bar{\bar{x}} = \frac{1}{m}\sum_{i=1}^{m} \bar{x}_i \\ \hat{\sigma} &= \frac{\bar{R}}{d_2} = \frac{1}{d_2 m}\sum_{i=1}^{m} R_i, \end{aligned} \tag{2}$$

where $\bar{x}_i = n^{-1}(x_{1i} + \cdots + x_{ni})$, $R_i = \max(x_{1i} \ldots x_{ni}) - \min(x_{1i} \ldots x_{ni})$, and d_2 is the mean of the relative range, and can be found in the appendices of most statistical process

control texts (Montgomery, 2013). Thus, the UCL, LCL, and Center Line ("CL") can now be calculated by:

$$\begin{aligned} UCL &= \bar{\bar{x}} + \frac{3}{d_2\sqrt{n}}\bar{R} \\ CL &= \bar{\bar{x}} \\ LCL &= \bar{\bar{x}} - \frac{3}{d_2\sqrt{n}}\bar{R}, \end{aligned} \tag{3}$$

where $3/\left(d_2\sqrt{n}\right)\bar{R}$ is sometimes referred to as the constant, "A_2," which can also be found in the appendices of several statistical process control texts (Montgomery, 2013). However, when the sample size increases to approximately $n = 10$ or $n = 12$, Montgomery (2013) noted that the range method of estimating σ loses efficiency, and thus it is recommended to instead use the sample standard deviation, s, which is calculated as:

$$s = \sqrt{\frac{1}{n-1}\sum_{i=1}^{n}(x_i - \bar{x})^2}. \tag{4}$$

However, while it is well-known that the sample variance, s^2, is an unbiased estimator of the population variance, σ^2, s is not an unbiased estimator of the population standard deviation. In fact, the expected value of s is $c_4\sigma$, where c_4 is a constant whose value is a function of the sample size, and is another tabled value commonly found in statistical process control texts (Montgomery, 2013). The estimator for μ_0 will remain the same as in (3), and the new estimator for σ, given m historical samples of size n becomes:

$$\hat{\sigma} = \frac{\bar{s}}{c_4} = \frac{1}{m(c_4)} \sum_{i=1}^{m} s_i. \quad (5)$$

Thus, the UCL, LCL, and CL can be calculated by:

$$\begin{aligned} UCL &= \bar{\bar{x}} + \frac{3\bar{s}}{c_4\sqrt{n}} \\ CL &= \bar{\bar{x}} \\ LCL &= \bar{\bar{x}} - \frac{3\bar{s}}{c_4\sqrt{n}}. \end{aligned} \quad (6)$$

Montgomery (2013) also recommended using the sample standard deviation as an estimate for the unknown process standard deviation in cases where the sample size is variable from sample to sample.

Control Charts for Detecting Small Mean Shifts

As mentioned in Chapter I, there are issues in using a Shewhart-style chart under certain circumstances. First, it is known that Shewhart-style charts are not particularly effective at detecting small shifts of the mean away from target ($\leq 1.5\sigma$) (Montgomery, 2013). Second, while there are techniques available to use an $\bar{X}$-chart in the case when $n = 1$, such as the Moving Range chart, this charting technique's in-control performance is "generally much worse" than that of a standard $\bar{X}$-chart (Montgomery, 2013). Montgomery (2013) noted that the cause of this phenomenon is that the moving range values are correlated, and the Moving Range chart does not consider the correlation between plotting statistics. Finally, the Shewhart-style framework does consider the entire sequence of sample plotting statistics taken. The "Exponentially Weighted Moving

Average (EWMA)" chart and the "Cumulative Summation (CUSUM)" chart correct for these shortcomings (Montgomery, 2013).

Exponentially weighted moving average chart. The EWMA control chart is a technique based on geometric moving averages (Roberts, 1959). An EWMA control chart possesses the same three components present in a Shewhart-style chart: the target value, μ_0, the UCL and the LCL (Roberts, 1959). However, since it takes into consideration the entire sequence of observations, the computation of the EWMA's UCL and LCL will differ from the control limits for the $\bar{X}$-chart.

Allow Z_i to represent the EWMA plotting statistic at sample i. Roberts (1959) proposed calculating Z_i as:

$$Z_i = r\bar{X}_i + (1 - r)Z_{i-1}, \tag{7}$$

where $0 < r \leq 1$ and $Z_0 = \mu_0$. Roberts (1959) showed that the expectation and variance of Z_i, assuming the $\bar{X}_i$'s are independent, are:

$$E[Z_i] = \mu_0 \tag{8}$$

$$Var[Z_i] = \sigma_{Z_i} = \sqrt{\frac{r}{2 - r}[1 - (1 - r)^{2i}]}\sigma_{\bar{X}}, \tag{9}$$

which as $i \to \infty$, the variance will approach an asymptote of:

$$Var[Z_i] = \sigma_{Z_i} = \sqrt{\frac{r}{2 - r}}\sigma_{\bar{X}}. \tag{10}$$

Therefore, the UCL, LCL, and CL can be computed by:

$$\begin{aligned} UCL &= \mu_0 + k\sigma_{Z_i} \\ CL &= \mu_0 \\ LCL &= \mu_0 - k\sigma_{Z_i}, \end{aligned} \tag{11}$$

where k denotes the number of standard deviations in both the positive and negative direction the UCL and LCL are away from μ_0, respectively. Note, while the notation given in (9) and (10) denotes the sample statistic being taken as the sample mean (which implies a sample size of $n > 1$), the EWMA charting scheme can also be used in the case when $n = 1$ (Montgomery, 2013). Also of note, it is assumed here that operators have a reasonably accurate estimate of the measured process' standard deviation, denoted in (9) and (10) as $\sigma_{\bar{X}}$ (Montgomery, 2013). Further, EWMA charts are desirable in practice as they are "very insensitive to the normality assumption" (Montgomery, 2013).

Montgomery (2013) recommended to use values of r between 0.05 and 0.25 (where smaller values of r are recommended when protecting against smaller shifts from target and vice versa) and that using $2.6 \leq k \leq 3.05$ "works reasonably well" with larger values of k being paired with larger values of r. Using $r = 0.1$ and $k = 2.7$ will yield in-control performance of $ARL_0 \approx 500$ (Montgomery, 2013).

Cumulative summation control chart. Page (1954) proposed an alternative control charting technique to the Shewhart-style charts referred to as the "Cumulative Summation (CUSUM)" chart. Based upon Wald's Sequential Likelihood Ratio Test, the CUSUM chart plots cumulative deviations from some target value, μ_0, in both the positive and negative direction (Wald, 1945; Page, 1954). Like the $\bar{X}$-chart and the EWMA chart, the CUSUM chart is also comprised of a target value, a UCL, and a LCL. If

an operator wished to monitor a process' mean, the plotting statistic to be used for the CUSUM chart at sample i is defined as:

$$C_i = \sum_{j=1}^{i} (\bar{X}_j - \mu_0). \tag{12}$$

In order to determine if the process has possibly shifted away from target, it is necessary to calculate control limits to compare against the cumulative deviations. If using the statistic in (12), derivation of control limits would depend on knowledge of the distribution of the underlying statistic being monitored as well as the distribution of the sum of those statistics. There are two other common techniques used to calculate the control limits: one is called the "V-Mask" and the other is called the "Tabular Method" (Montgomery, 2013). Montgomery (2013) recommends use of the Tabular Method, and thus, that is what will be discussed here. In the Tabular Method, the previously given plotting statistic is modified into a positive and negative plotting statistic and these are given by:

$$\begin{aligned} S_i^+ &= \max[0, x_i - (\mu_0 + k) + S_{i-1}^+] \\ S_i^- &= \max[0, (\mu_0 - k) - x_i + S_{i-1}^-], \end{aligned} \tag{13}$$

where $S_0^+ = S_0^- = 0$, and k is a constant referred to as a "slack value," and is commonly chosen to be one-half of the size of the shift desired to protect against (Montgomery, 2013). For example, if it is desired to protect against shifts of 1σ, $k = 1/2$. As shown in (13), there are two plotting statistics for CUSUM charts when using the Tabular Method. S_i^+ represents the plotting statistic for positive deviations from μ_0 and S_i^- represents the plotting statistic for negative deviations from μ_0. Here, x_i could be a sample statistic such

as the sample mean, but it could also be an individual observation in the case where $n = 1$. Note, like the EWMA charting scheme, it is assumed an accurate estimate of the process standard deviation is available (Montgomery, 2013).

S_i^+ and S_i^- are compared to a control limit commonly referred to as h. If $S_i^+ > h$ or $S_i^- > h$, this signals to the operator that a shift may have taken place (Montgomery, 2013). A feature of the CUSUM chart is that not only is the operator alerted that a shift has taken place, the construction of the plotting statistic, being cumulative deviations from target, will also show the operator at what point the shift began to occur. Therefore, more information can be utilized when searching for an assignable cause.

Operators must choose a value of h such that the CUSUM chart attains a desired value of ARL_0, and this value of h will differ depending on the distribution of the underlying process being monitored (Montgomery, 2013). There have been several different proposed approaches to determining this value. Page (1954) gave an integral equation for the exact value of ARL_0 given a particular value of h and a specified probability density function of the monitored process. The integral equation is difficult to find a direct solution to, and thus, alternative approaches to estimating ARL_0 given a particular value of h and a specified probability density function have been proposed in the time since. Brook & Evans (1972) approached the problem by regarding a CUSUM chart as a Markov chain. Reynolds (1975) used a Brownian motion approximation. Woodall (1983) utilized numerical quadrature in his approximation. Montgomery (2013) recommended, if the monitored process follows a normal distribution, that setting $k = 1/2$ and $h = 4.77$ will yield $ARL_0 = 370$. Gan (1991) also gave recommendations

for selecting k and h such that the CUSUM chart would perform "optimally," assuming the monitored process follows a standard normal distribution.

Review of Control Charts for Multiple Stream Processes

In the prior descriptions of the $\bar{X}$-chart, the EWMA chart, and the CUSUM chart, the process being monitored are considered "single stream processes," where operators are interested in only monitoring the mean from a single process. In practice, there may be instances where multiple streams are desired to be monitored. As mentioned in Chapter I, a "Multiple Stream Process (MSP)" is one where observations being taken during a single sample consist of numeric measurements from multiple individual sources or "streams" (Montgomery, 2013). For example, the number of transactions separate bank tellers within the same bank process over the course of an hour would be an MSP. As an additional example, identical models of automobiles being manufactured on separate assembly lines would also be an MSP. In such cases, several different MSP charts have been proposed as this type of process is common in practice and differs from traditional, univariate charting techniques (Montgomery, 2013).

Boyd's Group Control Chart

Boyd (1950) proposed a "Group Control Chart (GCC)" to monitor an MSP which utilizes the general framework of a Shewhart-style $\bar{X}$-chart, including an UCL and a LCL. To construct the control limits, m preliminary samples of size n are taken from each of the s streams as if an $\bar{X}$-chart were being used for each of the streams (Montgomery, 2013). Then, the UCL and LCL are computed by aggregating the observations into a single, overall "grand mean," denoted $\bar{\bar{x}}$, and "grand range," denoted $\bar{R}$. The equations for calculating the control limits are given by:

$$UCL = \bar{\bar{x}} + \frac{3}{d_2\sqrt{n}}\bar{R}$$
$$LCL = \bar{\bar{x}} - \frac{3}{d_2\sqrt{n}}\bar{R}, \quad (14)$$

where the constant d_2, whose value is a function of the sample size taken at the individual stream level, has the same meaning as in the standard $\bar{X}$-chart described in (3) (Montgomery, 2013). The plotting statistic used in Boyd's GCC at a given future sample is both the minimum and maximum sample mean values taken from the s streams (2013). For example, if $s = 4$ streams were being monitored, and the sample means taken at future sample number i were $\bar{X}_{1i} = 21.1$, $\bar{X}_{2i} = 21.4$, $\bar{X}_{3i} = 21.6$, and $\bar{X}_{4i} = 22.0$, then the means plotted against the control limits would be $\bar{X}_{1i}$ and $\bar{X}_{4i}$. If the minimum and maximum mean values from the s streams are within the control limits, then it is straightforward to recognize that all the other mean values would also be within the control limits.

Montgomery (2013) pointed to some potential issues when using Boyd's GCC. As samples are taken from each of the s streams, this technique may become overly cumbersome when the number of streams becomes prohibitively large. Furthermore, as information from only the minimum and maximum mean values are considered, data from the remaining $s - 2$ streams is omitted. Thus, this technique inefficiently uses collected data. Another issue with Boyd's GCC is the lack of care provided to the correlation between the streams, and this can either substantially inflate or deflate ARL_0 to an unacceptable level (Mortell & Runger, 1995). Grimshaw, Bryce & Meade (1999) proposed widening the control limits of Boyd's GCC to account for this. Grimshaw et al.

(1999) also recommended widening the limits to account for the tendency of the chart's ARL_0 to deteriorate as the number of streams being monitored becomes large.

Nelson (1986) recommended use of a "runs rule" to ameliorate the ARL_0 problem in Boyd's GCC which can be used with or without control limits. Runs rules are similar to control limits in that they help operators make decisions about the in or out-of-control nature of the process being monitored. However, instead of comparing a statistic to a control limit, the patterns formed in sequential observations are analyzed. They are often an attractive alternative to a more complex charting scheme due to their simple nature (Nelson & Stephenson, 1996). Nelson (1986) suggested that if one monitored stream produces the maximum or minimum observed $\bar{X}_i$ for $r = 4$ consecutive points, then this signals a possible out-of-control stream. Nelson & Stephenson (1996) also proposed additional runs rules for Boyd's GCC. However, additional rules can add complexity to a monitoring scheme and should be implemented cautiously (Montgomery, 2013).

Mortell and Runger's Group Control Chart

Mortell & Runger (1995) outlined many of the aforementioned issues with Boyd's GCC and proposed several alternative charting techniques. Their basic premise in all of the proposed charting schemes is that MSP variance among the s streams can be partitioned into between-stream variation and within-stream variation. Thus, they propose use of a model quite similar to a one-way random effect analysis of variance (ANOVA) model. Let Y_{tjk} be the kth measurement from the jth stream at time t. Thus, the MSP model can be written in scalar notation as:

$$Y_{tjk} = \mu_0 + A_t + \epsilon_{tjk}, \tag{15}$$

where $A_t \sim N(0, \sigma_a^2)$ represents the mean difference in measurement from target value μ_0 across all s streams, and $\epsilon_{tjk} \sim N(0, \sigma^2)$ represents the mean difference measurement k on stream j is away from $\mu_0 + A_t$ (Mortell & Runger, 1995; Montgomery, 2013). It is also assumed A_t and ϵ_{tjk} are independent of each other, but the A_t's might not necessarily be independent of each other (Mortell & Runger, 1995). For charting, the authors proposed using two different charts: one to monitor common variation (i.e., shifts in the mean of A_t) and one to monitor shifts in a single stream with respect to the others (i.e., shifts in the mean of ϵ_{tjk}) (Mortell & Runger, 1995).

To monitor common variation among the streams, the authors proposed a Shewhart-style $\bar{X}$-chart. In this technique, the authors propose taking sample means of size n from each of the s streams, aggregating them into an overall mean, and using this as the plotting statistic (Mortell & Runger, 1995). While this is like Boyd's GCC, with the exception being the overall mean of the sample means is the plotting statistic, the key difference between the two techniques is in how the control limits are computed. Instead of using the individual sample size, n, in the control limit construction, the authors instead use the overall sample size, $n \times s$, in the control limit construction. Clearly, this increase in sample size will narrow the width of the control limits from those in Boyd's GCC given in (14) thereby making it more sensitive to simultaneous and equal shifts across all streams (Mortell & Runger, 1995). However, one problem the authors noted in using this technique is the problem of the A_t's possibly being autocorrelated, which may deteriorate chart performance.

To monitor shifts in a single stream with respect to the others, the authors recommended using the maximum range among stream means in a Shewhart, EWMA

(using weighting values of r of 0.1, 0.3, and 0.8), and CUSUM-style frameworks (Mortell & Runger, 1995). That is, their proposed plotting statistic is:

$$R_t = \max_j Y_{tj} - \min_j Y_{tj}. \tag{16}$$

To evaluate the performance of their proposed techniques, the authors conducted a simulation study to estimate the in-control and out-of-control ARL for shifts in both a single stream and in multiple streams. They consider shifts from a target value of $\mu_0 = 0$ to 0.5, 1, 1.5, and 2 for processes comprised of 2, 3, 5, 10, and 20 streams (Mortell & Runger, 1995). Across the various conditions, the CUSUM chart tended to perform most optimally, both in terms of in-control and out-of-control performance. However, the authors recommend use of the two-chart technique in the case when a large number of streams are being monitored (Mortell & Runger, 1995).

The conceptualization of an MSP described by (15) has been extended to other studies. Epprecht, Barbosa & Simões (2011) essentially combined Mortell and Runger's R_t chart with the Boyd's GCC chart for monitoring shifts of a single stream. The authors recommended estimating $\hat{\mu}_0 + \hat{A}_t = \hat{b}_t$ by taking samples of size n from each of the m streams and calculating the sample mean (Epprecht et al, 2011). Then, they propose subtracting $\hat{b}_t$ from each sample mean from each stream at each time point t, which they refer to as $\hat{e}_{ti.}$ (Epprecht et al., 2011). Therefore, at each time point, there will be as many $\hat{e}_{ti.}$'s as there are streams being monitored. Now, as in Boyd's GCC, the minimum and maximum $\hat{e}_{ti.}$ are plotted against an upper and lower control limit (Epprecht et al., 2011). Via simulation, the authors showed their charting scheme to have superior performance, in terms of ARL_1, to Mortell and Runger's R_t chart for shifts of $> 1\sigma$ (Epprecht et al.,

2011). However, it was unclear whether $\hat{b}_t$ ought to be estimated in Phase I analysis and remain static for Phase II analysis or if it ought to be calculated for each Phase II sample. Additionally, the improved performance of Epprecht's proposed charting scheme over Mortell and Runger's R_t chart was marginal in most cases (Epprecht et al., 2011).

Runger, Alt & Montgomery (1996) also utilized (15) to produce a multivariate control chart. They considered the observations from each stream taken at time t to be a vector, $\boldsymbol{Y_t}$ with an associated covariance matrix $\boldsymbol{\Sigma} = \sigma_a^2\mathbf{1}\mathbf{1}^{\boldsymbol{T}} + \sigma^2\boldsymbol{I}$, where the variance terms are those described by (15), $\mathbf{1}$ denotes a vector whose elements are all equal to 1, $(.)^{\boldsymbol{T}}$ denotes the transpose of a vector or matrix, and $\boldsymbol{I}$ denotes the identity matrix (Runger et al., 1996). Through the principal component analysis (PCA) framework, the authors effectively developed Hotelling's T^2 statistic, except with differing projection matrices used in the quadratic form (Runger et al., 1996). Essentially, Hotelling's T^2 chart is akin to the sum of squares regression statistic used in classical hypothesis testing whereas this charting statistic is analogous to the mean corrected sum of squares total statistic also used in classical hypothesis testing (Ravishanker & Dey, 2002; Runger et al., 1996). That is, the proposed charting statistic is $S^2 = \sigma^{-2}\boldsymbol{Y}^{\boldsymbol{T}}(\boldsymbol{I} - s^{-1}\mathbf{1}\mathbf{1}^{\boldsymbol{T}})\boldsymbol{Y}$. From linear model theory, if $\boldsymbol{Y} \sim \boldsymbol{N_S}(\boldsymbol{\mu}, \boldsymbol{\Sigma})$, then $S^2 \sim \chi^2(s-1, \nu = \sigma^{-2}\boldsymbol{\mu}^{\boldsymbol{T}}(\boldsymbol{I} - s^{-1}\mathbf{1}\mathbf{1}^{\boldsymbol{T}})\boldsymbol{\mu})$ as $(\boldsymbol{I} - s^{-1}\mathbf{1}\mathbf{1}^{\boldsymbol{T}})$ is a symmetric, idempotent positive definite matrix (Ravishanker & Dey, 2002). The authors note that while this scheme would not be effective in detecting shifts in all streams, that it would be effective in detecting shifts in one or multiple streams (Runger et al., 1996). Additionally, the authors recommended that their S^2 statistic can be used in a multivariate CUSUM or multivariate EWMA charting scheme in order to more effectively detect small shifts away from target (Runger et al., 1996).

Meneces' Control Chart for Each Stream Technique

Meneces et al. (2008) noted that the historically cumbersome technique of using an $\bar{X}$-chart for each stream in an MSP has been alleviated by modern computing resources. However, the authors noted that the main problem with using a chart for each stream is the decrease in ARL_0 (or equivalently, an increase in the Type I error rate, α) due to cross-correlation between pairs of streams, which is defined as ρ (Meneces et al., 2008). Consider the case when $\rho = 0$. The probability of observing an out-of-control point at sample number i given the process is in control across all of the s streams being individually monitored is approximately $s\alpha$ (Meneces et al., 2008). This implies that as the number of streams increases, so too will the probability of making a Type I error. The method the authors suggest using to correct the inflated error rate is to widen the control limits to be greater than the classical half-width of three, as given in (3), (6), and (14), as $\rho \to 0$ and $s \to \infty$ (Meneces et al., 2008). The authors obtained estimates for the half-widths to be used to obtain a Type I error rate of $\alpha = 0.0027$, which yields $ARL_0 = 370$ (Meneces et al., 2008). Table 1 gives the simulated and recommended values to use in place of three for various numbers of streams being monitored.

In order to assess the performance of the $\bar{X}$-chart for each stream technique, the authors used direct comparison to and Boyd's GCC and the Mortell and Runger's Shewhart $\bar{X}$-chart to monitor shifts in a single stream with respect to the others (Meneces et al., 2008). In this comparison, the authors used industry data from an in-control MSP where $s = 14$ and the total number of samples taken was 53 (Meneces et al., 2008). Calculating a mean pairwise correlation between the 14 streams of $\hat{\rho} = 0.2782$, the authors decided to use a half-width value $L = 3.72$, which is nearly the mean of the

recommend half-width values for $s = 10$ and $s = 20$ given in Table 1 (Meneces et al., 2008). In their scheme, they did not observe an out-of-control point, as would be expected. However, Boyd's GCC and the Mortell and Runger chart both observed out-of-control points incorrectly, with the former scheme observing more than 10 (Meneces et al., 2008).

Table 1

Recommended Control Limit-Half Width Values

Number of Streams	Control Limit Half-Width
1	3.00
2	3.20
5	3.46
10	3.64
20	3.82
50	4.04
100	4.20

Meneces et al. (2008) noted that the primary value in their proposed charting scheme is with respect to the distinguishing of a shift in a single stream. Since data is being collected and used for each individual stream, the observed data are used more efficiently than in Boyd's GCC or in Mortell and Runger's charts (Meneces et al., 2008). Additionally, the authors suggested that in practice, while individual streams produce the same output, that it may not necessarily the case that they all have the same target value (Meneces et al., 2008). In such cases, erroneous conclusions may be drawn by the schemes proposed by Boyd and Mortell and Runger (Meneces et al., 2008).

Other Multiple Stream Process Monitoring Techniques

To the author's knowledge, the control charting schemes described previously represent nearly all of the academic studies regarding MSP monitoring. However, there do exist other studies which also contribute to the MSP body of literature which will be described here.

A mixture distribution approach. Vicentin et al. (2018) proposed a new Shewhart-style charting scheme to monitor the location parameters of an MSP. The authors conceptualized an MSP as a mixture distribution where each stream has its own, unique albeit related distribution (Vicentin et al., 2018). For example, the authors used four normal distributions with differing means and variances (Vicentin et al., 2018). However, the authors acknowledged that the MSP might not be evident, as would possibly be in the case where a seemingly identical part is purchased from multiple suppliers (Vicentin et al., 2018). Thus, identifying the number of streams becomes an important task to the efficacy of the chart. However, the authors only proposed use of visual inspection of historical samples via a histogram or other graphical aid to identify the appropriate number of streams to be monitored (Vicentin et al., 2018). As such, the proposed plotting statistic is the sample mean, which is calculated without respect to the proposed number of streams in the MSP (Vicentin et al., 2018). The authors developed control limits in a similar manner to (3), except taking into consideration that the plotting statistic may come from any of the monitored streams and that the half-widths could be changed depending on the desired shift to be protected against (Vicentin et al., 2018).

To evaluate their chart's performance, the authors performed a simulation for various size shifts away from target. However, instead of determining how quickly the

charting scheme can detect shifts in a single stream with respect to the others, they shifted multiple streams simultaneously (Vicentin et al., 2018). Additionally, the authors' simulation monitored four streams, and has been mentioned previously, the number of streams being monitored changes the efficacy of the charting scheme (Mortell & Runger, 1995; Meneces et al., 2008). Therefore, no direct comparison to any of the aforementioned charting schemes was made or could be made. Generally, as the shifts increase in magnitude in both the positive and negative direction in the streams, the chart signal more quickly (Vicentin et al., 2018). The authors noted this shortcoming of their analysis in the conclusions and recommended a direct comparison study in the future (Vicentin et al., 2018).

A fractional, adaptive sampling approach. As has been mentioned, one of the benefits of Boyd's GCC or Mortell and Runger's R_t charting schemes is that only one chart is being used for each of the s streams being monitored, which can be a desirable characteristic (Mortell & Runger, 1995; Montgomery, 2013). However, it may be cumbersome in practical environments to take a sample from each stream. Therefore, taking a sample from a fraction of the total number of streams may be more pragmatic approach (Lanning, 1998). Lanning (1998) suggested that such a sampling technique could be used in a $\bar{X}$-chart framework for monitoring an MSP. Moreover, it is normal to assume that if a plotting statistic plots near, but does not exceed a control limit, that operators may be more inclined to take larger samples at smaller time intervals (Lanning, 1998). To both ends, Lanning (1998) proposed taking a fixed sample from a fraction of the total number of streams at a fixed time interval and calculating an overall sample mean to be used as the plotting statistic in a $\bar{X}$-chart, as described previously. If the

sample mean plots near the target value, then the standard, fixed intervals between sampling continues (Lanning, 1998). "Near" here contextually means within "warning limits," which in an $\bar{X}$-chart are usually set to be $\pm 2\sigma$ instead of $\pm 3\sigma$ (Montgomery, 2013). If the sample mean exceeds the warning limits, then the sample size increases and the interval between samples is reduced (Lanning, 1999). The increase in sample size and reduction in time between observed samples must be determined prior to technique implementation and is often a function of physical limitations (Lanning, 1998). Montgomery (2013) noted that this technique is most effective in detecting a shift which affects all streams. It was also noted that use of the adaptive sampling technique is more effective in terms of the speed with which shifts are detected than the fixed interval sampling technique (Lanning, 1998; Montgomery, 2013).

Review of Some Nonparametric Tests

As mentioned in Chapter I, many of the common statistical hypothesis tests used in practice are dependent upon the variable of interest following a parametric distribution. Most commonly, it is assumed in traditional statistical testing and in the control charting schemes outlined in this chapter that the variable of interest is assumed to follow a normal or Gaussian distribution. However, in practical settings, this assumption may not reasonably be met, or it may be difficult if not impossible to verify. When this is the case, the conclusions drawn from use of a parametric test or charting technique may be erroneous (Conover, 1999). In such cases, and "when the price of making a wrong decision is high," it would be of use to utilize inferential tests and charting techniques which do not assume the variable of interest follows any particular distribution (Conover, 1999). Such tests and charting schemes are considered to be "nonparametric" in nature,

as the variable of interest has no parametric distributional assumption upon it. Several nonparametric inferential tests have been developed as alternatives to their parametric analogues. Of these, many nonparametric tests have been found to be preferable to their parametric counterparts, in terms of asymptotic relative efficiency, especially when the variable of interest comes from a heavy-tailed distribution (Conover, 1999). Additionally, several nonparametric control charting techniques which use nonparametric test statistics have been proposed as substitutes to the classical control charts discussed previously in this chapter.

One Population Nonparametric Tests

In research settings, it may be of interest for a researcher to make a determination, that is, test a hypothesis, about the unknown value of a single population's mean, denoted μ. In introductory statistics courses, the well-known parametric inferential test used to test the null hypothesis, $H_0: \mu = \mu_0$ versus an alternative hypothesis, $H_1: \mu \neq \mu_0$ (which could be one-sided) is referred to as a "one population t-test" (Montgomery, 2013). However, the t-test assumes the variable of interest follows a normal distribution. If this is not the case or cannot be reasonably assumed, some nonparametric alternatives to the one population t-test are the Sign Test and Wilcoxon's Signed Rank Test (Conover, 1999).

Sign test. The Sign Test, while nonparametric in nature, does have two primary assumptions (Conover, 1999). First, the sampled observations must be independent of each other. Second, data must be measured on at least an ordinal measurement scale for statements such as "less than" or "greater than" to have meaning. The Sign Test's statistical hypotheses are like that of the one population t-test with the exception that

inference is made about the population median instead of the population mean (Conover, 1999). Let $\tilde{\mu}$ denote the unknown population median and $\tilde{\mu}_0$ denote a hypothesized value of the population median under H_0. The hypotheses then being tested are the null $H_0: \tilde{\mu} = \tilde{\mu}_0$ versus the alternative $H_1: \tilde{\mu} \neq \tilde{\mu}_0$ (where again, the alternative could be one-sided) (Conover, 1999).

The procedure to obtain the test statistic for the Sign Test is straightforward. Let $x_1, x_2, \ldots, x_n$ denote a random sample from some population with an unknown median $\tilde{\mu}$. Then take the difference between each x_i and $\tilde{\mu}_0$. If $x_i = \tilde{\mu}_0$, then it is recommended to omit that data point (Conover, 1999). Let n^* represent the total number of observations for which $x_i \neq \tilde{\mu}_0$. Let ST denote the test statistic for the Sign Test. It is computed as:

$$ST = \sum_{i=1}^{n^*} I(x_i > \tilde{\mu}_0), \tag{17}$$

where $I(x_i > \tilde{\mu}_0) = 1$ if $x_i - \tilde{\mu}_0 > 0$ and $I(x_i > \tilde{\mu}_0) = 0$ otherwise. If H_0 is true, it would be expected that $ST = n^*/2$. Thus, under H_0, $ST \sim BIN(n^*, p = 0.50)$ (Conover, 1999). P-values associated with a particular value of ST can be found using either tabled values found in the appendices of most statistical texts or using statistical software applications. Additionally, for $n^* > 20$, ST can be standardized to the standard normal distribution using the Central Limit Theorem (Conover, 1999). This standardized test statistic is given by:

$$ST_{Standardized} = \frac{(T + 0.5) - 0.5n^*}{0.5\sqrt{n^*}}. \tag{18}$$

Wilcoxon signed rank test. Wilcoxon (1945) developed inferential tests based on ranking procedures which bear his name. When a single population is being analyzed,

the Wilcoxon Signed Rank Test (WSRT) test can be applied (Conover, 1999). The statistical hypotheses tested by the WSRT are identical to those tested by the Sign Test (i.e., $H_0: \tilde{\mu} = \tilde{\mu}_0$ versus $H_1: \tilde{\mu} \neq \tilde{\mu}_0$). The two main differences between these one sample nonparametric tests are the underlying assumptions and the testing procedure. With respect to the assumptions, in addition to assuming the sample data were randomly selected and thus independent of each other, the WSRT also assumes the measurement scale of the variable of interest is at least interval and that the population's underlying distribution is symmetric (Conover, 1999).

The testing procedure, while still straightforward, requires additional steps beyond those required by the Sign Test (Conover, 1999). Let $x_1, x_2, \ldots, x_n$ denote a random sample of size n from some population. Then let $D_i = x_i - \tilde{\mu}_0$, where x_i's for which $x_i = \tilde{\mu}_0$ are omitted from the analysis making the analyzed sample size n^* (Conover, 1999). Now, rank the $|D_i|$ such that $|D_{(1)}| < |D_{(2)}| < \cdots < |D_{(n^*)}|$, and let $R_{(i)}$ denote the ranking of $|D_{(i)}|$. If two or more $|D_{(i)}|$ are tied in value, then assign each tied value the mean of the $R_{(i)}$ values occupied by those tied values (Conover, 1999). For example, if two $|D_{(i)}|$ were both tied for the second smallest value, then they would both be assigned $R_{(i)} = 0.5(2 + 3) = 2.5$. Let W^+ denote the test statistic for the WSRT. The value of W^+ is then calculated by:

$$W^+ = \sum_{i=1}^{n^*} (R_{(i)}) I(D_{(i)}), \tag{19}$$

where $I(D_{(i)}) = 1$ if $D_{(i)} > 0$ and $I(D_{(i)}) = 0$ if $D_{(i)} < 0$. Thus, the statistic is the sum of the positive ranks. Quantiles for the exact null distribution of W^+ can be found in the

appendices of several statistical texts for small values of n^* (Conover, 1999). Thus, p-values associated with a value of W^+ can be found in these texts in addition to statistical software programs. Like ST, W^+ can also be standardized using:

$$W^+_{Standardized} = \frac{\sum_{i=1}^{n^*}\left(R_{(i)}\right)I\left(D_{(i)}\right)}{\sqrt{\sum_{i=1}^{n^*}\left(\left(R_{(i)}\right)I\left(D_{(i)}\right)\right)^2}}. \quad (20)$$

In cases where the somewhat more restrictive assumptions of the WSRT are met, it is preferable over the Sign Test in terms of statistical power (Conover, 1999).

Two Independent Population Nonparametric Tests

In some research situations, the comparison of two independent population's means is desired. The statistical hypotheses being tested are the null $H_0: \mu_1 = \mu_2$ versus the alternative $H_1: \mu_1 \neq \mu_2$. Traditionally, the parametric test used to test the given hypotheses is referred to as an "two independent populations t-test." Like the one population t-test, the two independent populations t-test is dependent upon the variable of interest being normally distributed (Montgomery, 2013). When this assumption is not met, two alternative nonparametric test that could be used are called the Median Test and the Mann-Whitney Test (Conover, 1999).

The median test. The Median Test is a nonparametric alternative to the two independent populations t-test. As is the case with the aforementioned nonparametric one population tests, inference is made with respect to the population medians and not the means (Conover, 1999). Thus, the hypotheses being tested by the Median Test are the null $H_0: \tilde{\mu}_1 = \tilde{\mu}_2$ versus the alternative $H_1: \tilde{\mu}_1 \neq \tilde{\mu}_2$.

Like the independent populations t-test, it is assumed that observations from either population are independent of each other, and that observations within each group are also independent of each other (Conover, 1999). More specifically, it is assumed under the null that for $p = 0.5$, each population is sampled from an independent binomial distribution (Snedecor & Cochran, 1989; Conover, 1999). The measurement scale of the variable of interest must be at least ordinal for statements such as "less than" and "greater than" to have meaning. Additionally, since under the null hypothesis it is assumed both populations have the same median, then it is also assumed that observations from both populations have the same probability of exceeding the median (Conover, 1999). Also, as this test is an application of the traditional χ^2 Goodness of Fit test, it must also meet those additional assumptions as well. Primarily, the expected cell frequencies (i.e., $(row\ total) \times (column\ total)/N$) must be ≥ 5 in order for the asymptotic approximate null distribution to be accurate (Conover, 1999; Agresti, 2007).

Let $x_1, x_2, \ldots, x_{n_1}$ and $y_1, y_2, \ldots, y_{n_2}$ denote random samples of size n_1 and n_2 from the two independent populations. Aggregate the data and find the median of the total sample which is denoted $\tilde{\tilde{\mu}}$. Now, create a 2×2 contingency table where the columns denote observations from either population, the top row denotes observations exceeding $\tilde{\tilde{\mu}}$, and the bottom row denotes observations which are less than or equal to $\tilde{\tilde{\mu}}$ (Conover, 1999). Table 2 graphically shows the data structure the Median Test uses. Under the null hypothesis, both populations are assumed to have the same median. Additionally, as the samples n_1 and n_2 are assumed to be taken from two binomial distributions, O_{11} and O_{12} are assumed to be distributed as binomial random variables.

That is $O_{11} \sim BIN(n_1, p = a/N)$ and $O_{12} \sim BIN(n_2, p = a/N)$. If $n_1 = n_2$, then $O_{1i} \sim BIN(n, p = 0.5N)$, $i = 1,2$.

Table 2

Contingency Table Used for Median Test

Sample	Population 1	Population 2	Totals
$> \tilde{\tilde{\mu}}$	O_{11}	O_{12}	a
$\leq \tilde{\tilde{\mu}}$	O_{21}	O_{22}	b
Totals	n_1	n_2	N

Let MT denote the Median Test's test statistic. It is calculated by:

$$MT = \frac{N^2}{ab} \sum_{i=1}^{2} \frac{\left(O_{1i} - \frac{n_i a}{N}\right)^2}{n_i} \ . \tag{21}$$

While perhaps less evident than the standardized Sign Test and WSRT test statistics, the Median Test statistic is the sum of two squared standardization of the two binomial random variables. However, since a and b are assumed fixed, one of the O_{1i}'s can be written in terms of the other. Thus, the squared standardized test statistic implies $MT \dot{\sim} \chi^2(1)$ as $N \to \infty$ (Conover, 1999).

The Mann-Whitney test. Mann & Whitney (1947) developed a nonparametric test to statistically determine if one random variable is stochastically larger than another random variable using ranks in a nearly identical way as Wilcoxon. In fact, the Mann-Whitney Test presented in this section is sometimes alternatively referred to as the "Wilcoxon Rank-Sum Test" (Wang et al., 2017). The Mann-Whitney (MW) Test tests the null hypothesis $H_0: \tilde{\mu}_1 = \tilde{\mu}_2$ against the alternative $H_1: \tilde{\mu}_1 \neq \tilde{\mu}_2$. As was the case for the Median Test, the MW Test also assumes independence between groups and within

groups (Conover, 1999). Additionally, the variable of interest must be measured at least on the ordinal scale for ranking to be performed (Conover, 1999).

To calculate the test statistic, first let $x_1, x_2, \dots, x_{n_1}$ and $y_1, y_2, \dots, y_{n_2}$ denote two mutually independent random samples such that $n_1 + n_2 = N$. The data is then aggregated and assigned a rank. Let $R(X_i)$ and $R(Y_j)$ denote the respective rankings assigned to X_i and Y_j for all i and j. Much like the WSRT statistic, tied values are assigned the mean of the rankings the tied values would hold (Conover, 1999). Let MW denote the MW test statistic. If there are a minimal number of ties, the test statistic can be calculated as:

$$MW = \sum_{i=1}^{n_1} R(X_i). \tag{22}$$

Conover (1999) recommended use of an alternative test statistic in the case when many ties are present. This alternative is the standardization of MW and is given by:

$$MW_{Standardized} = \frac{\left(MW - \frac{n_1(N+1)}{2}\right)}{\sqrt{\frac{n_1 n_2}{N(N-1)} \sum_{i=1}^{N} R_{(i)}^2 - \frac{n_1 n_2 (N+1)^2}{4(N-1)}}}, \tag{23}$$

where $\sum_{i=1}^{N} R_{(i)}^2$ denotes the squared ranks for all observations across both samples (Conover, 1999). Critical values and their associated p-values can be found in the appendices of many statistical texts as well as in several statistical software programs. Similar to the relationship of the Sign Test and the WSRT, the MW Test may be preferable to the Median Test in terms of statistical power while the latter tends to be more efficient when the data come from heavy-tailed distributions (Conover, 1999).

Multiple Independent Population Nonparametric Tests

In research settings, researchers may be interested in comparing means between multiple independent populations. Here, the hypotheses being tested are the null $H_0: \mu_1 = \mu_2 = \cdots \mu_c$ versus the alternative $H_1: \mu_i \neq \mu_j$ for at least one pair of (i, j) where $i \neq j$. The parametric testing procedure commonly used to test these hypotheses is a one-way ANOVA F-test (Montgomery, 2013). Like the one population t-test and the two independent populations t-test, the ANOVA F-test assumes the variable of interest for each of the c independent populations are normally distributed with possibly differing means and equal variances (Montgomery, 2013). As mentioned in the description of the other nonparametric tests, normality may not always be reasonably assumed, and therefore, nonparametric alternatives may be more appropriate. Two nonparametric alternatives which could be used are the Extended Median Test and the Kruskal-Wallis Test.

The extended median test. The naming convention of this particular test points to its purpose: extending the Median Test previously described to C independent populations. Thus, instead of an application of a χ^2 Goodness of Fit test of two binomial samples, it is an application of a χ^2 Goodness of Fit test of C binomial samples (Conover, 1999; Snedecor & Cochran, 1989). Therefore, all of the assumptions and general testing procedures presented in the Median Test's description are the same for the Extended Median Test (EMT) as well (Conover, 1999). The EMT tests the statistical hypotheses: $H_0: \tilde{\mu}_1 = \tilde{\mu}_2 = \cdots \tilde{\mu}_c$ versus $H_1: \tilde{\mu}_i \neq \tilde{\mu}_j$ for at least one pair of (i, j) where $i \neq j$ (Conover, 1999). Table 3 presents the extension of Table 2 to the case where c populations are being compared.

Table 3

Contingency Table Used for Extended Median Test

Sample	Population 1	Population 2	...	Population c	Totals
$> \tilde{\tilde{\mu}}$	O_{11}	O_{12}	...	O_{1c}	a
$\leq \tilde{\tilde{\mu}}$	O_{21}	O_{22}	...	O_{2c}	b
Totals	n_1	n_2	...	n_c	N

Let EM denote the test statistic for the EMT. It is calculated in an identical way to what is shown in (21), with the summation going across all c populations.

$$EM = \frac{N^2}{ab}\sum_{i=1}^{c}\frac{\left(O_{1i} - \frac{n_i a}{N}\right)^2}{n_i}. \tag{24}$$

Like the Median Test, $EM \dot{\sim} \chi^2(C-1)$ as $N \to \infty$ (Conover, 1999). Therefore, critical values and p-values can be readily found in the appendices of most any statistical text and in statistical software programs. However, it should be noted that there are three primary limitations for the EMT which also hold for the Median Test. First, as $\tilde{\tilde{\mu}}$ is estimated from the empirical sample rather than being specified *a priori,* the results are strongly dependent on $\tilde{\tilde{\mu}}$ being a reasonable estimator of the true population median. If the sample sizes between groups are small or greatly vary, $\tilde{\tilde{\mu}}$ may not be accurate. Second, if the populations have dramatically different medians, the cell expectation assumption may not be met. Third, this test is effectively a quantile test where only one quantile is being considered (Conover, 1999). It may be the case that the populations have the same median, but their other quantiles drastically differ.

Kruskal-Wallis test. Kruskal & Wallis (1952) extended the MW test to the case when more than two independent populations are being compared. As a result, the

assumptions for the MW test are nearly identical to those of the Kruskal-Wallis (KW) Test (Conover, 1999). It is assumed each of the c populations are mutually independent, the observations within each sample are also independent, and the measurement scale of the variable of interest is assumed to be at least ordinal (Conover, 1999). In addition, it is also assumed that either each of the C populations have identical distribution functions or "some of the populations tend to yield larger values than other populations do" (Conover, 1999). The KW Test tests the hypotheses: H_0: *The c populations have identical distribution functions* versus H_1: *At least one of the populations yields larger observations than at least one other population*.

Let $x_{j1}, x_{j2}, \dots, x_{jn_j}$ denote a random sample from the jth population of size n_j, where $\sum_{j=1}^{c} n_j = N$. Let KWT denote the test statistic for the KW Test. To calculate KWT, first aggregate the samples together and assign ranks to each of the N observations. (Conover, 1999). The same procedure is used for tied observations as was described in the sections on the WRST and MW Test. Let $R(X_{ij})$ denote the rank of the X_{ij}th observation and let $R_i = \sum_{j=1}^{n_i} R(X_{ij})$, $i = 1 \dots n_i$. Then, KWT can be calculated by:

$$KWT = \frac{1}{S^2}\left(\sum_{i=1}^{c} \frac{R_i^2}{n_i} - \frac{N(N+1)^2}{4}\right), \tag{25}$$

where:

$$S^2 = \frac{1}{N-1}\left(\sum_{\substack{All \\ Ranks}} R(X_{ij})^2 - \frac{N(N+1)^2}{4}\right). \tag{26}$$

The exact null distribution of KWT can be cumbersome to calculate (Conover, 1999). Consequently, tabled quantiles found in the appendices of statistical texts are often limited to a small number of values for c and n_j. Conover (1999) recommended use of the asymptotic $\chi^2(C-1)$ approximation. In deciding which of the nonparametric tests to use when comparing multiple independent populations, the KW Test is preferable (in terms of asymptotic relative efficiency) to the EMT when the variable of interest comes from a normal or light-tailed distribution (Conover, 1999). The EMT is preferable in terms of asymptotic relative efficiency to the KW Test when the variable of interest comes from a heavy-tailed distribution (Conover, 1999).

Review of Some Nonparametric Control Charting Techniques

As stated in the previous section, nonparametric tests are of value when the assumptions of their parametric counterparts are not met or cannot be verified, and the "price of making a wrong decision is high" (Conover, 1999). In business settings where quality management techniques are employed, specifically through use of control charts, there may exist many costly wrong decisions. As mentioned in the discussion on relevant control charts, all have an assumption of the monitored process following a normal distribution. Chakraborti et al. (2001) noted that in cases where this assumption is not met that the performance of the control chart, in terms of ARL_0 and ARL_1, may substantially deteriorate. Consequently, operators may be receiving frequent false alarms, or they may be alerted of a shift in the process' mean after a large number of nonconformities have been produced. In either scenario, the cost to a business may be sizeable and faith in the quality management program may wane. Therefore, it would be of value to employ and

further develop charting techniques which are nonparametric in nature to avoid such problems (Chakraborti et al., 2001).

A Shewhart-Style Sign Test Chart

Amin et al. (1995) noted that performance of the classical $\bar{X}$-chart may be negatively impacted in the presence of non-normal data. Therefore, the authors proposed use of the one population Sign Test statistic, as given in (17), as the plotting statistic in a Shewhart-style framework (Amin et al., 1995). One assumption the authors made for mathematical simplicity was that the variable of interest is continuous such that $P[x_i - \tilde{\mu}_0 = 0] = 0$ (Amin et al., 1995). It is straightforward to see from (17) that $0 \leq ST \leq n$ under H_0. Additionally, the null distribution of ST is symmetric about $n/2$ (Amin et al., 1995). As a result, for some desired ARL_0, a control limit the authors denote "a_2" can be determined by solving:

$$ARL_0 = \frac{1}{P(|ST| \geq a_2)}. \tag{27}$$

To compare the performance of their chart with respect to the traditional $\bar{X}$-chart, the authors carried out a simulation study using both standard two-sided charts and one-sided positive charts (Amin et al., 1995). Here, random samples of size $n = 10$ were generated from several distributions, including light-tailed, heavy-tailed, and skewed (Amin et al., 1995). The simulated samples were then monitored using both charting techniques, and ARL_1 values were estimated for shifts away from target of various magnitudes. The authors noted that the performance of the $\bar{X}$-chart is superior to their Shewhart-style chart when the underlying data were generated from the normal and uniform distributions (Amin et al., 1995). However, when the data were generated from heavy-tailed or skewed distributions, and the size of the shift was small ($< 1\sigma$), their

chart was found to be superior (Amin et al., 1995). The preferable performance was especially evident when the technique was one-sided (Amin et al., 1995).

A Cumulative Summation-Style Sign Test Chart

Amin et al. (1995) also proposed a CUSUM-style chart where the observations are the values of the Sign Test statistic. In their technique, samples of size n are taken, and their proposed CUSUM plotting statistics are given by:

$$S_t^+ = \sum_{i=1}^{t}(ST_i - k) - \min_{0 \le u \le t}\left(\sum_{i=1}^{u}(ST_i - k)\right)$$
$$S_t^- = \max_{0 \le u \le t}\left(\sum_{i=1}^{u}(ST_i - k)\right) - \sum_{i=1}^{t}(ST_i - k)\,. \tag{28}$$

Like the standard CUSUM procedure described before, if either of the plotting statistics exceeds some control limit h, then this is evidence to the operator that a shift may have taken place (Amin et al., 1995). Treating the CUSUM plotting statistics like a Markov chain, the authors were able to estimate values of k for various sized shifts from target (Amin et al., 1995). The authors then performed a simulation study to determine which values of k and h would yield a desired value of ARL_0 (Amin et al., 1995). To evaluate the performance of their proposed CUSUM chart, the authors compared its performance via simulation to the performance of a CUSUM which used $\bar{X}$ for each sample (Amin et al., 1995). The CUSUM using $\bar{X}$ tended to perform better than the Sign Test CUSUM when the data came from a uniform distribution (Amin et al., 1995). However, the performance of the Sign Test CUSUM was far superior to that of the $\bar{X}$ CUSUM for heavy-tailed and skewed distributions (Amin et al., 1995). Interestingly, the authors noted that the Sign Test CUSUM was even more effective than the $\bar{X}$ CUSUM

when monitoring small shifts from target when the data were normally distributed (Amin et al., 1995). Additionally, the authors also made note that the Sign Test CUSUM performed better than their proposed Shewhart-style Sign Test chart, as the distributions and shifts considered in both simulations were identical (Amin et al., 1995).

A Cumulative Summation Chart Based on the Wilcoxon Signed Rank Test

Bakir & Reynolds (1979) developed a CUSUM charting technique using the WSRT statistic. In their technique, individual observations are either grouped together naturally or artificially such that a group $(x_{i1}, x_{i2}, \dots, x_{ig})$ constitutes a future sample i (Bakir & Reynolds, 1979). The authors refer to their grouped technique as "Grouped Signed Rank (GSR)" chart. The authors slightly modify the test statistic given in (19) to be the sum of all ranks as opposed to the sum of all positive ranks (Bakir & Reynolds, 1979). Let R_{ij} denote the rank of x_{ij} within the group $(|x_{i1}|, |x_{i2}|, \dots, |x_{ig}|)$ for $i = 1,2, \dots$ and $j = 1,2, \dots g$ (Bakir & Reynolds, 1979). For sample number i, define the Bakir and Reynolds WSRT statistic as:

$$SR_i = \sum_{j=1}^{g} sgn(x_{ij}) R_{ij} \,. \tag{29}$$

The upper and lower CUSUM plotting statistics proposed by the authors are nearly identical to those given in (28) with the exception of replacing ST_i with SR_i given in (29) (Bakir & Reynolds, 1979; Amin et al., 1995). As was the case with the other described CUSUM techniques, one of the purposes of the authors' study was to determine for which values of h and k the in-control performance of the GSR technique would yield desirable ARL_0 (Bakir & Reynolds, 1979). Much like other proposed

CUSUM techniques, the authors treated the GSR CUSUM as a Markov chain to estimate its in-control performance for various combinations of k and h via computer simulation (Bakir & Reynolds, 1979). Unlike other proposed CUSUM techniques, the authors showed that the choice of k and h for the GSR CUSUM is dependent upon the skewness or lack thereof of the underlying probability distribution function (Bakir & Reynolds, 1979). Considering a symmetric distribution is an assumption of the WSRT, this additional simulation was warranted (Bakir & Reynolds, 1979; Conover, 1999).

To assess the performance of their chart, the authors compared the GSR CUSUM to a standard CUSUM chart (which assumed normality) and the traditional $\bar{X}$-chart (Bakir & Reynolds, 1979). They considered two cases: one where natural grouping (i.e., samples of size $n = 10$ were taken at each time point) was assumed and one where individual observations constituted the sample, and thus artificial grouping took place (Bakir & Reynolds, 1979). In the former case, the authors used $\bar{x}_i$ as the plotting statistic in the standard CUSUM and $\bar{X}$-charts, and SR_i for the observed value in the GSR CUSUM (Bakir & Reynolds, 1979). In the latter case, the authors used x_i as the plotting statistic for the standard CUSUM and $\bar{X}$-charts and waited until 10 individual observations had been accumulated to calculate SR_i in their GSR CUSUM (Bakir & Reynolds, 1979). The authors compared ARL_1 of the three charts in both cases when the data came from the normal, uniform, double exponential, and Cauchy distributions (Bakir & Reynolds, 1979). The uniform distribution is an example of a light-tailed distribution, while the latter two distributions represent heavy-tailed distributions.

Through simulation, the authors determined that the GSR CUSUM is not quite as effective as the standard CUSUM when the data are normally distributed (Bakir &

Reynolds, 1979). They also noted that the GSR CUSUM is less efficient than the standard CUSUM as it required 10 observations before a point could be plotted (Bakir & Reynolds, 1979). This was found to be the case of all the studied distributions besides the heavy-tailed distributions. Interestingly, it was shown that the GSR CUSUM was more effective at detecting small shifts than the $\bar{X}$-chart when the data were normal (Bakir & Reynolds, 1979). In the case where data came from the uniform distribution, the ungrouped $\bar{X}$-chart was shown to have superior performance (Bakir & Reynolds, 1979). Finally, it was shown that when the data came from the double exponential distribution, the GSR CUSUM's performance "is at least as good as the parametric procedures" (Bakir & Reynolds, 1979). The GSR CUSUM's ability to detect shifts from data coming from the very heavy-tailed Cauchy distribution was far superior to that of the parametric alternatives (Bakir & Reynolds, 1979).

A Shewhart-style Chart Based on the Mann-Whitney Test

Chakraborti & van de Wiel (2008) proposed a univariate control chart which made use of the MW Test statistic. While the MW Test is commonly used to compare two independent populations, the authors creatively applied the MW Test's procedure to a univariate process within a Shewhart-style framework (Chakraborti & van de Wiel, 2008). They define one independent group to be a historical, in-control sample of size m, (denoted $x_1 \dots x_m$) and the other independent group to be the hth future sample of size n (denoted $y_1 \dots y_n$) (Chakraborti & van de Wiel, 2008). They then define the Mann-Whitney plotting statistic for future sample h as:

$$M_{XY}^{h} = \sum_{i=1}^{m}\sum_{j=1}^{n} I(x_i < y_j)\,. \tag{30}$$

Note, the Mann-Whitney Test statistic given in (30) differs from the Mann-Whitney Test statistic given in (22). The statistic in (22) is an equivalent alternative to (30). Wang et al. (2017) showed $M_{XY}^{h} = MW - m(m+1)/2$. Chakraborti & van de Wiel (2008) noted that since $0 \leq M_{XY}^{h} \leq mn$, and since M_{XY}^{h} is symmetric about $mn/2$, that probabilistic control limits can be calculated for M_{XY}^{h} for some specified α. Like a standard Shewhart-style chart, if $M_{XY}^{h} > U_{mn}$ or $M_{XY}^{h} < L_{mn}$, then this signals to the operator that the process may have gone out of control (Chakraborti & van de Wiel, 2008).

To calculate ARL_0 and ARL_1, the authors used an approximation to the exact integral solution for average run length (Chakraborti & van de Wiel, 2008). This approach is an alternative to indirectly estimating by performing a large number of simulation iterations, counting the number of points in-between the out-of-control observations, and taking the mean of those counts to be the average run length. Because the integral, much like Page's integral, is not easily solved directly, the authors proposed and compared several techniques to both quickly and accurately estimate ARL's (Chakraborti & van de Wiel, 2008). The most effective technique used a Monte Carlo approximation where K iterations were taken (Chakraborti & van de Wiel, 2008). Let $\hat{p}_u(x_i)$ denote the estimated probability of a Type I error as estimated by the Lugannani-Rice formula (Jensen, 1995). The estimated average run length is given by:

$$\hat{ARL}_0 \approx \frac{1}{K}\sum_{i=1}^{K}\frac{1}{\hat{p}_U(x_i)}\,. \tag{31}$$

The authors compared the performance of their chart to that of a traditional $\bar{X}$-chart in the presence of normal, double exponential, and gamma distributions for shifts from target ranging from 0.5 – 3 (Chakraborti & van de Wiel, 2008). In the case of the normal distribution, it was found that the $\bar{X}$-chart was more effective in detecting smaller shifts than the proposed chart, but the differences waned as the shifts approached three (Chakraborti & van de Wiel, 2008). In the case of the heavy-tailed double exponential distribution, the proposed charting technique was found to be more effective in detecting smaller shifts than the $\bar{X}$-chart, but those differences also became scant as the shifts approached three (Chakraborti & van de Wiel, 2008). Finally, in the presence of the skewed gamma distribution, the proposed chart was again found to more quickly detect small shifts away from target than the $\bar{X}$-chart (Chakraborti & van de Wiel, 2008).

A Cumulative Summation Chart Based on the Mann-Whitney Test

Wang et al. (2017) proposed a CUSUM style chart based on the MW Test in a similar way to the technique proposed by Chakraborti & van de Wiel (2008). Besides the primary difference in the structure of the charting schemes, another distinction between the two Mann-Whitney charts is how the observations from future samples are collected. In Chakraborti's Shewhart-style MW chart, future samples of size n are iteratively collected to create a sequence of MW Test statistics (Chakraborti & van de Wiel, 2008). In the MW CUSUM proposed by Wang et al. (2017), the authors take future samples of size $n = 1$. As explained previously, waiting to take samples of $n > 1$ may be more inefficient than techniques where individual observations are allowable (Bakir & Reynolds, 1979). An additional difference between the two Mann-Whitney charts is that

Wang et al. (2017) standardize the MW Test statistic, which is advised in cases where the sample size is variable from sample to sample (Montgomery, 2013).

Let $MW_{t,l}$ denote the MW Test statistic under the proposed framework. The expectation and variance of the MW Test statistic are given by:

$$E\left[MW_{t,l}\right] = \frac{t(l-t)}{2} \tag{32}$$

$$Var\left[MW_{t,l}\right] = \frac{t(l-t)(l+1)}{12}. \tag{33}$$

Thus, the standardized MW Test statistic under this framework is given by:

$$SMW_{t,l} = \frac{MW_{t,l} - E\left[MW_{t,l}\right]}{\sqrt{Var\left[MW_{t,l}\right]}}. \tag{34}$$

The upper and lower CUSUM statistics are given by:

$$\begin{aligned} S_J^+(m,n) &= max\left[0, S_{j-1}^+(m,n) + SMW_{j,(m+n)} - k\right] \\ S_J^-(m,n) &= max\left[0, S_{j-1}^-(m,n) + SMW_{j,(m+n)} + k\right], \end{aligned} \tag{35}$$

where $S_0^+(m,n) = S_0^-(m,n) = 0$, and $k = 0.5$ (Wang et al., 2017). Note, the exact null distribution of the MW Test statistic is a function of the analyzed sample size (Conover, 1999). When the analyzed sample size is small, the standardized value cannot reasonably be assumed to be approximately distributed as a standard normal distribution. It is only in the case that $n \to \infty$ (the practical interpretation of which is debated, but $n > 30$ is a commonly used guideline) that such an approximation is reasonable (Montgomery, 2013). Wang et al. (2017) concluded that because the observed value to be used in the CUSUM framework would only approach the standard normal distribution as the number of future observations became large, and because the sample size for each $SMW_{t,l}$ is variable, a dynamic control limit, $h(m,n)$, should be used instead of the traditional static

control limit, h. This approach closely mirrors what was described in the section on calculating control limits for the EWMA chart.

Since $h(m,n)$ is variable, the approaches described in prior sections regarding estimating h could not be used. Instead, the authors performed a simulation to obtain a value of $h(m,n)$ given a specified ARL_0 and a given reference sample size m for each future sample $n = 1,2, \ldots 490$ (Wang et al., 2017). The authors chose $ARL_0 = 100, 200, 370,$ and 500, and $m = 10, 50$ (Wang et al., 2017). As the number of future samples becomes large, $h(m,n)$ approaches a static figure for each combination of ARL_0 and m (Wang et al., 2017).

To assess the out-of-control performance of their chart, the authors compared their technique to an existing nonparametric technique which utilized the MW Test statistic in an EWMA framework (Zhou, Zou, Zhang & Wang, 2007). The authors used simulated data from the standard normal, $\chi^2(4)$, $t(4)$, and lognormal distributions where shifts in the mean varied from $0.00 - 3.00$ in small increments (Wang et al., 2017). Additionally, the authors introduced the shift at various points in the sequence as the construction of $SMW_{t,l}$ would seem to make it more sensitive to small shifts if it contains a large amount of in-control observations and vice versa (Wang et al., 2017). As shown, for large shifts, both charts performed almost equally as well across all studied distributions (Wang et al., 2017). For smaller shifts, the proposed CUSUM performed slightly better across all studied distributions (Wang et al., 2017). Of note, the estimated ARL_1 values varied only minimally across the studied distributions (Wang et al., 2017). The result would be congruent with the MW Test's assumptions as there is no assumption regarding the underlying shape of the distribution (Conover, 1999).

Nonparametric Multiple Stream Processes Control Chart

As has been noted, the purpose of all control charting schemes is to quickly detect a true shift in some monitored process or processes (Montgomery, 2013). A variety of control charting techniques have been developed to meet the needs of organizations and practitioners. MSP charts have been developed in the case when an organization collects observations from multiple, separate data points called "streams" (Boyd, 1950; Mortell & Runger, 1995; Meneces et al., 2008; Montgomery, 2013). The MSP control charting schemes described in Chapter II all assumed the underlying processes being monitored followed normal distributions and the various proposed techniques and recommendations were based upon the normality assumption (Boyd, 1950; Mortell & Runger, 1995; Meneces et al., 2008). Chakraborti et al. (2001) noted that in practice, processes may not necessarily follow any known parametric distribution, let alone a normal distribution. It is therefore of value to use nonparametric control charting techniques when the assumption of normality is not known or cannot reasonably be assumed (Chakraborti et al., 2001). However, a review of the literature found no specific mention of nonparametric MSP control charting schemes. Thus, it is the purpose of this dissertation to address this apparent gap in the literature by constructing a new nonparametric MSP control chart using the Extended Median Test within a CUSUM framework.

CHAPTER III

METHODS

A Proposed Cumulative Summation Nonparametric Multiple Stream Process Control Chart

In this chapter, a new nonparametric control chart for monitoring a multiple stream process (MSP) is proposed. Chart development is based upon a modification of the Extended Median Test (EMT) statistic given by (24). The EMT statistic is to be used as the observation within a, two-sided cumulative summation (CUSUM) framework, as given by (12). As noted in Chapter I, this new chart is referred to as the "Nonparametric Extended Median Test Cumulative Summation (NEMT-CUSUM) Chart."

Research Questions

As stated in Chapter I, the research questions guiding this study are as follows:

Q1 What value of the parameter δ of the NEMT-CUSUM chart yields the commonly desired ARL_0 values of 200, 370, and 500 which correspond to Type I error rates of $\alpha = 0.005, 0.0027,$ and 0.002?

Q2 For a specified value of ARL_0, what is the statistical power yielded when a subset of the C monitored streams has shifted away from target, considering different magnitude shifts, number of monitored streams, and sample sizes of the streams?

Q3 How does the performance of the NEMT-CUSUM chart, in terms of ARL_1, compare to the performance of the Boyd, Mortell and Runger, and Meneces MSP charts in the presence of data coming from normal, light-tailed, heavy-tailed, and skewed distributions when half of the monitored streams shift from the target median of magnitudes ranging from 0 to 3 in increments of 0.25 have occurred?

The EMT was chosen to be the nonparametric test used for monitoring a MSP for one main reason. The testing procedure underlying the EMT is more straightforward than that of the Kruskal-Wallis Test as there are fewer steps and fewer calculations (Conover, 1999). However, the EMT can be further simplified to directly be an application of a χ^2 Goodness of Fit test, as is shown. Therefore, if the proposed charting scheme, using a slight modification to the EMT, were to be implemented in a practical setting, it would seem less likely than the Kruskal-Wallis Test to cause confusion. Dr. Deming's 13th point in his 14-point framework is to continually educate employees on the quality management program (Montgomery, 2013). Markedly, the employees ought to clearly understand the use of the control charting schemes being used to monitor product and service quality (Montgomery, 2013). Thus, it would be of benefit for control charts to be clear to understand as well as efficient and effective in detecting shifts away from target. The EMT can reasonably be justified to meet the former benefit, and the purpose of this study was to address the degree to which the second benefit is met.

The CUSUM framework was chosen as the charting technique to be used for the reasons described in Chapter II. The CUSUM technique is more effective than the classical Shewhart-style charts in detecting small shifts ($< 1.5\sigma$) away from target (Montgomery, 2013). Furthermore, the entire sequence of observations is taken into consideration in the CUSUM plotting statistics (as shown in (12)) rather than only the latest observation (Montgomery, 2013). Additionally, (12) was used rather than the common tabular method as shown in (13) as it allows the Type I error rate α to be fixed from sample to sample, which may or may not be the case when using the tabular method (Adams, Woodall & Lowry, 1992).

Before describing the methods used to address the research questions stated in Chapter I, it is of benefit to mention the practical assumptions used in this study. First, it is assumed that a reasonable estimate of the target value of the median, denoted $\tilde{\mu}_0$, is known either from technical specifications or historical estimates. Second, the EMT as described in Chapter II and the χ^2 Goodness of Fit test upon which it is based assumes the populations or streams in this case are independent. While other studies described situations in which the streams had some degree of correlation, it will be assumed the streams are independent here. Additionally, it is also assumed the streams are sampled as independent binomial random variables not only at each sampled time point, but also between all sampled time points (i.e., no autocorrelation). Third, while the number of groups or streams the EMT can analyze could be arbitrarily large but finite, for assessing ARL_1 performance of the competing charting schemes in this study, the number of streams was fixed at $C = 10$. Fourth, the EMT statistic, as described by (43), allows samples from each of the C groups to be of varying sizes. In this study for assessing ARL_1 performance, the sample size is equal and fixed across all samples. Finally, the total sample size was taken to be large enough such that the asymptotic properties of the EMT statistic could be leveraged.

Chart Construction

Distribution of Monitored Statistic

In this section, the proposed methodology for constructing the NEMT-CUSUM is given. Let $x_{i1t} \ldots x_{in_it}$ denote a random sample of size n_i from stream i at time t where $t = 1,2 \ldots$, and $i = 1,2, \ldots, C$. Let the random samples from each stream be mutually independent and assume that all of the streams have the same target median, $\tilde{\mu}_0$. At time

t, using the random samples taken, obtain the frequencies of observations from each sample taken which are either $\geq \tilde{\mu}_0$ or $< \tilde{\mu}_0$. Let O_{1t}, O_{2t} ... O_{ct} denote the frequencies of observations from each sampled stream which are either $\geq \tilde{\mu}_0$ or $< \tilde{\mu}_0$. Then, Table 4 can be constructed where the O_{it}'s denote frequencies $\geq \tilde{\mu}_0$.

Table 4

Table Used for Modified Extended Median Test

Frequency of Observations $\geq \tilde{\mu}_0$	O_{1t}	O_{2t}	...	O_{ct}
Sample sizes	n_{1t}	n_{2t}	...	n_{Ct}

If each stream has the same median, then it can be assumed that:

$$O_{it} \sim BIN(n_{it}, p_0 = 0.5), \forall\ (i,t) \tag{36}$$

which implies that a random observation taken from each stream is assumed to have the same probability of exceeding $\tilde{\mu}_0$, and:

$$\begin{aligned} E[O_{it}] &= n_{it}p_0 \\ Var[O_{it}] &= n_{it}p_0(1-p_0). \end{aligned} \tag{37}$$

Consequently, in order for $n_{it}p_0 = n_{it}(0.5) \geq 5$, as is assumed in order to use the χ^2 approximation, then $n_{it} \geq 10$ (Conover, 1999; Agresti, 2007). Now, using all relevant information, it is apparent that the modified EMT is a direct application of a χ^2 Goodness of Fit test. Assuming each $n_{it}(0.5) \geq 5$, then each O_{it} can be standardized to become independent, approximate standard random variables. That is,

$$\frac{O_{it} - n_{it}p_0}{\sqrt{n_{it}p_0(1-p_0)}} \dot{\sim} N(0,1). \tag{38}$$

Agresti (2007) noted that the approximation becomes better as $n_{it} \to \infty$. If the sampled streams are mutually independent, the covariance between them is well known to be zero. Additionally, it is also well known that the variance of the sum of independent random variables is the sum of each respective random variable's variance term.

It is important to note a relationship between sums independent normal random variables. Let $X_1 \dots X_N$ denote independent normal random variables with means $\mu_1 \dots \mu_N$ and standard deviations $\sigma_1 \dots \sigma_N$ and let $Z = \sum_{i=1}^{N} X_i$. Using the moment generating function of the normal distribution, the moment generating function of Z is:

$$
\begin{aligned}
&M_Z(t) = E[\exp(Zt)] \\
&= E\left[\exp\left(\left(\sum_{i=1}^{N} X_i\right)t\right)\right] \\
&= E\left[\exp\left(tX_1 + tX_2 + \cdots + t_{X_N}\right)\right] \\
&= E[\exp(tX_1)]E[\exp(tX_2)] \dots E[\exp(tX_N)] \\
&= (\exp(\mu_1 t + \sigma_1^2 t^2 0.5)) \dots (\exp(\mu_N t + \sigma_N^2 t^2 0.5)) \\
&= \left(\exp\left(t\sum_{i=1}^{N} \mu_i + 0.5t^2 \sum_{i=1}^{N} \sigma_i^2\right)\right) \\
&\Rightarrow Z \sim N\left(\sum_{i=1}^{N} \mu_i\,, \sum_{i=1}^{N} \sigma_i^2\right).
\end{aligned}
\tag{39}
$$

For a sample taken at time t, define EMT_t to be the sum of the standardized O_{it}'s. Then, as a result of (38) and (39):

$$
EMT_t = \sum_{i=1}^{C}\left(\frac{O_{it} - n_{it}p_0}{\sqrt{n_{it}p_0(1-p_0)}}\right) \dot{\sim} N(\mu = 0, \sigma^2 = C). \tag{40}
$$

Thus, for the sample taken at time t, one value of EMT_t will be obtained. As the distribution given in (40) is the null distribution, small deviations of EMT_t away from 0 in either the positive or negative direction implies that none of the streams may have shifted away from $\tilde{\mu}_0$. Conversely, large deviations of EMT_t away from 0 implies that at least one of the streams may have a different median than $\tilde{\mu}_0$. EMT_t will serve as the statistic monitored by the CUSUM framework.

Distribution of Cumulative Summation Statistic

For each sample taken at time t, one EMT_t will be calculated. Then, the CUSUM statistic to be used for monitoring the MSP will have the form given by (12). Let S_t denote the CUSUM statistic at time $= 1,2, \ldots$. Then, let its value be defined as:

$$S_t = \sum_{j=1}^{t} EMT_j \, . \tag{41}$$

Since EMT_t and subsequently S_t can vary in both the positive and negative direction, each S_t will be compared to UCL_t and LCL_t where:

$$\begin{aligned} UCL_t &= E[S_t] + \delta\sqrt{Var[S_t]} \\ LCL_t &= E[S_t] - \delta\sqrt{Var[S_t]} \, , \end{aligned} \tag{42}$$

and where UCL_t and LCL_t will vary for a specified value of α for each time t. If $S_t > UCL_t$ or $S_t < LCL_t$, then it is signaled to the operator that a shift away from target may have occurred in one or multiple of the streams being monitored. In order to calculate these limits, the distribution of S_t must first be derived. From the computation of S_t, it is clear that:

$$S_t = S_{t-1} + EMT_t. \tag{43}$$

The result in (43) implies that S_t is dependent upon S_{t-1}. However, there are two different approaches to addressing the dependency. The first approach conditions S_t upon S_{t-1} and thus is conceptualized much like classical regression with fixed predictors. The second approach conceptualizes (43) as a random walk process, which is used in time series applications (Wei, 2007). Of note, a random walk process is a special case of a first order autoregressive process (AR-1) (Wei, 2007). With respect to the former conceptualization, since S_{t-1} is a known quantity, as in regression, the randomness inherent in S_t comes from EMT_t. Therefore, like the general linear model:

$$S_t | S_{t-1} \dot{\sim} N(S_{t-1}, C). \tag{44}$$

Using the result given by (44), UCL_t and LCL_t can be obtained by:

$$\begin{aligned} UCL_t &= S_{t-1} + \delta\sqrt{C} \\ LCL_t &= S_{t-1} - \delta\sqrt{C}\,, \end{aligned} \tag{45}$$

where $t = 1$, $S_0 = 0$. Note, UCL_t and LCL_t are indexed by time, which implies that the control limits are dynamic, and not static as is the case with the tabular CUSUM method (Montgomery, 2013). This property allows α to be fixed from sample to sample. This, in conjunction with the asymptotic property of the EMT_t's, allows relatively straightforward computation of ARL_0 and ARL_1.

Now, with respect to the conceptualization of (43) as a random walk process, and as aforementioned, a random walk is a special case of an AR-1 process (Wei, 2007). Let

$\{Z_t\}$ denote a random walk series with white noise process $a_t \sim N(0, \sigma^2)$ where all a_t are independent for all $t = 1,2, \ldots$. Then, the random walk process is defined by:

$$Z_t = Z_{t-1} + a_t. \tag{46}$$

The expectation of the process described by (46) is:

$$\begin{aligned} E[Z_t] &= E\left[\sum_{j=1}^{t} a_j\right] \\ &= \sum_{j=1}^{t} E[a_j] \\ &= t(0) = 0, \end{aligned} \tag{47}$$

and its variance is defined in a similar way by:

$$\begin{aligned} Var[Z_t] &= Var\left[\sum_{j=1}^{t} a_j\right] \\ &= \sum_{j=1}^{t} Var[a_j] \\ &= t\sigma^2. \end{aligned} \tag{48}$$

Of note, the result in (48) shows that a random walk process is not stationary since its variance depends on t. Now, using (47) and (48), along with the knowledge that $Var[EMT_j] = C$, the results in (47) and (48) can be input into (42) such that:

$$\begin{aligned} UCL_t^* &= \delta\sqrt{tC} \\ LCL_t^* &= -\delta\sqrt{tC}. \end{aligned} \tag{49}$$

Like what was computed in (45), (49) shows that UCL_t^* and LCL_t^* will change with time when treating S_t as a random walk process. In this case, they will increase in their respective positive and negative directions with each step by magnitude $\sqrt{t}$. This property of having dynamic limits is useful since α can be fixed across all time points, as is the case with the conditional regression conceptualization of S_t.

While either conceptualization of S_t could be used to create and use the NEMT-CUSUM control chart, this work utilized the conditional regression conceptualization. There are two main reasons for this. First, even though the control limits given in (45) change with the conditional mean, S_{t-1}, the magnitude of the difference between UCL_t and LCL_t is fixed across all observed time points as:

$$\begin{aligned} UCL_t - LCL_t &= S_{t-1} + \delta\sqrt{C} - S_{t-1} + \delta\sqrt{C} \\ &= 2\delta\sqrt{C}\,. \end{aligned} \tag{50}$$

The difference between the control limits given in (49) will increase with time as $UCL_t^* - LCL_t^* = 2\delta\sqrt{tC}$. When plotting S_t, having a fixed width between the limits makes the chart easier to visually inspect, especially for large t. The second reason for using the conditional regression conceptualization as opposed to the marginal random walk conceptualization is related to the calculation of ARL_0 and the interpretation of α. In all of the control charts described in Chapter II, and as is generally the case in control charting techniques, ARL_0 is defined as the expected number of samples taken before a false alarm signals when the process is in-control. As an example, assume a classical CUSUM chart is set up such that the control limit h were set such that $ARL_0 \approx 370$. If 10,000 CUSUM series were simulated, each of them would signal a false alarm at some

time point, but these would vary. One may be 90, one may be 1000, but their sample mean would be approximately 370. However, in the random walk conceptualization of S_t, the same approach could not be taken since the distribution depends on t. Notice, this is also true for the EWMA chart when the sample number is small and the steady-state control limits cannot be used. However, the control limits for the EWMA approach an asymptotic value as shown in (9) and (10). The control limits in (49) will not approach an asymptote as $t \to \infty$.

Thus, in order to have a nominal ARL_0 and α as thought of in the classical sense, practical implementation of the random walk chart would have to have t fixed at some upper value and then the chart would need to be reset at $t = 1$. This is due to α. The Type I error rate α is the probability of a false alarm or in traditional hypothesis testing, it is the probability of rejecting the null hypothesis when the null hypothesis is indeed true. As an example, if a one-population t-test were performed 1,000 times on the same population, and if the null hypothesis were true, it would be expected that 1000α of those tests would show statistical significance incorrectly. The same result would be yielded for the random walk S_t, but only if t was fixed. Thus, one of the attractive features of the CUSUM framework, namely the consideration of the whole series of observations, becomes somewhat limited. Certainly, the conditional regression S_t is also nonstationary because its mean varies, but the problem described here is not exacerbated in the same way it is as in the random walk conceptualization and this is shown through the simulation study results presented in Chapter IV. For these two reasons, the conditional regression S_t was used in this work.

Assessing the In-Control Performance of the Proposed Charting Technique

The first research question guiding this study is to determine which values of δ should be used to obtain common ARL_0 values of 200, 370, and 500 which correspond to Type I error rates of $\alpha = 0.005, 0.0027,$ and 0.002. This question can be reframed as one of conditional probability.

Let $\tilde{\mu}_1, \tilde{\mu}_2, \ldots, \tilde{\mu}_C$ denote the true medians for each of the monitored streams, and also let $p_1, p_2, \ldots, p_c$ denote the true probability parameters of each stream's binomial distribution. If all streams have not shifted away from the specified, common target median, $\tilde{\mu}_0$, then it is implied that $\tilde{\mu}_0 = \tilde{\mu}_1 = \cdots = \tilde{\mu}_C$ and $p_0 = p_1 = \cdots = p_C$. Then, for a given value of α and given that all C streams have not shifted from their common target median, $\tilde{\mu}_0$, it is desired to determine what values of UCL_t and LCL_t ought to be used such that the probability of S_t exceeding either control limit thereby signaling a false alarm is equal to a specified α. Mathematically, this can be written as:

$$P[(S_t > UCL_t) \cup (S_t < LCL_t) | \tilde{\mu}_0 = \tilde{\mu}_1 = \tilde{\mu}_2 = \cdots = \tilde{\mu}_C] = \alpha. \tag{51}$$

However, since $S_t > UCL_t$ and $S_t < LCL_t$ are disjoint events, and as the normal distribution is symmetric about its mean, it would be sufficient to examine:

$$P[S_t < LCL_t | \tilde{\mu}_0 = \tilde{\mu}_1 = \tilde{\mu}_2 = \cdots = \tilde{\mu}_C] = \frac{\alpha}{2}. \tag{52}$$

If the inverse cumulative distribution function of the standard normal distribution is denoted Φ^{-1}, then:

$$\begin{aligned} \frac{LCL_t - S_{t-1}}{\sqrt{c}} &= \Phi^{-1}\left(\frac{\alpha}{2}\right) \\ \frac{S_{t-1} - \delta\sqrt{c} - S_{t-1}}{\sqrt{c}} &= \Phi^{-1}\left(\frac{\alpha}{2}\right) \\ -\delta &= \Phi^{-1}\left(\frac{\alpha}{2}\right) \\ \Rightarrow \delta &= \Phi^{-1}\left(1 - \frac{\alpha}{2}\right). \end{aligned} \tag{53}$$

While UCL_t and LCL_t can be found for some α, C, and t without much strain, example tabled values of δ_t, UCL_t and LCL_t are also given in Chapter IV for $\alpha = 0.005, 0.0027, 0.002$, $C = 1,2,\ldots,10$ and $t = 1,2,\ldots,20$.

Assessing the Out-of-Control Performance of the Proposed Charting Technique

After the control limits required to achieve a specified value of ARL_0 have been determined, the second research question, which examined the out-of-control performance of the NEMT-CUSUM can be addressed. If α denotes the probability of making a Type I error, then let β denote the probability of making a Type II error. In terms of control charts, a Type II error occurs when a shift away from target has taken place, but the chart does not signal. As was the case with the first research question, the probability of making a Type II error can be written as a conditional probability. When the MSP being monitored is in-control for all streams, it is implied $\tilde{\mu}_0 = \tilde{\mu}_1 = \cdots = \tilde{\mu}_C$. This further implies that for all O_{it}'s, the probability parameter in their binomial distributions are all equal to $p_0 = 0.5$. If one or more of the medians of the monitored streams have shifted away from $\tilde{\mu}_0$ to some value $\tilde{\mu}_A$, it is implied that at least one of the streams' probability parameter has shifted away from $p_0 = 0.5$ to some other value p_A. Let p_0 and p_A be related by:

$$p_A = p_0 + \gamma, \tag{54}$$

where:

$$-p_0 < \gamma < 1 - p_0. \tag{55}$$

To note, the interpretation of γ and p_A differs somewhat from the classical interpretation of a shift away from target. If Table 4 is used as the framework for the proposed charting scheme, where the O_{it}'s are the frequency of observations being equal to or exceeding $\tilde{\mu}_0$, then p_0 is interpreted as the probability of an observation being equal to or exceeding $\tilde{\mu}_0$ under the in-control or null assumptions. However, if p_0 shifts to p_A for some number of streams, this implies that $\tilde{\mu}_0$ may not be the 50th percentile for those number of streams, but rather the $100(1 - p_A)$th percentile. For example, if $p_A = 0.50 + 0.25 = 0.75$ for some number of streams, then it is implied that the probability of an observation meeting or exceeding $\tilde{\mu}_0$ is 0.75 for those number of streams. If 0.75 of the observations should fall at or in excess of $\tilde{\mu}_0$, then $1 - 0.75 = 0.25$ of the observations would be less than $\tilde{\mu}_0$. By definition, $\tilde{\mu}_0$ would be the 25th percentile for those shifted streams and not the 50th percentile under the in-control assumptions.

Let C_0 denote the number of streams for which a shift has not occurred and let C_A denote the number of streams for which a shift has occurred. Note, while shifts of varying magnitudes could occur in all streams, it is assumed here that the shift occurring in the C_A streams is of the same magnitude. At time t, the shifted statistic, denoted EMT_t^*, would then have the form:

$$EMT_t^* = \sum_{i=1}^{C_0} \frac{O_{it} - n_i p_0}{\sqrt{n_{it} p_0 (1 - p_0)}} + \sum_{i=C_0+1}^{C} \frac{O_{it} - n_{it} p_A}{\sqrt{n_{it} p_A (1 - p_A)}}. \tag{56}$$

Then, at time t, β is the probability of S_t not exceeding either control limit given that C_A number of streams' probability parameters have shifted away from p_0 to p_A. This can be written in mathematical notation by:

$$P\left[LCL_t \leq S_t \leq UCL_t \middle| \tilde{\mu}_0 = \tilde{\mu}_1 = \cdots = \tilde{\mu}_{C_0}, \tilde{\mu}_A = \tilde{\mu}_{C_0+1} = \cdots = \tilde{\mu}_C\right] = \beta, \tag{57}$$

or equivalently using the complement:

$$\begin{aligned} P\left[(S_t > UCL_t) \cup (S_t < LCL_t) \middle| \tilde{\mu}_0 = \tilde{\mu}_1 = \cdots = \tilde{\mu}_{C_0}, \tilde{\mu}_A = \tilde{\mu}_{C_0+1} = \cdots = \tilde{\mu}_C\right] \\ = 1 - \beta. \end{aligned} \tag{58}$$

(58) can be conceptualized as the probability of the chart signaling when a shift has taken place, and is sometimes referred to as "statistical power." Since the events are disjoint, (58) can be rewritten as:

$$\begin{aligned} &P\left[S_t > UCL_t \middle| \tilde{\mu}_0 = \tilde{\mu}_1 = \cdots = \tilde{\mu}_{C_0}, \tilde{\mu}_A = \tilde{\mu}_{C_0+1} = \cdots = \tilde{\mu}_C\right] \\ &+ P\left[S_t < LCL_t \middle| \tilde{\mu}_0 = \tilde{\mu}_1 = \cdots = \tilde{\mu}_{C_0}, \tilde{\mu}_A = \tilde{\mu}_{C_0+1} = \cdots = \tilde{\mu}_C\right] = 1 - \beta. \end{aligned} \tag{59}$$

In order to empirically determine β, the distribution of S_t must be derived when a shift has taken place. Let this distribution be referred to as the "alternative distribution." Using (56), the alternative distribution can be written as a function of the null distribution. Let the sums of the standardized in-control streams and out-of-control streams be denoted as the quantities Q_t and H_t, respectively. That is:

$$\begin{aligned} Q_t &= \sum_{i=1}^{C_0} \frac{O_{it} - n_{it}p_0}{\sqrt{n_{it}p_0(1-p_0)}} \\ H_t &= \sum_{i=C_0+1}^{C} \frac{O_{it} - n_{it}p_A}{\sqrt{n_{it}p_A(1-p_A)}} \end{aligned} \tag{60}$$

H_t can be rewritten as:

$$
\begin{aligned}
H_t &= \sum_{i=C_0+1}^{C} \frac{O_{it} - n_{it}p_A}{\sqrt{n_{it}p_A(1-p_A)}} \\
&= \sum_{i=C_0+1}^{C} \frac{O_{it} - n_{it}(p_0+\gamma)}{\sqrt{n_{it}\big((p_0+\gamma)(1-p_0-\gamma)\big)}} \\
&= \sum_{i=C_0+1}^{C} \frac{O_{it} - n_{it}p_0 - n_i\gamma}{\sqrt{(n_{it}p_0 + n_{it}\gamma)\big((1-p_0)-\gamma\big)}} \\
&= \sum_{i=C_0+1}^{C} \frac{O_{it} - n_{it}p_0 - n_i\gamma}{\sqrt{n_{it}p_0(1-p_0) - n_{it}p_0\gamma + n_{it}(1-p_0)\gamma - n_{it}\gamma^2}} \\
&= \sum_{i=C_0+1}^{C} \frac{O_{it} - n_{it}p_0 - n_{it}\gamma}{\sqrt{n_{it}p_0(1-p_0)\left[1 - \frac{\gamma}{1-p_0} + \frac{\gamma}{p_0} - \frac{\gamma^2}{p_0(1-p_0)}\right]}} \\
&= \frac{1}{\sqrt{1 - \frac{\gamma}{1-p_0} + \frac{\gamma}{p_0} - \frac{\gamma^2}{p_0(1-p_0)}}} \sum_{i=C_0+1}^{C} \frac{O_{it} - n_{it}p_0}{\sqrt{n_{it}p_0(1-p_0)}} \\
&\quad - \sum_{i=C_0+1}^{C} \frac{n_{it}\gamma}{\sqrt{n_{it}p_0(1-p_0)\left[1 - \frac{\gamma}{1-p_0} + \frac{\gamma}{p_0} - \frac{\gamma^2}{p_0(1-p_0)}\right]}}.
\end{aligned}
\tag{61}
$$

Now, defining the sum of the sample sizes of the out-of-control streams as n_{C_A}, let:

$$\theta = \frac{1}{\sqrt{1 - \frac{\gamma}{1-p_0} + \frac{\gamma}{p_0} - \frac{\gamma^2}{p_0(1-p_0)}}}$$

$$\varepsilon = \sum_{i=C_0+1}^{C} \frac{n_{it}\gamma}{\sqrt{n_{it}p_0(1-p_0)\left[1 - \frac{\gamma}{1-p_0} + \frac{\gamma}{p_0} - \frac{\gamma^2}{p_0(1-p_0)}\right]}} \tag{62}$$

$$= \frac{n_{C_A}\gamma}{\sqrt{n_{C_A}p_0(1-p_0)\left[1 - \frac{\gamma}{1-p_0} + \frac{\gamma}{p_0} - \frac{\gamma^2}{p_0(1-p_0)}\right]}}.$$

Combining (61) and (62), H_t is now function of the null distribution being scaled and shifted by some constants as:

$$H_t = \theta \sum_{i=C_0+1}^{C} \frac{O_{it} - n_{it}p_0}{\sqrt{n_{it}p_0(1-p_0)}} - \varepsilon \dot{\sim} N(\mu = -\varepsilon, \sigma^2 = C_A\theta) \tag{63}$$

Since under the null distribution $Q_t \dot{\sim} N(0, C_0)$, and since it is still assumed the monitored streams, regardless of their in-control or out-of-control status, are independent, then:

$$EMT_t^* = Q_t + H_t \dot{\sim} N(-\varepsilon, C_0 + C_A\theta). \tag{64}$$

Let S_t^* denote the shifted plotting statistic. Then, as in (44),

$$S_t^* = S_{t-1}^* + EMT_t^*. \tag{65}$$

Therefore, using the same conditional distribution structure as (44),

$$S_t^* | S_{t-1}^* \dot{\sim} N(S_{t-1}^* - \varepsilon, C_0 + C_A\theta). \tag{66}$$

To calculate the exact probability given by (59), UCL_t and LCL_t must first be calculated under the in-control assumptions, as given in the previous section. Then, using these control limits and the result given by (66), statistical power can be directly calculated for

a given α, γ, n_{C_A}, C_A, and C_0. In control charting literature, it is common to present graphical representations of statistical power for a given control charting technique, which are referred to as "operating characteristic (OC) curves," (Montgomery, 2013). Here, the y-axis denotes the complement of power, β, the x-axis denotes the magnitude of the shift, γ in this instance, and multiple curves are plotted for various sample sizes (Montgomery, 2013). In Chapter IV, power curves are presented for $C = 1, 5, 10, 15$, and 20, $C_A = C - 1$ (with the exception of $C = 1$, where $C_A = 1$), $n_{C_A} = 10(C_A), 20(C_A), 30(C_A), 50(C_A)$, and $100(C_A)$, $\gamma \in (0, 0.50)$, and $\alpha = 0.005, 0.0027$, and 0.002.

Comparing the Performance of the Proposed Charting Scheme to Other Multiple Stream Process Control Charts

The third research question posed in Chapter I was to compare the performance of the NEMT-CUSUM to that of the Boyd, Mortell and Runger, and Meneces MSP Charting Schemes. The performance was assessed when monitoring $C = 10$ streams in the presence of normal and non-normal data when $C_A = 5$ streams shift away from target of magnitudes ranging from $0 - 3$ in increments of 0.25. The comparison was made in terms of ARL_1. A Monte Carlo computer simulation was performed using the statistical software package R to address this research question (R Core Team, 2018).

Random samples of size $n = 10$ were generated from four different distributions for each of the $C = 10$ monitored streams. The in-control forms of these distributions are: the normal distribution with a mean of 1 and a standard deviation of 1, $N(\mu = 1, \sigma = 1)$, the light-tailed uniform distribution on the [0,1] interval, $UNIF(0,1)$, the heavy-tailed Laplacian distribution with scale parameter 1 and location parameter 1, $Laplace(\theta =$

$1, \eta = 1$), and the positively-skewed exponential distribution with scale parameter of 1, $EXP(\theta = 1)$. The normal distribution's in-control mean is $\mu = 1$. The uniform distribution's in-control mean is $\mu = 0.5$. The Laplacian distribution's in-control mean is $\mu = \eta = 1$. The exponential distribution's in-control mean is $\mu = \theta = 1$. To assess the out-of-control performance, the means of these distributions were shifted by magnitudes ranging from 0 – 3 in increments of 0.25. For example, the normal distribution's mean was shifted from 0.25 – 3. Table 5 contains all combinations of charting schemes and magnitudes of shift for the normal distribution. This table was replicated for all distributions under consideration. Note, ARL_{1ijk} denotes the estimated ARL_1 value for the kth magnitude of shift for the jth distribution being monitored by the ith charting scheme.

Table 5

Estimated Average Run Lengths for Competing Control Charting Schemes

Distribution and Target Value	$N(1,1), \mu_0 = 1$			
	Charting Scheme			
Magnitude of Shift	NEMT-CUSUM	Boyd's GCC	Mortell & Runger's R_t Chart	Meneces Chart for Every Stream
$0.25\mu_0$	ARL_{11111}	ARL_{12111}	ARL_{13111}	ARL_{14111}
$0.50\mu_0$	ARL_{11121}	ARL_{12121}	ARL_{13121}	ARL_{14121}
$0.75\mu_0$	ARL_{11131}	ARL_{12131}	ARL_{13131}	ARL_{14131}
$1\mu_0$	ARL_{11141}	ARL_{12141}	ARL_{13141}	ARL_{14141}
$1.25\mu_0$	ARL_{11151}	ARL_{12151}	ARL_{13151}	ARL_{14151}
$1.50\mu_0$	ARL_{11161}	ARL_{12161}	ARL_{13161}	ARL_{14161}
$1.75\mu_0$	ARL_{11171}	ARL_{12171}	ARL_{13171}	ARL_{14171}
$2.00\mu_0$	ARL_{11181}	ARL_{12181}	ARL_{13181}	ARL_{14181}
$2.25\mu_0$	ARL_{11191}	ARL_{12191}	ARL_{13191}	ARL_{14191}
$2.50\mu_0$	$ARL_{111(10)1}$	$ARL_{121(10)1}$	$ARL_{131(10)1}$	$ARL_{141(10)1}$
$2.75\mu_0$	$ARL_{111(11)1}$	$ARL_{121(11)1}$	$ARL_{131(11)1}$	$ARL_{141(11)1}$
$3.00\mu_0$	$ARL_{111(12)1}$	$ARL_{121(12)1}$	$ARL_{131(12)1}$	$ARL_{141(12)1}$

To determine the ARL_1 for the NEMT-CUSUM, random samples of size $n = 10$ were generated for each of the C_A streams from each of the comparison distributions assuming $\tilde{\mu}_0$ is equal to the in-control mean. The C_A streams' samples were generated from a shifted distribution whereas the other $10 - C_A$ streams' samples were generated from the in-control distribution. Then, the procedure described to calculated EMT_t, S_t, and UCL_t and LCL_t was performed for $t = 1,2, \ldots, 10000$. Each S_t was iteratively

compared to UCL_t and LCL_t. When $S_t > UCL_t$ or $S_t < LCL_t$, t was saved in a separate vector. Then, the mean difference of all recorded t's was taken to be an estimate of ARL_1 for the given distribution, number of out-of-control streams, and magnitude of shift. This procedure was performed 10000 times and the mean of the estimated ARL_1 values was taken to be the true ARL_1 estimate. This process was repeated for all considered shifts away from target.

To determine the ARL_1 for Boyd's GCC, $m = 25$ preliminary samples of size $n = 10$ from the in-control distribution were generated for each of the $C = 10$ streams. These preliminary samples were taken from the in-control distributions mentioned previously to construct the in-control UCL and LCL, as described by (14). After the control limits were calculated, samples of size $n = 10$ from each of the four distributions for a specified shift away from target were generated for each of the C_A streams whereas the other $C - C_A$ streams had data generated from the in-control distribution. The means of each sample were stored in a matrix of dimension 100000×10. Each row of the matrix was considered a sample. The minimum and maximum of each row was iteratively compared to the control limits. When the minimum or maximum of a row exceeded either control limit, the row number was recorded in a separate vector. The mean of the difference between the elements of the separate vector was taken to be the estimate for ARL_1 for a given distribution and a given shift away from target. This process was repeated for all considered shifts away from target.

To determine ARL_1 for the Mortell and Runger MSP Shewhart-style chart to monitor shifts in a single stream with respect to the others, the same technique for data generation as was used for Boyd's GCC was employed. Since R_t, as described by (16),

does not have a simple distributional form, control limits were determined by simulation. A sample of size 100000 was generated for each of the four in-control distributions, and the values associated with the 0.00135^{th} and 0.99865^{th} quantiles were taken to be the LCL and UCL, respectively. The control limits derived from these quantiles are traditionally associated with $ARL_0 = 370$ for Shewhart-style charts (Montgomery, 2013).

After the control limits were calculated, samples of size $n = 10$ were generated for each stream, with C_A streams having data from the shifted distribution and $10 - C_A$ streams having data from the in-control distribution. The observations were aggregated and R_t was calculated. This was performed 100000 times and the R_t's were stored in a 100000×1 dimensional vector. Then, the R_t's were iteratively compared to the control limits. When a value of R_t exceeded either control limit, the row number within the vector was recorded. The mean of the differences between the elements within the vector was taken to be an estimate of ARL_1 for a given distribution and a given shift away from target. Again, this process was repeated for all considered shifts away from target.

To estimate ARL_1 for the Meneces MSP charting scheme, the in-control control limits first had to be computed. Using Table 1, the mean of the proposed values of L for $s = 2$ and $s = 5$ was taken to be the half-width ($L = 3.33$). $m = 25$ preliminary samples of size $n = 10$ were taken from each of the $C = 10$ streams from the in-control distribution. The overall mean of the preliminary samples was the used as the estimate for the center line. The overall standard deviation of the preliminary samples was taken to be the estimate of the MSP's standard deviation to be used in computing the control limits. Then, the UCL and LCL were computed as in (1).

After constructing the control limits, samples of size $n = 10$ were taken for each stream, with C_A samples being generated from the shifted distribution and $10 - C_A$ samples being generated from the in-control distribution. The sample means were computed for each stream. 100000 means were generated for each distribution for each stream. These means were stored in a matrix of dimension 100000×10, where each row denotes a sample number and each column denotes a monitored stream. The rows were iteratively compared to the control limits. If a row contained a mean from one of the streams which exceeded either control limit, the row number was saved in a separate vector. The mean of the differences of the elements in this separate vector was taken to be the estimate of ARL_1 for a given number of streams out-of-control, C_A, and a given shift away from target. The process was repeated for all considered shifts away from target.

In Chapter IV, tabled values for δ_t, UCL_t, and LCL_t, graphs of the power curves, and the results of the simulations described here are given both tabularly and graphically. In Chapter V, conclusions, recommendations for use of the NEMT-CUSUM chart, study limitations, and future studies are also given.

CHAPTER IV

RESULTS

In this chapter, results for the research questions proposed in Chapter I are presented. First, tabled values of δ, UCL_t and LCL_t are provided for various values of α and C, as specified in Chapter III. Second, OC curves are given for $\gamma \in (0, 0.50)$, and several values of α, C, C_A, and n_{C_A}, as also stated in Chapter III. Finally, ARL_1 comparisons are made between the NEMT-CUSUM, Boyd's GCC, Mortell and Runger's R_t chart, and the Meneces MSP charting scheme as given in Chapter III and as shown in Table 5.

Specifying Control Limits for Proposed Control Charting Scheme

The aim of the first research question is to find values of δ, and consequently UCL_t and LCL_t, such that α can be fixed at a specified value. Values of α are typically chosen to be 0.005, 0.0027, or 0.002 which generally correspond to ARL_0 values of 200, 370, and 500, respectively. As discussed in Chapter III, the control limits of the NEMT-CUSUM are dynamic such that α can be fixed across all time points. This implies that for practical implementation, UCL_t and LCL_t must be specified at each time point in order for α to remain fixed. Using (48) will yield these values for a given value of α at time t for a given number of monitored streams, C, and an observed S_{t-1}. From (53), it was shown that:

$$\delta = \Phi^{-1}\left(1 - \frac{\alpha}{2}\right), \tag{67}$$

and therefore the UCL_t and LCL_t can be calculated by:

$$\begin{aligned} UCL_t &= S_{t-1} + \left(\Phi^{-1}\left(1 - \frac{\alpha}{2}\right)\right)\sqrt{C} \\ LCL_t &= S_{t-1} - \left(\Phi^{-1}\left(1 - \frac{\alpha}{2}\right)\right)\sqrt{C}, \end{aligned} \tag{68}$$

where Φ^{-1} denotes the inverse cumulative distribution function of the standard normal distribution, and $S_0 = 0$. It is clear that calculation of these control limits depends on the value of S_{t-1} (i.e., the limits are dynamic and specific to the observed data). Because of this, traditional tabled values of the control limits cannot be calculated for a general case. However, the computation of the limits for an example data set is shown to illustrate how this could be done in practice.

The subsequent tables give the values of δ, UCL_t and LCL_t, for $t = 1,2,\ldots,20$, and $C = 1,2,\ldots,10$. Table 6 is for $\alpha = 0.005$, Table 7 is for $\alpha = 0.0027$, and Table 8 is for $\alpha = 0.002$. Note, the example data was generated from the standard normal distribution for all considered streams. The subsequent tables give the values of UCL_t, LCL_t, and δ for $t = 1,2,\ldots,20$, and $C = 1,2,\ldots,10$. Table 6 contains the EMT_t statistics calculated for each C considered. Note, the underlying data used to generate the EMT_t statistics was randomly generated from the standard normal distribution (i.e., $\tilde{\mu}_0 = 0$) where the sample size from each stream was taken to be $n = 10$. The columns of Table 6 denote the EMT_t statistic for each considered C and the rows denote the time, t. Table 7 contains calculated control limits for $\alpha = 0.005$, Table 8 is for $\alpha = 0.0027$, and Table 9 is for $\alpha = 0.002$.

Table 6

Extended Median Test Statistics Used to Generate Control Limits

	Number of Streams *C*									
t	1	2	3	4	5	6	7	8	9	10
1	1.26	1.26	0.63	0.63	0.00	0.63	-0.63	-0.63	1.26	2.53
2	0.63	0.63	0.00	0.00	1.90	2.53	0.63	-0.63	-0.63	-1.90
3	-0.63	-0.63	0.00	1.26	0.63	0.00	1.26	2.53	2.53	3.79
4	-1.26	0.00	0.63	1.26	0.63	-0.63	-0.63	0.00	0.00	-0.63
5	0.00	1.26	1.26	3.79	2.53	2.53	3.79	3.79	4.43	3.16
6	-0.63	0.00	1.90	2.53	1.26	0.63	0.63	1.90	3.79	6.32
7	-0.63	0.00	-1.26	-2.53	-1.90	-0.63	0.63	1.26	1.90	0.00
8	-0.63	-0.63	-1.26	-0.63	0.00	1.26	0.63	1.26	0.63	0.63
9	-0.63	-1.90	-1.90	-1.26	-1.26	-1.90	-2.53	-4.43	-5.06	-5.69
10	-0.63	-1.26	-3.16	-3.79	-3.16	-3.16	-3.16	-2.53	-1.90	0.00
11	-0.63	-2.53	-1.90	-1.26	-1.26	-0.63	-1.90	-1.90	-1.90	-0.63
12	-0.63	-1.26	-1.26	-1.26	-1.26	-1.26	-1.90	-3.16	-3.16	-3.79
13	0.00	1.26	1.90	1.90	1.90	2.53	3.16	3.79	3.79	3.79
14	1.26	3.79	3.79	3.79	3.79	5.06	6.32	6.96	6.32	7.59
15	1.26	0.00	0.63	1.90	1.90	2.53	1.26	1.26	1.26	1.26
16	0.00	-1.26	-0.63	-0.63	-0.63	-0.63	-0.63	-0.63	-0.63	-1.26
17	0.00	0.63	0.63	0.00	-0.63	-1.90	-2.53	-3.16	-1.90	-1.90
18	1.26	2.53	3.16	3.79	2.53	3.79	5.06	4.43	4.43	5.06
19	0.63	0.00	-1.26	-1.26	-2.53	-3.16	-2.53	-2.53	-1.90	-3.16
20	-0.63	-3.16	-3.16	-1.90	-1.26	-1.90	-1.90	-1.26	-2.53	-3.16

Table 7

Calculated Control Limits for Type I Error Rate of 0.005

	Number of Streams C									
	$\delta = 2.8070$									
t	1	2	3	4	5	6	7	8	9	10
1	-2.8, 2.8	-4.0, 4.0	-4.9, 4.9	-5.6, 5.6	-6.3, 6.3	-6.9, 6.9	-7.4, 7.4	-7.9, 7.9	-8.4, 8.4	-8.9, 8.9
2	-1.5, 4.1	-1.4, 6.5	-1.1, 8.7	-1.2, 10.0	-2.5, 10.1	-3.1, 10.7	-4.9, 10.0	-4.8, 11.1	-3.4, 13.5	-5.1, 12.7
3	-0.9, 4.7	-0.2, 7.8	0.2, 9.9	0.1, 11.3	-0.6, 12.0	-1.8, 11.9	-3.0, 11.9	-3.5, 12.4	-3.4, 13.5	-5.1, 12.7
4	0.4, 6.0	1.1, 9.0	2.7, 12.5	3.2, 14.5	2.6, 15.1	2.0, 15.7	2.1, 16.9	0.3, 16.2	1.1, 17.9	-1.3, 16.5
5	-0.3, 5.3	-0.8, 7.1	-1.1, 8.7	-0.6, 10.7	-1.2, 11.3	-1.8, 11.9	-3.0, 11.9	-6.0, 9.8	-6.5, 10.3	-8.9, 8.9
6	-0.9, 4.7	-2.1, 5.9	-3.6, 6.1	-1.8, 9.4	-3.1, 9.4	-3.7, 10.0	-6.2, 8.7	-9.8, 6.0	-9.7, 7.2	-13.3, 4.4
7	-2.2, 3.4	-2.7, 5.2	-3.6, 6.1	-1.8, 9.4	-3.1, 9.4	-4.3, 9.4	-6.8, 8.1	-10.5, 5.4	-9.1, 7.8	-13.3, 4.4
8	-2.8, 2.8	-3.3, 4.6	-4.9, 4.9	-3.1, 8.1	-4.4, 8.2	-6.2, 7.5	-6.2, 8.7	-11.1, 4.8	-9.7, 7.2	-13.9, 3.8
9	-2.8, 2.8	-2.1, 5.9	-3.6, 6.1	-3.7, 7.5	-5.6, 6.9	-8.8, 5.0	-11.2, 3.6	-16.8, -0.9	-16.0, 0.8	-19.0, -1.2
10	-2.2, 3.4	-0.2, 7.8	-3.0, 6.8	-1.2, 10.0	-3.7, 8.8	-6.2, 7.5	-9.3, 5.5	-14.3, 1.6	-15.4, 1.5	-18.4, -0.6
11	-0.3, 5.3	1.7, 9.7	-0.4, 9.3	0.7, 11.9	-2.5, 10.1	-5.0, 8.8	-9.3, 5.5	-15.5, 0.4	-16.6, 0.2	-22.2, -4.4
12	-0.3, 5.3	1.1, 9.0	-1.1, 8.7	-1.2, 10.0	-5.6, 6.9	-8.8, 5.0	-13.8, 1.1	-19.3, -3.4	-21.7, -4.9	-26.6, -8.8
13	-2.2, 3.4	-0.2, 7.8	-0.4, 9.3	-1.2, 10.0	-6.3, 6.3	-8.1, 5.6	-13.8, 1.1	-20.0, -4.1	-21.7, -4.9	-25.3, -7.6
14	-2.8, 2.8	-0.2, 7.8	-0.4, 9.3	-1.8, 9.4	-6.3, 6.3	-9.4, 4.3	-13.8, 1.1	-18.7, -2.8	-21.1, -4.2	-26.0, -8.2
15	-2.2, 3.4	1.1, 9.0	0.8, 10.6	0.7, 11.9	-3.1, 9.4	-6.2, 7.5	-11.2, 3.6	-14.9, 1.0	-17.3, -0.4	-25.3, -7.6
16	-1.5, 4.1	3.0, 10.9	4.0, 13.7	5.8, 17.0	0.0, 12. 6	-1.2, 12.6	-5.5, 9.3	-8.6, 7.3	-12.8, 4.0	-19.0, -1.2
17	-0.3, 5.3	4.3, 12.2	7.2, 16.9	9.6, 20.8	4.5, 17.0	4.5, 18.3	1.4, 16.3	-0.4, 15.5	-6.5, 10.3	-11.4, 6.3
18	-1.5, 4.1	3.6, 11.6	7.2, 16.9	9.6, 20.8	5.7, 18.3	6.4, 20.2	4.6, 19.4	1.5, 17.4	-5.3, 11.6	-9.5, 8.2
19	-0.9, 4.7	5.5, 13.5	9.7, 19.4	12.1, 23.3	9.5, 22.1	11.5, 25.2	10.3, 25.1	7.2, 23.1	0.4, 17.3	-2.6, 15.2
20	-0.9, 4.7	6.1, 14.1	9.7, 19.4	12.7, 24.0	8.9, 21.5	12.1, 25.8	10.3, 25.1	8.5, 24.4	2.3, 19.2	0.0, 17.7

Table 8

Calculated Control Limits for Type I Error Rate of 0.0027

	Number of Streams C									
	$\delta = 3.0000$									
t	1	2	3	4	5	6	7	8	9	10
1	-3.0, 3.0	-4.2, 4.2	-5.2, 5.2	-6.0, 6.0	-6.7, 6.7	-7.3, 7.3	-7.9, 7.9	-8.5, 8.5	-9.0, 9.0	-9.5, 9.5
2	-1.7, 4.3	-1.7, 6.8	-1.4, 9.0	-1.6, 10.4	-2.9, 10.5	-3.6, 11.1	-5.4, 10.5	-5.3, 11.6	-3.9, 14.1	-5.7, 13.3
3	-1.1, 4.9	-0.4, 8.0	-0.1, 10.3	-0.3, 11.7	-1.0, 12.4	-2.3, 12.4	-3.5, 12.4	-4.1, 12.9	-3.9, 14.1	-5.7, 13.3
4	0.2, 6.2	0.8, 9.3	2.4, 12.8	2.9, 14.9	2.1, 15.6	1.5, 16.2	1.5, 17.4	-0.3, 16.7	0.5, 18.5	-1.9, 17.1
5	-0.5, 5.5	-1.1, 7.4	-1.4, 9.0	-0.9, 11.1	-1.6, 11.8	-2.3, 12.4	-3.5, 12.4	-6.6, 10.4	-7.1, 10.9	-9.5, 9.5
6	-1.1, 4.9	-2.3, 6.1	-3.9, 6.5	-2.2, 9.8	-3.5, 9.9	-4.2, 10.5	-6.7, 9.2	-10.4, 6.6	-10.3, 7.7	-13.9, 5.1
7	-2.4, 3.6	-3.0, 5.5	-3.9, 6.5	-2.2, 9.8	-3.5, 9.9	-4.8, 9.9	-7.3, 8.6	-11, 6.0	-9.6, 8.4	-13.9, 5.1
8	-3.0, 3.0	-3.6, 4.9	-5.2, 5.2	-3.5, 8.5	-4.8, 8.6	-6.7, 8.0	-6.7, 9.2	-11.6, 5.3	-10.3, 7.7	-14.5, 4.4
9	-3.0, 3.0	-2.3, 6.1	-3.9, 6.5	-4.1, 7.9	-6.1, 7.3	-9.2, 5.5	-11.7, 4.1	-17.3, -0.4	-16.6, 1.4	-19.6, -0.6
10	-2.4, 3.6	-0.4, 8.0	-3.3, 7.1	-1.6, 10.4	-4.2, 9.2	-6.7, 8.0	-9.8, 6.0	-14.8, 2.2	-16.0, 2.0	-19.0, 0.0
11	-0.5, 5.5	1.4, 9.9	-0.8, 9.6	0.3, 12.3	-2.9, 10.5	-5.5, 9.2	-9.8, 6.0	-16.1, 0.9	-17.2, 0.8	-22.8, -3.8
12	-0.5, 5.5	0.8, 9.3	-1.4, 9.0	-1.6, 10.4	-6.1, 7.3	-9.2, 5.5	-14.3, 1.6	-19.9, -2.9	-22.3, -4.3	-27.2, -8.2
13	-2.4, 3.6	-0.4, 8.0	-0.8, 9.6	-1.6, 10.4	-6.7, 6.7	-8.6, 6.1	-14.3, 1.6	-20.5, -3.5	-22.3, -4.3	-25.9, -7.0
14	-3.0, 3.0	-0.4, 8	-0.8, 9.6	-2.2, 9.8	-6.7, 6.7	-9.9, 4.8	-14.3, 1.6	-19.2, -2.3	-21.6, -3.6	-26.6, -7.6
15	-2.4, 3.6	0.8, 9.3	0.5, 10.9	0.3, 12.3	-3.5, 9.9	-6.7, 8.0	-11.7, 4.1	-15.4, 1.5	-17.9, 0.1	-25.9, -7.0
16	-1.7, 4.3	2.7, 11.2	3.7, 14.1	5.4, 17.4	-0.4, 13.0	-1.7, 13.0	-6.0, 9.8	-9.1, 7.9	-13.4, 4.6	-19.6, -0.6
17	-0.5, 5.5	4.0, 12.5	6.8, 17.2	9.2, 21.2	4.0, 17.5	4.0, 18.7	0.9, 16.8	-0.9, 16.1	-7.1, 10.9	-12.0, 7.0
18	-1.7, 4.3	3.3, 11.8	6.8, 17.2	9.2, 21.2	5.3, 18.7	5.9, 20.6	4.1, 20.0	1.0, 18.0	-5.8, 12.2	-10.1, 8.9
19	-1.1, 4.9	5.2, 13.7	9.4, 19.7	11.7, 23.7	9.1, 22.5	11.0, 25.7	9.8, 25.6	6.7, 23.7	-0.1, 17.9	-3.2, 15.8
20	-1.1, 4.9	5.9, 14.4	9.4, 19.7	12.3, 24.3	8.5, 21.9	11.6, 26.3	9.8, 25.6	8.0, 24.9	1.8, 19.8	-0.6, 18.3

Table 9

Calculated Control Limits for Type I Error Rate of 0.002

	Number of Streams C									
	$\delta = 3.0902$									
t	1	2	3	4	5	6	7	8	9	10
1	-3.0, 3.1	-4.2, 4.4	-5.2, 5.4	-6.0, 6.2	-6.7, 6.9	-7.3, 7.6	-7.9, 8.2	-8.5, 8.7	-9.0, 9.3	-9.5, 9.8
2	-1.8, 4.4	-1.8, 6.9	-1.6, 9.1	-1.8, 10.6	-3.1, 10.7	-3.8, 11.4	-5.6, 10.7	-5.6, 11.9	-4.2, 14.3	-6.0, 13.6
3	-1.2, 5.0	-0.6, 8.2	-0.3, 10.4	-0.5, 11.9	-1.2, 12.6	-2.5, 12.6	-3.7, 12.6	-4.3, 13.2	-4.2, 14.3	-6.0, 13.6
4	0.1, 6.3	0.7, 9.4	2.2, 12.9	2.7, 15.0	1.9, 15.8	1.3, 16.4	1.3, 17.7	-0.5, 17.0	0.2, 18.8	-2.2, 17.4
5	-0.6, 5.6	-1.2, 7.5	-1.6, 9.1	-1.1, 11.2	-1.9, 12.0	-2.5, 12.6	-3.7, 12.6	-6.8, 10.6	-7.4, 11.2	-9.8, 9.8
6	-1.2, 5.0	-2.5, 6.3	-4.1, 6.6	-2.4, 10	-3.7, 10.1	-4.4, 10.7	-6.9, 9.4	-10.6, 6.8	-10.5, 8.0	-14.2, 5.3
7	-2.5, 3.7	-3.1, 5.6	-4.1, 6.6	-2.4, 10.0	-3.7, 10.1	-5.0, 10.1	-7.5, 8.8	-11.3, 6.2	-9.9, 8.6	-14.2, 5.3
8	-3.1, 3.1	-3.7, 5.0	-5.4, 5.4	-3.7, 8.7	-5.0, 8.8	-6.9, 8.2	-6.9, 9.4	-11.9, 5.6	-10.5, 8.0	-14.8, 4.7
9	-3.1, 3.1	-2.5, 6.3	-4.1, 6.6	-4.3, 8.1	-6.3, 7.5	-9.5, 5.7	-12.0, 4.4	-17.6, -0.1	-16.9, 1.7	-19.9, -0.3
10	-2.5, 3.7	-0.6, 8.2	-3.5, 7.2	-1.8, 10.6	-4.4, 9.4	-6.9, 8.2	-10.1, 6.3	-15.1, 2.4	-16.2, 2.3	-19.3, 0.3
11	-0.6, 5.6	1.3, 10.1	-0.9, 9.8	0.1, 12.5	-3.1, 10.7	-5.7, 9.5	-10.1, 6.3	-16.3, 1.2	-17.5, 1.0	-23.1, -3.5
12	-0.6, 5.6	0.7, 9.4	-1.6, 9.1	-1.8, 10.6	-6.3, 7.5	-9.5, 5.7	-14.5, 1.9	-20.1, -2.6	-22.6, -4.0	-27.5, -7.9
13	-2.5, 3.7	-0.6, 8.2	-0.9, 9.8	-1.8, 10.6	-6.9, 6.9	-8.8, 6.3	-14.5, 1.9	-20.8, -3.3	-22.6, -4.0	-26.2, -6.7
14	-3.1, 3.1	-0.6, 8.2	-0.9, 9.8	-2.4, 10.0	-6.9, 6.9	-10.1, 5.0	-14.5, 1.9	-19.5, -2.0	-21.9, -3.4	-26.8, -7.3
15	-2.5, 3.7	0.7, 9.4	0.3, 11.0	0.1, 12.5	-3.7, 10.1	-6.9, 8.2	-12.0, 4.4	-15.7, 1.8	-18.1, 0.4	-26.2, -6.7
16	-1.8, 4.4	2.6, 11.3	3.5, 14.2	5.2, 17.6	-0.6, 13.2	-1.9, 13.3	-6.3, 10.1	-9.4, 8.1	-13.7, 4.8	-19.9, -0.3
17	-0.6, 5.6	3.9, 12.6	6.7, 17.4	9.0, 21.4	3.8, 17.7	3.8, 19.0	0.7, 17.0	-1.2, 16.3	-7.4, 11.2	-12.3, 7.2
18	-1.8, 4.4	3.2, 12	6.7, 17.4	9.0, 21.4	5.1, 18.9	5.7, 20.9	3.8, 20.2	0.7, 18.2	-6.1, 12.4	-10.4, 9.1
19	-1.2, 5.0	5.1, 13.9	9.2, 19.9	11.5, 23.9	8.9, 22.7	10.8, 25.9	9.5, 25.9	6.4, 23.9	-0.4, 18.1	-3.4, 16.1
20	-1.2, 5.0	5.7, 14.5	9.2, 19.9	12.2, 24.5	8.3, 22.1	11.4, 26.5	9.5, 25.9	7.7, 25.2	1.5, 20.0	-0.9, 18.6

Examining the control limit values from left to right across the rows of Table 7, Table 8, and Table 9, the limits generally increase in magnitude. This is to be expected as the asymptotic variance of S_t is a function of the number of monitored streams. Additionally, it is noted that the limits also tend to increase in magnitude as t increases. This result is also unsurprising as S_t is a cumulative summation.

Determining Statistical Power of the Proposed Charting Scheme

The purpose of the second research question was to find the statistical power of the NEMT-CUSUM charting scheme. While this can be determined exactly by (59) and (66) for a given C, C_A, n_{C_A}, γ, α, and some prior value S_{t-1}^*, it may be of use to practitioners to have graphical representations for quick reference. Such graphs, referred to as "operating characteristic (OC) curves" are customary accompaniments for many common control charting techniques (Montgomery, 2013). However, like the calculation of the control limits, the alternative distribution depends on S_{t-1}^* as:

$$S_t^* | S_{t-1}^* \dot{\sim} N(S_{t-1}^* - \varepsilon, C_0 + C_A\theta), \tag{69}$$

where:

$$\theta = \frac{1}{\sqrt{1 - \frac{\gamma}{1-p_0} + \frac{\gamma}{p_0} - \frac{\gamma^2}{p_0(1-p_0)}}}, \tag{70}$$

$$\varepsilon = \frac{n_{C_A}\gamma}{\sqrt{n_{C_A}p_0(1-p_0)\left[1 - \frac{\gamma}{1-p_0} + \frac{\gamma}{p_0} - \frac{\gamma^2}{p_0(1-p_0)}\right]}}. \tag{71}$$

Therefore, in a similar way to the calculation of the control limits, OC curves are generated using example data, as a general OC curve cannot be plotted. In lieu of this, for

a particular combination of C, C_A, n_{C_A}, and α, one thousand random values of S^*_{t-1} were generated given some value of γ and β was calculated for each value. Then, the mean of the calculated β's was taken to be the true β. Figure 1 through Figure 3 represent some of the curves proposed in Chapter III. The remainder can be observed in Appendix A.

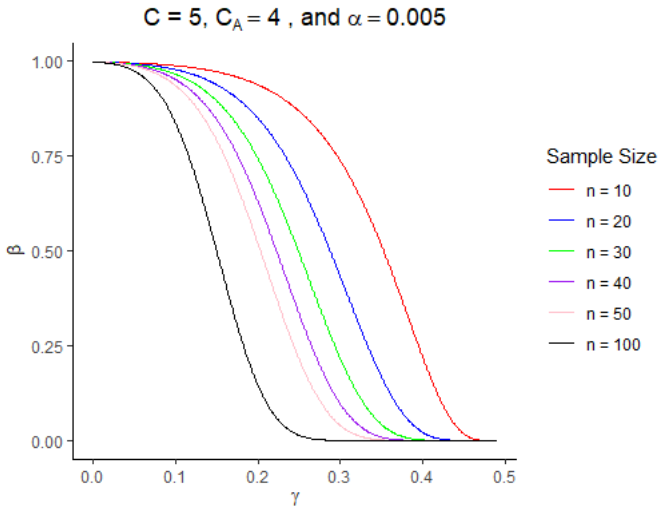

Figure 1. Operating Characteristic Curve for C = 5, CA = 4, and Type I Error Rate of 0.005

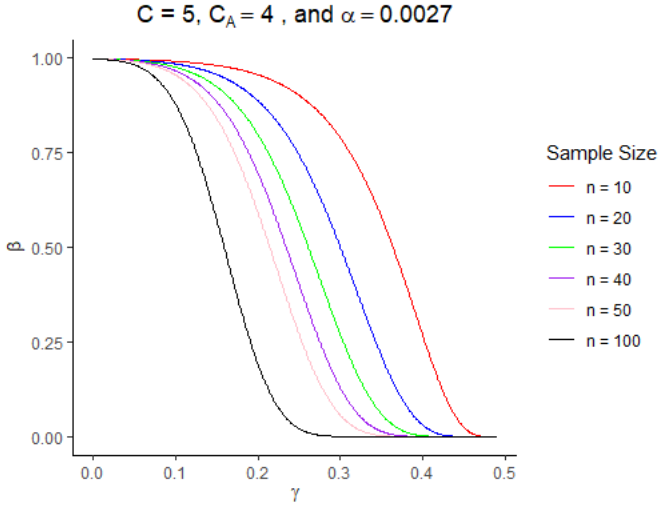

Figure 2. Operating Characteristic Curve for C = 5, CA = 4, and Type I Error Rate of 0.0027

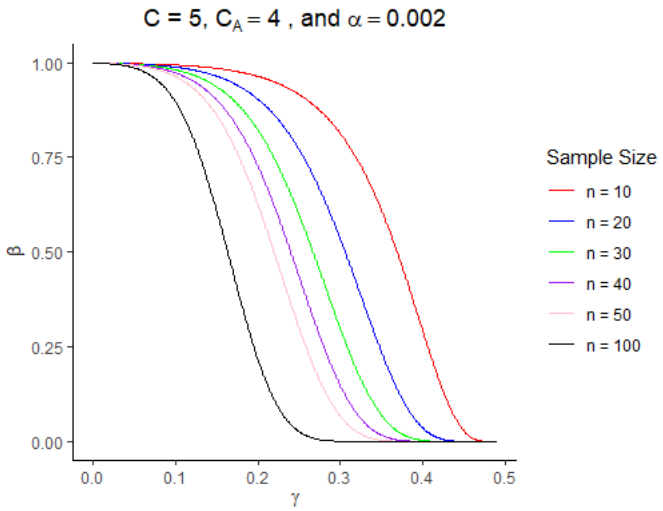

Figure 3. Operating Characteristic Curve for C = 5, CA = 4, and Type I Error Rate of 0.002

Observing Figure 1 through Figure 3, several interesting phenomena are observed. First, as the γ approaches its upper limit, the NEMT-CUSUM charting scheme has a lower probability of making a Type II error (i.e., greater power), and thus is more likely to signal an out-of-control point, as would be expected. Second, it is clear that as the sample size increases, the NEMT-CUSUM becomes more sensitive to smaller shifts in γ as noted by the steepening of the slopes of the OC curves within each figure. This graphical result is also to be expected due to the result obtained in (62) as ε is a function of the sample size, n_{C_A}. However, the differences between the steepness of the curves shown in Figure 1, Figure 2, and Figure 3, while slightly different, do not appear to be dramatically different.

Chart Performance Comparison Results

For the third research question, the performance of the NEMT-CUSUM is compared to existing MSP monitoring techniques. As stated in Chapter III, the comparison will be in terms of ARL_1 considering different magnitudes of shifts and different distributions. The results, which mirror the structure provided in Table 5, are

given in Table 9, Table 10, Table 11, and Table 12. The code used for this simulation can be found in Appendix B. Note, the MSP technique with the smallest ARL_1 will be bolded, as this scheme would be found to have performed most optimally. Additionally, and as noted in Chapter III, all control limits were set such that $ARL_0 \approx 370$ (i.e., $\alpha = 0.0027$) for fair comparison. It should further be noted that for the normal, uniform, and Laplacian distributions, their means and medians are equivalent. However, for the exponential distribution, it can be shown that $\tilde{\mu} = \lambda \ln(2)$, where $\lambda = \mu$. This equivalency was used in the ARL simulation for the NEMT-CUSUM.

Table 10

Average Run Length Comparison for Normally Distributed Data

Distribution and Target Value	$N(1,1), \mu_0 = 1$			
	Charting Scheme			
Magnitude of Shift	NEMT-CUSUM	Boyd's GCC	Mortell & Runger's R_t Chart	Meneces Chart for Every Stream
$0.25\mu_0$	2.2901	6.9035	8.2731	**2.1566**
$0.50\mu_0$	**6.4076**	52.1487	35.3933	8.6791
$0.75\mu_0$	**37.1485**	531.5027	187.2411	62.6334
$1\mu_0$	286.6044	1897.0392	302.0182	259.6250
$1.25\mu_0$	**45.6954**	205.1646	167.8463	65.3986
$1.50\mu_0$	**8.8978**	19.6906	35.7976	9.0865
$1.75\mu_0$	4.2448	3.5996	8.5067	**2.2110**
$2.00\mu_0$	4.2718	1.3700	2.8217	**1.1438**
$2.25\mu_0$	6.1042	1.0259	1.4750	**1.0058**
$2.50\mu_0$	5.2248	1.0003	1.0958	**1.0000**
$2.75\mu_0$	2.6851	**1.0000**	1.0100	**1.0000**
$3.00\mu_0$	1.6893	**1.0000**	1.0004	**1.0000**

In Table 10, which represents the case when the parametric MSP charts would be would be appropriate to use, it is clear that Meneces charting technique seems to be most effective comparing the parametric charting schemes. This result is congruent with what Meneces et al (2008) also found in their analysis. However, for small shifts, the NEMT-CUSUM chart was found to have superior performance.

Table 11

Average Run Length Comparison for Uniformly Distributed Data

Distribution and Target Value	$UNIF(0,1)\ \mu_0 = 0.50$			
	Charting Scheme			
Magnitude of Shift	NEMT-CUSUM	Boyd's GCC	Mortell & Runger's R_t Chart	Meneces Chart for Every Stream
$0.25\mu_0$	1.0008	**1.0000**	2.2752	**1.0000**
$0.50\mu_0$	**1.0010**	1.5013	16.2930	2.4576
$0.75\mu_0$	**9.4895**	24.1163	172.2190	57.1274
$1\mu_0$	286.3873	97.6778	360.2254	183.7638
$1.25\mu_0$	44.3936	**2.8504**	14.6257	3.3182
$1.50\mu_0$	12.6879	**1.0838**	2.0183	1.1083
$1.75\mu_0$	6.7086	**1.0020**	1.1109	1.0028
$2.00\mu_0$	4.9340	**1.0000**	1.0081	1.0001
$2.25\mu_0$	4.2453	**1.0000**	1.0005	**1.0000**
$2.50\mu_0$	3.9218	**1.0000**	**1.0000**	**1.0000**
$2.75\mu_0$	3.9063	**1.0000**	**1.0000**	**1.0000**
$3.00\mu_0$	4.0185	**1.0000**	**1.0000**	**1.0000**

In Table 11, the uniform distribution, which represents an example of a light-tailed distribution, was the data situation analyzed. For downward shifts away from target, the NEMT-CUSUM tended to perform more optimally. However, and as generally the case when comparing nonparametric and parametric tests in the presence of light-tailed data, the parametric charting schemes were more powerful than the NEMT-CUSUM in all upward shifts considered (Conover, 1999).

Table 12

Average Run Lengths Comparison for Laplacian Distributed Data

Distribution and Target Value	$Laplace(1,1)\ \mu_0 = 1$			
	Charting Scheme			
Magnitude of Shift	NEMT-CUSUM	Boyd's GCC	Mortell & Runger's R_t Chart	Meneces Chart for Every Stream
$0.25\mu_0$	**2.5284**	8.1230	47.4134	5.5130
$0.50\mu_0$	**5.9113**	25.6817	133.5194	15.5445
$0.75\mu_0$	**29.1895**	77.3210	256.7306	39.6770
$1\mu_0$	280.5016	129.1964	281.2655	51.6539
$1.25\mu_0$	35.5752	81.8567	254.8772	**25.3206**
$1.50\mu_0$	**8.3189**	27.4041	131.0118	9.0949
$1.75\mu_0$	4.5116	8.5979	46.3026	**3.4718**
$2.00\mu_0$	3.8905	3.1966	18.5632	**1.6697**
$2.25\mu_0$	4.6212	1.5945	7.3881	**1.1373**
$2.50\mu_0$	5.9305	1.1155	3.5348	**1.0153**
$2.75\mu_0$	6.5443	1.0113	2.0256	**1.0006**
$3.00\mu_0$	5.3362	1.0003	1.3921	**1.0000**

Table 12 gives the comparison of the considered charting techniques in the presence of heavy-tailed data, represented here by the Laplacian distribution. As has been the case in the other comparison tables, the NEMT-CUSUM tended to perform more optimally than its parametric alternatives for downward shifts. However, the Meneces charting scheme tended to signal an out-of-control point more quickly, on average, than

the other considered techniques, especially for relatively large, upward shifts away from target.

Table 13

Average Run Lengths Comparison for Exponentially Distributed Data

Distribution and Target Value	$EXP(1), \mu_0 = 1$			
	Charting Scheme			
Magnitude of Shift	NEMT-CUSUM	Boyd's GCC	Mortell & Runger's R_t Chart	Meneces Chart for Every Stream
$0.25\mu_0$	4.1754	**1.0000**	1.0002	**1.0000**
$0.50\mu_0$	7.3369	1.4178	1.9193	**1.0840**
$0.75\mu_0$	49.2004	16.7420	35.4300	**4.2939**
$1\mu_0$	281.7526	355.1449	332.5518	35.5473
$1.25\mu_0$	**57.7853**	702.4397	315.9681	73.0702
$1.50\mu_0$	**13.9108**	662.3800	336.7406	74.0793
$1.75\mu_0$	**5.4827**	774.0625	357.5699	72.6880
$2.00\mu_0$	**2.9666**	743.7669	289.9186	72.4554
$2.25\mu_0$	**1.9691**	711.8071	280.2704	71.4707
$2.50\mu_0$	**1.5450**	673.5448	237.6280	67.7610
$2.75\mu_0$	**1.2985**	806.1301	200.2691	68.5443
$3.00\mu_0$	**1.1790**	633.2692	197.7248	71.5165

Finally, Table 13 shows the comparison of the MSP charting techniques in the presence of skewed data, which is represented in these analyses by the exponential distribution. While the parametric MSP schemes were found to have superior performance to that of the NEMT-CUSUM for downward shifts away from target, the

latter performed substantially better than its parametric alternatives for upward shifts. Interestingly, the performance of the NEMT-CUSUM was fairly similar for the same magnitude of observed shift, but differing data situations with a slight exception for the uniform distribution. This general result is not necessarily surprising as the chart does not rely on the underlying data following a particular distribution.

To conclude, the results addressing the three research questions guiding this dissertation were presented. For the first research question, an example dataset was given to demonstrate how control limits can be computed for a specified value of α. While a general form for the computation of the control limits is given by (68), exact values of the control limits cannot be computed for a general case as they are dependent upon the previously observed value, S_{t-1}. With respect to the second research question, OC curves were estimated for various values of α, γ, C, C_A, and n_{C_A}. The OC curves had to be estimated rather than explicitly computed as the alternative distribution is also dependent on the previously observed value, S_{t-1}^{*}. Here, it was shown that larger sample sizes have a higher probability of detecting shifts of a smaller magnitude and that smaller values of α are slightly less powerful than larger values of α. Finally, with the third research question, the performance of the NEMT-CUSUM was compared to that of existing parametric MSP techniques. It was shown that the NEMT-CUSUM performed more optimally than the competing techniques across all data situations for small shifts away from target. It was also shown that the NEMT-CUSUM was substantially more effective at detecting shifts away from target when the underlying data came from the skewed exponential distribution. While the parametric techniques, and in particular the Meneces Chart for Each Stream technique, had preferable performance in some instances, their

performance varied across the compared distributions. The NEMT-CUSUM performed consistently across the examined data situations.

CHAPTER V

CONCLUSIONS

In this dissertation, a nonparametric cumulative summation (CUSUM) chart for monitoring multiple stream processes (MSP) based on a modified version of the classical nonparametric median test was developed. Referred to as the "Nonparametric Extended Median Test – Cumulative Summation (NEMT-CUSUM)", this chart was designed to be used in cases when chart operators have little or no knowledge of the monitored streams' underlying distribution. Chart development and procedural use were discussed in Chapter III. Theoretical results were also shown in Chapter III for both the in-control and out-of-control cases, given the assumptions described at the onset of the chapter hold. Finally, a simulation study was conducted to compare the performance of the NEMT-CUSUM to existing charting techniques whose assumptions are based on the underlying data coming from a normal distribution. Research questions one and two were addressed in Chapter III and the final research question was addressed in Chapter IV.

Discussion

Asymptotic Results

Three research questions guided this study. The goal of the first was to develop and compute control limits for the NEMT-CUSUM such that the Type I error rate, α, could be fixed across all observed time points. The theoretical construction of these limits was shown in Chapter III and exact limits were calculated for an example data set for the number of monitored streams being $C = 1,2,\dots,10$ and $\alpha = 0.005, 0.0027$, and 0.002 as

shown in Table 7, Table 8, and Table 9 in Chapter IV. Given that the assumptions of the NEMT-CUSUM are met (i.e., large sample sizes for each monitored stream, mutual independence of the streams, and independence of the samples taken between all time points), the calculation of these limits is relatively straightforward as given by (48) and (51). However, in practice it is common for tabled values of the control limits of a control limit to be calculated for use by practitioners (Montgomery, 2013). Because the mean of the plotting statistic, S_t, is the last observed plotting statistic, S_{t-1}, this is not possible for a general case. Consequently, it is necessary to create a computer program to compute the limits if the NEMT-CUSUM is to be widely used. This may create a barrier to adoption. It may also be of value to modify the existing charting scheme such that the plotting statistic is symmetric about a constant asymptotic mean rather than a varying one.

The purpose of the second research question was to calculate, both theoretically and empirically, the statistical power of the NEMT-CUSUM. The alternative distribution, given a fixed shift affecting some subset of the total number of monitored streams was derived in Chapter III. The theoretical distribution and formula for calculating statistical power was also given in Chapter III. For various combinations of the parameters of the alternative distribution, operating characteristic (OC) curves were presented in both Chapter IV and in Appendix A. Like the calculation of the control limits, the theoretical results found for statistical power depend on the independence and large-sample assumptions being met as well as the previous observation, S^*_{t-1}. Thus, it is not possible, given current chart construction, to calculate statistical power for a general case.

Additionally, in this dissertation it was assumed that if a shift occurred in a subset of the monitored streams that the same shift occurred in those streams. In practical

settings, shifts of differing magnitudes may occur in the shifted subset of streams. For example, if the number of monitored streams is $C = 10$ and the shifted number of streams is $C_A = 3$, the shift present in the first shifted stream, say γ_1, might be different then the shift present in the other two shifted streams, say γ_2. Thus, while some of the literature assumes a fixed shift on a subset of monitored streams, the results here could be further generalized for the case when the shifted streams are shifted away from target by differing magnitudes (Mortell & Runger, 1995).

Finally, because the NEMT-CUSUM only considers the hypothesized median in determining if a process is in-control or out-of-control, its power to detect a distributional shift (e.g., when both the location and scale parameters shift) is weakened. For example, if the null distribution is the standard normal distribution, but a subset of streams observe a shift in variance to say, $\sigma^2 = 25$, but the mean stayed constant, it is unlikely the NEMT-CUSUM would be able to efficiently detect the scale shift. Thus, it may be of value to design a nonparametric control chart which monitors several quantiles of the null distribution instead of only one.

Simulation Results

As mentioned in Chapter IV and as shown in Table 10, Table 11, Table 12, and Table 13, the estimated ARL values for the NEMT-CUSUM were generally consistent across the differing underlying data situations for the same observed shift away from target. This result is not surprising as the chart does not rely on the underlying data following a particular distribution, but it is an attractive feature for practitioners. The performance of the parametric charting schemes varied across the various data situations. Consider the case when the observed shift was $2.00\mu_0$. The normal, light-tailed estimated

ARL_1 values appeared adequate, but their performance in the presence of heavy-tailed and skewed data deteriorated. If a chart operator does not have knowledge of the underlying distribution, they may be risking the observed process operating in an out-of-control state for a substantial amount of time, which may cost the organization a substantial amount of time, money, or both. Therefore, "when the cost of making a mistake is high," it may be of more value to the operator to use this nonparametric scheme.

While this simulation study provided valuable insights, it also has limitations. First, the specified Type I error rate was taken to be $\alpha = 0.0027$. This traditionally corresponds to an in-control $ARL \approx 370$. In this analysis, the NEMT-CUSUM was consistently estimated to have an $ARL_0 \approx 280$. There are two likely causes for this large difference between nominal and empirical ARL_0. One, the probability of making a Type I error, α, is interpreted as the long-run proportion of runs of the NEMT-CUSUM which result in an improper out-of-control signal. Since the number of iterations used here was 10000, it may be the case that this was not large enough for the empirical ARL_0 to converge to the nominal ARL_0. Two, the sample size used for each stream at each time point was taken to be $n = 10$. While this meets the minimum sample typically recommended to use the asymptotic distributions, it may be the case that the minimum sample required is not quite large enough for the distribution of $S_t|S_{t-1}$ does not yet converge to $N(S_{t-1}, C)$.

The second limitation of this simulation study is time constraints. First, and as stated previously, the number of iterations was taken to be 10000. This number could be chosen to be 50000 or 100000 to perhaps yield more representative, accurate ARL_1

values, it would require additional computing time that was not available. Second, the were four distributions considered, while intended to illustrate chart performance in general distributional situations, do not represent all possible data situations. It would be of value to consider discrete data, data from mixture distributions (both the same and different), or autocorrelated data, among others. Going forward, it would be valuable to consider these other situations which may arise in practice in order to fully evaluate the performance of the NEMT-CUSUM.

Future Directions

If the assumptions of within and between stream independence and large sample sizes are met, the NEMT-CUSUM may be an attractive option for practitioners monitoring a multiple stream process. However, the main limitation of the technique is that calculation of the plotting statistic as well as the control limits is not as straightforward as compared to Boyd's GCC, Meneces Chart for each Stream, or even Mortell & Runger's R_t chart. Thus, and as mentioned, one expansion of the NEMT-CUSUM would be to modify the calculation of the plotting statistic, S_t, such that its mean and variance are constant across all time points. It is a nice feature of the NEMT-CUSUM that α is fixed across all trials through the use of dynamic control limits, but the necessity of some quantitative and statistical knowledge in order to calculate the control limits may create a barrier to wider implementation. Further, having the distribution of the plotting statistic not vary across the time would solve the limitation of not being able to calculate general tabled values of the control limits as well as general operating characteristic curves.

The second future direction for research to build upon the proposed charting scheme would be to determine how estimation of $\tilde{\mu}_0$ using some historical samples affects the performance of the NEMT-CUSUM. Using the sample median of a small number of historical samples may substantially underestimate or overestimate the true median, and thus, the performance of the chart may wane. It would be of value to practitioners to understand how estimating the target median affects chart performance.

Third, as mentioned in Chapter III, S_t could reasonably be conceptualized as a marginal random walk process. However, and as is the case with the conditional regression conceptualization of S_t, a random walk process is not stationary. The issue relating to it being nonstationary were described in Chapter III. To possibly address this issue, a first-order autoregressive model could be fit to the S_t series such that S_t is stationary (i.e., its mean and variance do not depend on t). Thus, static limits could be computed and the chart, while somewhat more cumbersome to initially set up, would be more straightforward to operate going forward. This would be of great value to explore in future studies.

Finally, and as also stated previously in this chapter, a limitation of designing a control chart to monitor a single quantile (i.e., a single location parameter) of the null distribution is that it is unlikely it would be efficient in detecting shifts in other quantiles. Therefore, it would be valuable to design a chart, still nonparametric in nature, which has the ability to detect such shifts in multiple stream processes. The Kruskal-Wallis nonparametric test or extending the $1 \times C$ contingency table used by the NEMT-CUSUM to an $R \times C$ contingency table, where R denotes the number of intervals desired to be monitored from the null distribution, could potentially be used to more broadly monitor

shifts away from the null distribution. While the calculation of the plotting statistic would likely be more complicated than what was presented in this dissertation, the potential of more efficiently detecting a variety of shifts away from target may outweigh the added complexity.

To conclude, the development of the NEMT-CUSUM control chart fills an apparent need in the body of literature regarding the monitoring of MSPs. Given that its assumptions are met, the results given in Chapter IV suggest that the NEMT-CUSUM is a promising alternative to existing parametric MSP monitoring techniques. However, even though it is nonparametric, the NEMT-CUSUM still relies upon some assumptions. If these are not met, it is likely its performance would deteriorate, and consequently, a charting technique with less or looser assumptions should be developed in the case when the assumptions are not met. Another future consideration is to develop a similar charting scheme, but one in which the calculation of both the plotting statistic and control limits are straightforward in nature. The implementation and use of the NEMT-CUSUM requires some statistical knowledge which may prevent its adoption in practice. Though, such barriers could be ameliorated if a chart operator was convinced of the value of this nonparametric charting scheme, and if a computer program was developed to make computation of the plotting statistic and control limits automated.

REFERENCES

Adams B.M., Woodall W.H., Lowry C.A. (1992) The Use (and Misuse) of False Alarm Probabilities in Control Chart Design. In: Lenz HJ., Wetherill G.B., Wilrich PT. (eds) Frontiers in Statistical Quality Control 4. Frontiers in Statistical Quality Control 4, vol 4. Physica, Heidelberg

Agresti, A. (2007). Introduction to categorical data analysis. Hoboken, NJ: Wiley.

Amin, R.W., Reynolds Jr., M.R., & Bakir, S.T. (1995). Nonparametric quality control charts based on the sign statistic. Communications in Statistics – Theory and Methods, 24(6), 1597-1623.

Bakir, S.T., & Reynolds Jr., M.R. (1979). A non parametric procedure for process control based on within group ranking. Technometrics, 21, 175-183.

Bersimis, S., Psarakis, S., & Panaretos, J. (2007). Multivariate statistical process control charts: An overview. Quality and Reliability Engineering International, 23(5), 517-543. doi:10.1002/qre.829

Boyd, D.F. (1950). Applying the group control chart for $\bar{x}$ and R. Industrial Quality Control, 7(3), 22-25.

Brook, D., & Evans, D. A. (1972). An approach to the probability distribution of cusum run length. Biometrika, 59(3), 539-549. doi:10.1093/biomet/59.3.539

Chakraborti, S., Van Der Laan, P., & Bakir, S. T. (2001). Nonparametric control charts: an overview and some results. Journal of Quality Technology, 33(3), 304-315.

Chakraborti, S., & van de Wiel, M. A. (2008). A nonparametric control chart based on the Mann-Whitney statistic. Beyond Parametrics in Interdisciplinary Research: Festschrift in Honor of Professor Pranab K. Sen Collections, 156-172. doi:10.1214/193940307000000112

Conover, W. J. (1999). Practical nonparametric statistics (3rd ed.). New York: Wiley.

Delavigne, K. T., & Robertson, J. D. (1994). Demings profound changes: When will the sleeping giant awaken? Englewood Cliffs, NJ: Prentice Hall.

Deming, W. E. (1981). Improvement of quality and productivity through action by management. National Productivity Review, 1(1), 12-22. doi:10.1002/npr.4040010105

Epprecht, E. K., Barbosa, L. F., & Simões, B. F. (2011). SPC of multiple stream processes: A chart for enhanced detection of shifts in one stream. Production, 21(2), 242-253. doi:10.1590/s0103-65132011005000022

Gan, F.F. (1991). An Optimal Design of CUSUM Quality Control Charts. Journal of Quality Technology, 23(4), 279-286.

Grimshaw, S. D., Bryce, G. R., & Meade, D. J. (1999). Control Limits For Group Charts. Quality Engineering, 12(2), 177-184. doi:10.1080/08982119908962575

History of Total Quality Management (TQM). (n.d.). Retrieved from http://asq.org/learn-about-quality/total-quality-management/overview/tqm-history.html

Jensen, J. L. (1995). Saddlepoint Approximations. Oxford University Press, New York.

Jirasettapong, P., & Rojanarowan, N. (2011). A Guideline to Select Control Charts for Multiple Stream Processes Control. Engineering Journal, 15(3), 1-14. doi:10.4186/ej.2011.15.3.1

Kruskal, W.H., & Wallis, W.A. (1952). Use of ranks in one-criterion variance analysis. Journal of the American Statistical Association, 47(260), 583-621.

Lanning, J. W. (1998). Methods for monitoring fractionally sampled multiple stream processes (Order No. 9837682). Available from ProQuest Dissertations & Theses Global. (304426706). Retrieved from https://unco.idm.oclc.org/login?url=https://search.proquest.com/docview/304426706?accountid=12832

Lowry, C., Woodall, W., Champ, C., & Rigdon, S. (1992). A Multivariate Exponentially Weighted Moving Average Control Chart. Technometrics, 34(1), 46-53. doi:10.2307/1269551

Mann, H.B., & Whitney, D.R. (1947). On a test of whether one of two random variables is stochastically larger than the other. The Annals of Mathematical Statistics, 18(1), 50-60.

Meneces, N.S., Olivera, S.A., Saccone, C.D., & Tessore, J. (2008). Statistical control of multiple-stream processes: a Shewhart control chart for each stream. Quality Engineering, 20(2), 185-194.

Montgomery, D. C. (2013). Statistical quality control: A modern introduction. Hoboken, NJ: Wiley.

Mortell, R., & Runger, G. (1995). Statistical process-control of multiple stream processes. Journal of Quality Technology, 27(1), 1-12. doi:10.1080/00224065.1995.11979554

Neave, H. R. (1990). The Deming dimension. Knoxville: SPC Press.

Nelson, L.S. (1986). Control chart for multiple stream processes. Journal of Quality Technology, 18(4), 255-256.

Nelson, P.R., & Stephenson, P.L. (1996). Runs tests for group control charts. Communications in Statistics – Theory and Methods, 25(11), 2739-2765.

Page, E.S. (1954). Continuous inspection schemes. Biometrika, 41(5), 100-115.

Pignatiello, J., & Runger, G. (1990). Comparisons of multivariate cusum charts. Journal of Quality Technology, 22(3), 173-186.

R Core Team. (2018). R: A Language and Environment for Statistical Computing. Vienna, Austria: R Foundation for Statistical Computing. Retrieved from https://www.r-project.org/

Ravishanker, N., & Dey, D. K. (2002). A first course in linear model theory. Boca Raton, FL: Chapman & Hall/CRC.

Reynolds, M. R. (1975). Approximations to the Average Run Length in Cumulative Sum Control Charts. Technometrics, 17(1), 65. doi:10.2307/1268002

Roberts, S. W. (1959). Control chart tests based on geometric moving averages. Technometrics, 1(3), 239-250. doi:10.1080/00401706.1959.10489860

Runger, G. C., Alt, F. B., & Montgomery, D. C. (1996). Controlling multiple stream processes with principal components. International Journal of Production Research, 34(11), 2991-2999. doi:10.1080/00207549608905074

Snedecor, G. W., & Cochran, W. G. (1989). Statistical Methods (8th ed.). Ames, IA: Blackwell Publishing Professional.

Shewhart, W. A. (1924). Some applications of statistical methods to the analysis of physical and engineering data. The Bell System Technical Journal, 3(1), 43-87. doi:10.1002/j.1538-7305.1924.tb01347.x

Vicentin, D. S., Silva, B. B., Piccirillo, I., Bueno, F. C., & Oprime, P. C. (2018). Monitoring process control chart with finite mixture probability distribution. International Journal of Quality & Reliability Management, 35(2), 335-353. doi:10.1108/ijqrm-11-2016-0196

Wald, A. (1945). Sequential Tests of Statistical Hypotheses. The Annals of Mathematical Statistics, 16(2), 117-186. doi:10.1214/aoms/1177731118

Walton, M. (1991). Deming management at work. New York, NY: Perigee Books, Putnam Publishing Group.

Wang, D., Zhang, L., & Xiong, Q. (2017). A non parametric CUSUM control chart based on the Mann-Whitney statistic. Communications in Statistics – Theory and Methods, 46(10), 4713-4725.

Wei, W. W. (2007). Time series analysis: Univariate and multivariate methods. Boston: Pearson Addison Wesley.

Wilcoxon, F. (1945). Individual comparisons by ranking methods. Biometrika, 1, 80-83.

Woodall, W. (1983). The Distribution of the Run Length of One-Sided CUSUM Procedures for Continuous Random Variables. Technometrics, 25(3), 295-301.

Woodall, W., & Montgomery, D. (2014). Some current directions in the theory and application of statistical process monitoring. Journal of Quality Technology, 46(1), 78-94.

Zhou, C., Zou, C., Zhang, Y., & Wang, Z. (2007). Nonparametric control chart based on change-point model. Statistical Papers, 50(1), 13-28. doi:10.1007/s00362-007-0054-7

Appendix A

Additional Operating Characteristic Curves

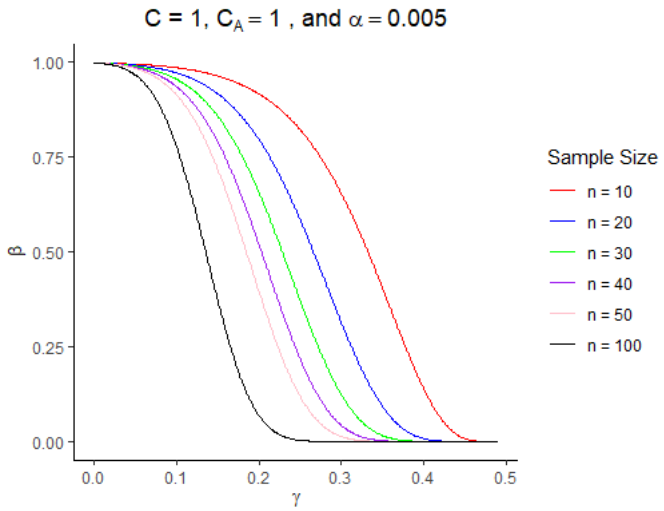

Figure 4. Operating Characteristic Curve for C = 1, CA = 1, and Type I Error Rate of 0.005

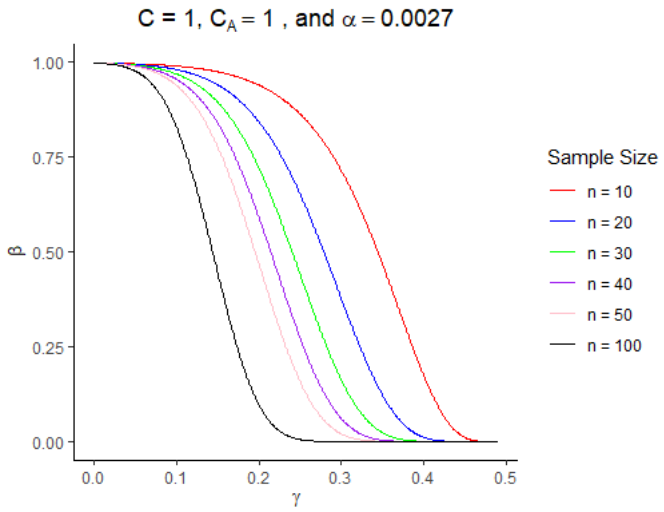

Figure 5. Operating Characteristic Curve for C = 1, CA = 1, and Type I Error Rate of 0.0027

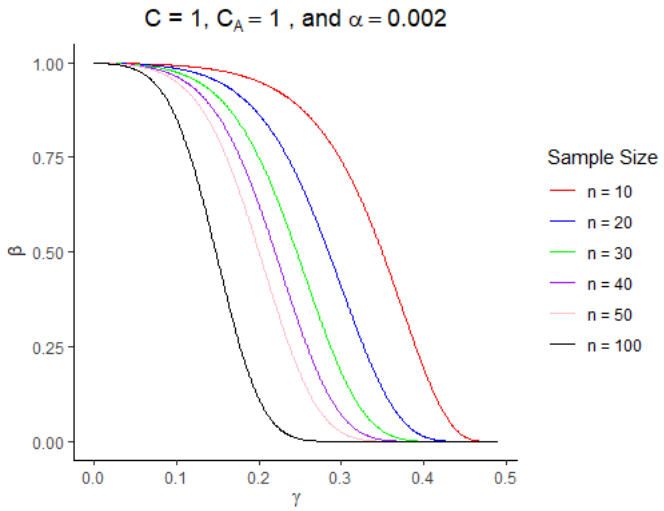

Figure 6. Operating Characteristic Curve for C = 1, CA = 1, and Type I Error Rate of 0.002

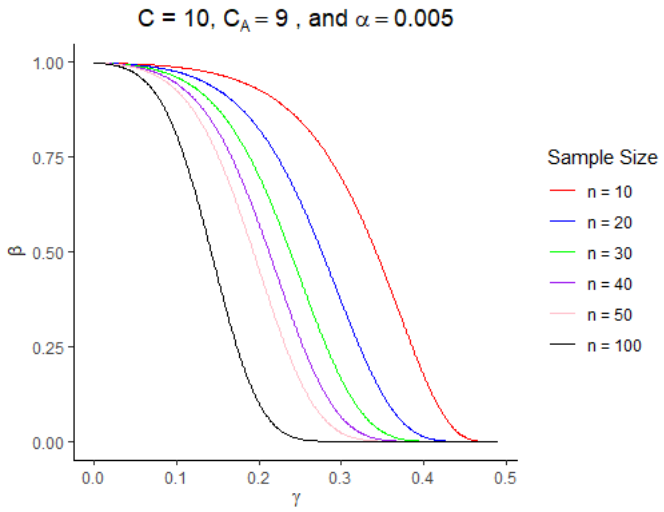

Figure 7. Operating Characteristic Curve for C = 10, CA = 9, and Type I Error Rate of 0.005

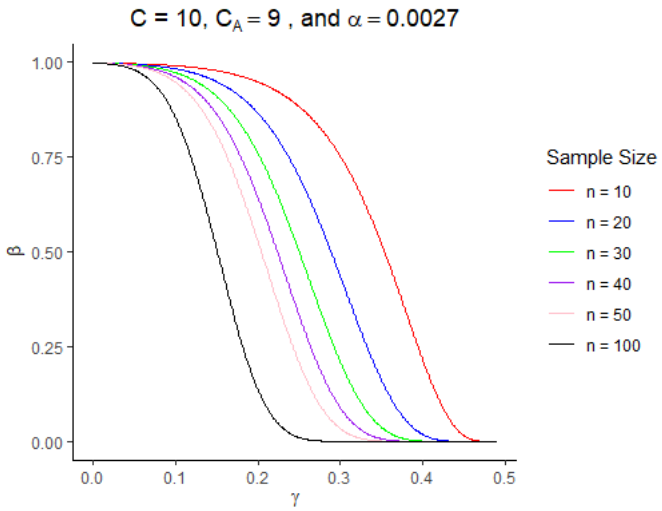

Figure 8. Operating Characteristic Curve for C = 10, CA = 9, and Type I Error Rate of 0.0027

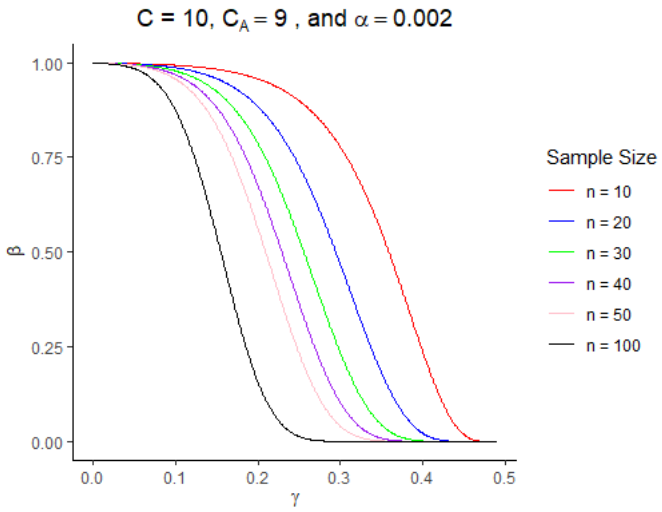

Figure 9. Operating Characteristic Curve for C = 10, CA = 9, and Type I Error Rate of 0.002

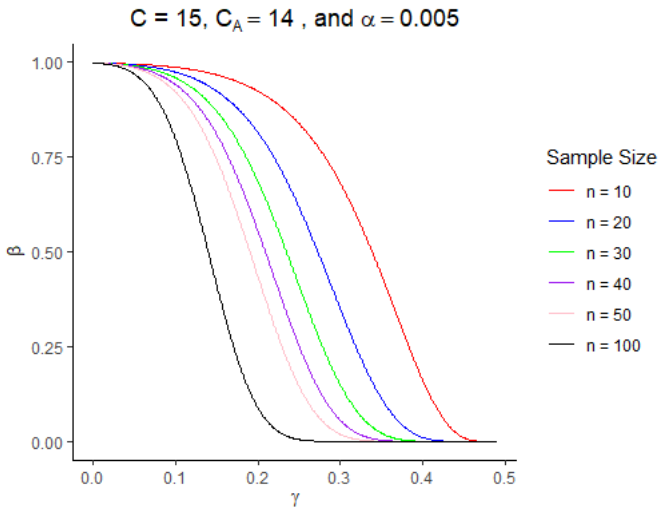

Figure 10. Operating Characteristic Curve for C = 15, CA = 14, and Type I Error Rate of 0.005

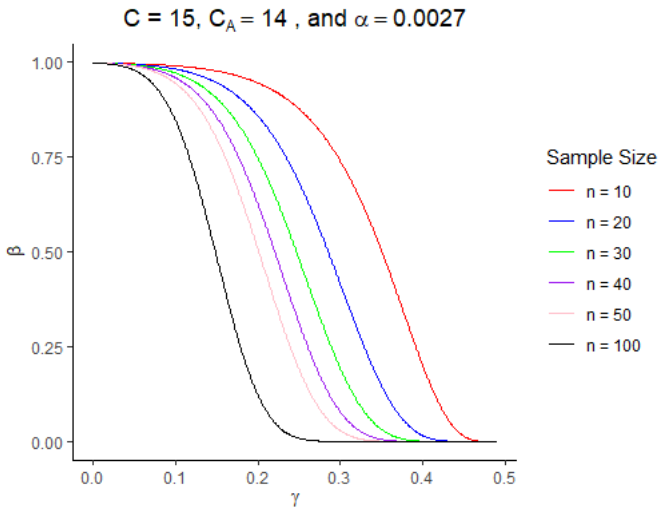

Figure 11. Operating Characteristic Curve for C = 15, CA = 14, and Type I Error Rate of 0.0027

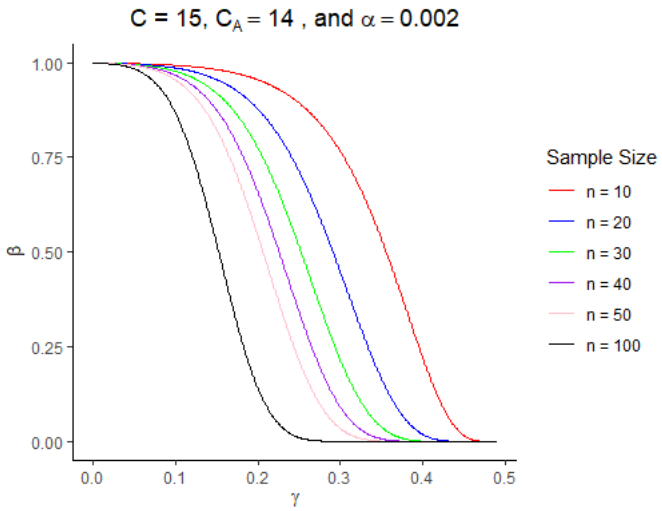

Figure 12. Operating Characteristic Curve for C = 15, CA = 14, and Type I Error Rate of 0.002

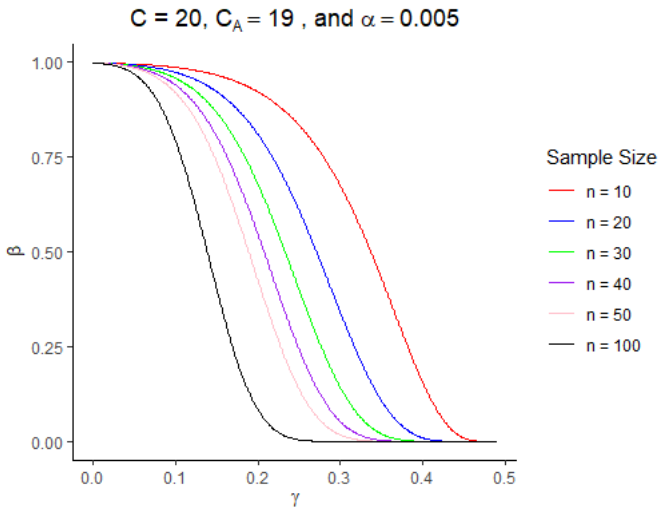

Figure 13. Operating Characteristic Curve for C = 20, CA = 19, and Type I Error Rate of 0.005

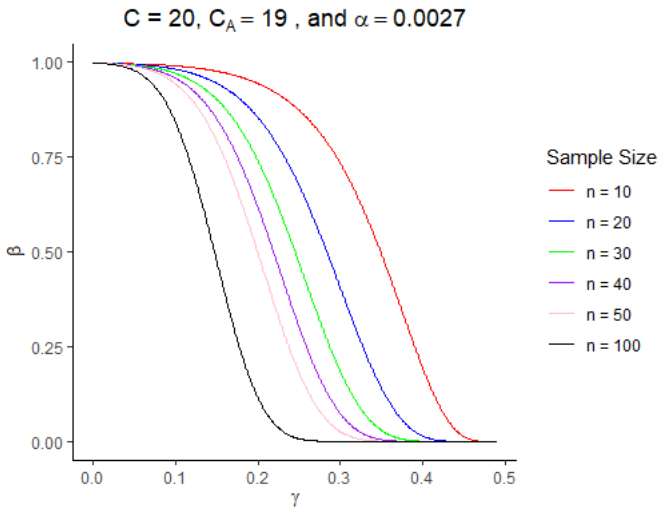

Figure 14. Operating Characteristic Curve for C = 20, CA = 19, and Type I Error Rate of 0.0027

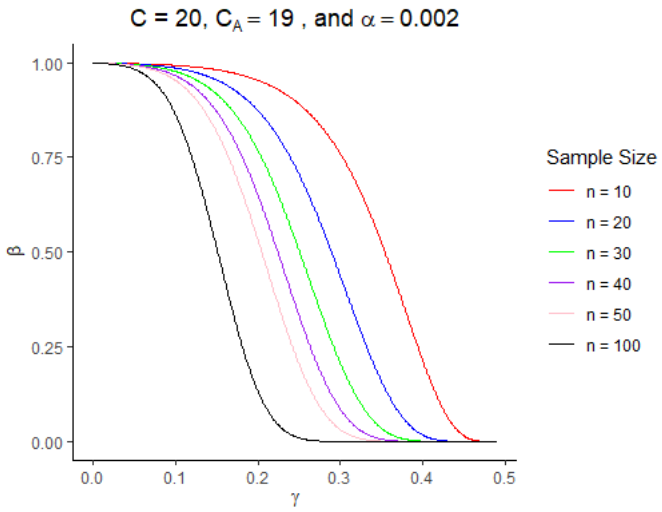

Figure 15. Operating Characteristic Curve for C = 20, CA = 19, and Type I Error Rate of 0.002

Appendix B

R Code

```
## Calculating Control Limits ##

## Set Seed ##

set.seed(123456)

n <- 10
p0 <- 0.5
streams <- seq(1,10,by=1)

alpha1 <- 0.005
alpha2 <- 0.0027
alpha3 <- 0.002

mu0 <- 0

## Generating Underlying Data ##

dat <- matrix(rnorm(200*10),ncol=10)

t1 <- dat[1:10,]
t2 <- dat[11:20,]
t3 <- dat[21:30,]
t4 <- dat[31:40,]
t5 <- dat[41:50,]
t6 <- dat[51:60,]
t7 <- dat[61:70,]
t8 <- dat[71:80,]
t9 <- dat[81:90,]
t10 <- dat[91:100,]
```

```
t11 <- dat[101:110,]

t12 <- dat[111:120,]

t13 <- dat[121:130,]

t14 <- dat[131:140,]

t15 <- dat[141:150,]

t16 <- dat[151:160,]

t17 <- dat[161:170,]

t18 <- dat[171:180,]

t19 <- dat[181:190,]

t20 <- dat[191:200,]


o1 <- matrix(nrow=10,ncol=20)


## Calculating Frequency >= mu0 ##


for(i in 1:10){


  o1[i,1] <- ifelse(is.na(table(t1[,i] > mu0)[2]) ==
'TRUE',0,table(t1[,i] > mu0)[2])

  o1[i,2] <- ifelse(is.na(table(t2[,i] > mu0)[2]) ==
'TRUE',0,table(t2[,i] > mu0)[2])

  o1[i,3] <- ifelse(is.na(table(t3[,i] > mu0)[2]) ==
'TRUE',0,table(t3[,i] > mu0)[2])

  o1[i,4] <- ifelse(is.na(table(t4[,i] > mu0)[2]) ==
'TRUE',0,table(t4[,i] > mu0)[2])

  o1[i,5] <- ifelse(is.na(table(t5[,i] > mu0)[2]) ==
'TRUE',0,table(t5[,i] > mu0)[2])

  o1[i,6] <- ifelse(is.na(table(t6[,i] > mu0)[2]) ==
'TRUE',0,table(t6[,i] > mu0)[2])

  o1[i,7] <- ifelse(is.na(table(t7[,i] > mu0)[2]) ==
'TRUE',0,table(t7[,i] > mu0)[2])

  o1[i,8] <- ifelse(is.na(table(t8[,i] > mu0)[2]) ==
'TRUE',0,table(t8[,i] > mu0)[2])
```

```
  o1[i,9] <- ifelse(is.na(table(t9[,i] > mu0)[2]) ==
'TRUE',0,table(t9[,i] > mu0)[2])

  o1[i,10] <- ifelse(is.na(table(t10[,i] > mu0)[2]) ==
'TRUE',0,table(t10[,i] > mu0)[2])

  o1[i,11] <- ifelse(is.na(table(t11[,i] > mu0)[2]) ==
'TRUE',0,table(t11[,i] > mu0)[2])

  o1[i,12] <- ifelse(is.na(table(t12[,i] > mu0)[2]) ==
'TRUE',0,table(t12[,i] > mu0)[2])

  o1[i,13] <- ifelse(is.na(table(t13[,i] > mu0)[2]) ==
'TRUE',0,table(t13[,i] > mu0)[2])

  o1[i,14] <- ifelse(is.na(table(t14[,i] > mu0)[2]) ==
'TRUE',0,table(t14[,i] > mu0)[2])

  o1[i,15] <- ifelse(is.na(table(t15[,i] > mu0)[2]) ==
'TRUE',0,table(t15[,i] > mu0)[2])

  o1[i,16] <- ifelse(is.na(table(t16[,i] > mu0)[2]) ==
'TRUE',0,table(t16[,i] > mu0)[2])

  o1[i,17] <- ifelse(is.na(table(t17[,i] > mu0)[2]) ==
'TRUE',0,table(t17[,i] > mu0)[2])

  o1[i,18] <- ifelse(is.na(table(t18[,i] > mu0)[2]) ==
'TRUE',0,table(t18[,i] > mu0)[2])

  o1[i,19] <- ifelse(is.na(table(t19[,i] > mu0)[2]) ==
'TRUE',0,table(t19[,i] > mu0)[2])

  o1[i,20] <- ifelse(is.na(table(t20[,i] > mu0)[2]) ==
'TRUE',0,table(t20[,i] > mu0)[2])


}


## Standardizing Frequencies to N(0,1) ##


E1 <- matrix(nrow = 10, ncol= 20)


for(i in 1:10){

  for(j in 1:20){

    E1[i,j] <- (o1[i,j] - n*p0)/sqrt(n*p0*(1-p0))
```

```
  }
}

## Calculating EMT Statistics for each considered C ##
##           and at each time point                 ##

EMT <- matrix(nrow=10,ncol=20)

for(i in 1:20){
  EMT[,i] <- cumsum(E1[,i])
}

## Write Table 6 to CSV ##

write.csv(t(round(EMT,2)),"table6.csv",row.names=F)

## Calculating St Matrix ##

St <- apply(t(EMT),2,FUN=function(x){cumsum(x)})


## Generating Control Limits ##

table7 <- matrix(nrow=20,ncol=10)
table71 <- matrix(nrow=20,ncol=10)
table8 <- matrix(nrow=20,ncol=10)
table81 <- matrix(nrow=20,ncol=10)
table9 <- matrix(nrow=20,ncol=10)
table91 <- matrix(nrow=20,ncol=10)
```

```
## First Limits when S0 = 0 ##


for(j in 1:10){
  table7[,j] <- round(-qnorm(alpha1/2)*sqrt(streams[j]),1)
  table71[,j]<- round(qnorm(alpha1/2)*sqrt(streams[j]),1)
  table8[,j] <- round(-qnorm(alpha2/2)*sqrt(streams[j]),1)
  table81[,j] <- round(qnorm(alpha2/2)*sqrt(streams[j]),1)
  table9[,j] <- round(-qnorm(alpha3/2)*sqrt(streams[j]),1)
  table91[,j] <- round(qnorm(alpha2/2)*sqrt(streams[j]),1)


}


for(i in 2:20){
  for(j in 1:10){


    table7[i,j] <- round(qnorm(alpha1/2,mean=St[(i-
1),j],sd=sqrt(streams[j]),lower.tail=F),1)


    table71[i,j] <- round(qnorm(alpha1/2,mean=St[(i-
1),j],sd=sqrt(streams[j]),lower.tail=T),1)


    table8[i,j] <- round(qnorm(alpha2/2,mean=St[(i-
1),j],sd=sqrt(streams[j]),lower.tail=F),1)


    table81[i,j] <- round(qnorm(alpha2/2,mean=St[(i-
1),j],sd=sqrt(streams[j]),lower.tail=T),1)


    table9[i,j] <- round(qnorm(alpha3/2,mean=St[(i-
1),j],sd=sqrt(streams[j]),lower.tail=F),1)


    table91[i,j] <- round(qnorm(alpha3/2,mean=St[(i-
1),j],sd=sqrt(streams[j]),lower.tail=T),1)
```

```
    }
}


big_table7 <- matrix(nrow=20,ncol=10)
big_table8 <- matrix(nrow=20,ncol=10)
big_table9 <- matrix(nrow=20,ncol=10)


for(i in 1:20){
  for(j in 1:10){
    big_table7[i,j] <- paste(paste(table71[i,j],",",
sep=""),table7[i,j],sep=" ")
    big_table8[i,j] <- paste(paste(table81[i,j],",",
sep=""),table8[i,j],sep=" ")
    big_table9[i,j] <- paste(paste(table91[i,j],",",
sep=""),table9[i,j],sep=" ")
    }
}


write.csv(big_table7,"table7.csv",row.names=F)
write.csv(big_table8,"table8.csv",row.names=F)
write.csv(big_table9,"table9.csv",row.names=F)
```

```
## Building OC Curves ##

## C, CA, & Alpha can be Modified ##

library(ggplot2)

spec_alpha <- 0.005
p0 <- 0.5
gamma_1 <- as.matrix(seq(0,0.49,by=0.001))
C <- 1
CA <- 1
C0 <- C - CA
sample_s1ze1 <- 10
sample_s1ze2 <- 20
sample_s1ze3 <- 30
sample_s1ze4 <- 40
sample_s1ze5 <- 50
sample_s1ze6 <- 100
n_ca1 <- CA*sample_s1ze1
n_ca2 <- CA*sample_s1ze2
n_ca3 <- CA*sample_s1ze3
n_ca4 <- CA*sample_s1ze4
n_ca5 <- CA*sample_s1ze5
n_ca6 <- CA*sample_s1ze6

theta_parm <- matrix(ncol=1,nrow=length(gamma_1))
eps_parm1 <- matrix(ncol=1,nrow=length(gamma_1))
eps_parm2 <- matrix(ncol=1,nrow=length(gamma_1))
eps_parm3 <- matrix(ncol=1,nrow=length(gamma_1))
eps_parm4 <- matrix(ncol=1,nrow=length(gamma_1))
```

```
eps_parm5 <- matrix(ncol=1,nrow=length(gamma_1))

eps_parm6 <- matrix(ncol=1,nrow=length(gamma_1))


for(i in 1:length(gamma_1)){

  theta_parm[i] <- 1/sqrt(1-(gamma_1[i]/(1-
p0))+(gamma_1[i]/p0)-(gamma_1[i]^2/(p0*(1-p0))))

  eps_parm1[i] <- (n_ca1*gamma_1[i])/sqrt(n_ca1*p0*(1-
p0)*(1-(gamma_1[i]/(1-p0))+(gamma_1[i]/p0)-
(gamma_1[i]^2/(p0*(1-p0)))))

  eps_parm2[i] <- (n_ca2*gamma_1[i])/sqrt(n_ca2*p0*(1-
p0)*(1-(gamma_1[i]/(1-p0))+(gamma_1[i]/p0)-
(gamma_1[i]^2/(p0*(1-p0)))))

  eps_parm3[i] <- (n_ca3*gamma_1[i])/sqrt(n_ca3*p0*(1-
p0)*(1-(gamma_1[i]/(1-p0))+(gamma_1[i]/p0)-
(gamma_1[i]^2/(p0*(1-p0)))))

  eps_parm4[i] <- (n_ca4*gamma_1[i])/sqrt(n_ca4*p0*(1-
p0)*(1-(gamma_1[i]/(1-p0))+(gamma_1[i]/p0)-
(gamma_1[i]^2/(p0*(1-p0)))))

  eps_parm5[i] <- (n_ca5*gamma_1[i])/sqrt(n_ca5*p0*(1-
p0)*(1-(gamma_1[i]/(1-p0))+(gamma_1[i]/p0)-
(gamma_1[i]^2/(p0*(1-p0)))))

  eps_parm6[i] <- (n_ca6*gamma_1[i])/sqrt(n_ca6*p0*(1-
p0)*(1-(gamma_1[i]/(1-p0))+(gamma_1[i]/p0)-
(gamma_1[i]^2/(p0*(1-p0)))))

}


alt_EMT1 <- matrix(nrow=1000,ncol=length(gamma_1))

alt_EMT2 <- matrix(nrow=1000,ncol=length(gamma_1))

alt_EMT3 <- matrix(nrow=1000,ncol=length(gamma_1))

alt_EMT4 <- matrix(nrow=1000,ncol=length(gamma_1))

alt_EMT5 <- matrix(nrow=1000,ncol=length(gamma_1))

alt_EMT6 <- matrix(nrow=1000,ncol=length(gamma_1))
```

```
for(i in 1:length(gamma_1)){

  alt_EMT1[,i] <- rnorm(1000,mean=-
eps_parm1[i],sd=sqrt(theta_parm[i]*CA))

  alt_EMT2[,i] <- rnorm(1000,mean=-
eps_parm2[i],sd=sqrt(theta_parm[i]*CA))

  alt_EMT3[,i] <- rnorm(1000,mean=-
eps_parm3[i],sd=sqrt(theta_parm[i]*CA))

  alt_EMT4[,i] <- rnorm(1000,mean=-
eps_parm4[i],sd=sqrt(theta_parm[i]*CA))

  alt_EMT5[,i] <- rnorm(1000,mean=-
eps_parm5[i],sd=sqrt(theta_parm[i]*CA))

  alt_EMT6[,i] <- rnorm(1000,mean=-
eps_parm6[i],sd=sqrt(theta_parm[i]*CA))

}


alt_St1 <- apply(alt_EMT1,2,FUN=function(x){cumsum(x)})

alt_St2 <- apply(alt_EMT2,2,FUN=function(x){cumsum(x)})

alt_St3 <- apply(alt_EMT3,2,FUN=function(x){cumsum(x)})

alt_St4 <- apply(alt_EMT4,2,FUN=function(x){cumsum(x)})

alt_St5 <- apply(alt_EMT5,2,FUN=function(x){cumsum(x)})

alt_St6 <- apply(alt_EMT6,2,FUN=function(x){cumsum(x)})


## Calculate Control L1m1ts ##


UCL1 <- matrix(nrow=1000,ncol=length(gamma_1))

LCL1 <- matrix(nrow=1000,ncol=length(gamma_1))

UCL2 <- matrix(nrow=1000,ncol=length(gamma_1))

LCL2 <- matrix(nrow=1000,ncol=length(gamma_1))

UCL3 <- matrix(nrow=1000,ncol=length(gamma_1))

LCL3 <- matrix(nrow=1000,ncol=length(gamma_1))

UCL4 <- matrix(nrow=1000,ncol=length(gamma_1))

LCL4 <- matrix(nrow=1000,ncol=length(gamma_1))
```

```
UCL5 <- matrix(nrow=1000,ncol=length(gamma_1))
LCL5 <- matrix(nrow=1000,ncol=length(gamma_1))
UCL6 <- matrix(nrow=1000,ncol=length(gamma_1))
LCL6 <- matrix(nrow=1000,ncol=length(gamma_1))

UCL1[1,] <- -qnorm(spec_alpha/2)*sqrt(C)
LCL1[1,] <- qnorm(spec_alpha/2)*sqrt(C)
UCL2[1,] <- -qnorm(spec_alpha/2)*sqrt(C)
LCL2[1,] <- qnorm(spec_alpha/2)*sqrt(C)
UCL3[1,] <- -qnorm(spec_alpha/2)*sqrt(C)
LCL3[1,] <- qnorm(spec_alpha/2)*sqrt(C)
UCL4[1,] <- -qnorm(spec_alpha/2)*sqrt(C)
LCL4[1,] <- qnorm(spec_alpha/2)*sqrt(C)
UCL5[1,] <- -qnorm(spec_alpha/2)*sqrt(C)
LCL5[1,] <- qnorm(spec_alpha/2)*sqrt(C)
UCL6[1,] <- -qnorm(spec_alpha/2)*sqrt(C)
LCL6[1,] <- qnorm(spec_alpha/2)*sqrt(C)
```

```
for(i in 2:1000){

  for(j in 1:length(gamma_1)){

    UCL1[i,j] <- qnorm(spec_alpha/2,mean=alt_St1[(i-
1),j],sd=sqrt(C),lower.tail=F)

    LCL1[i,j] <- qnorm(spec_alpha/2,mean=alt_St1[(i-
1),j],sd=sqrt(C),lower.tail=T)

    UCL2[i,j] <- qnorm(spec_alpha/2,mean=alt_St2[(i-
1),j],sd=sqrt(C),lower.tail=F)

    LCL2[i,j] <- qnorm(spec_alpha/2,mean=alt_St2[(i-
1),j],sd=sqrt(C),lower.tail=T)

    UCL3[i,j] <- qnorm(spec_alpha/2,mean=alt_St3[(i-
1),j],sd=sqrt(C),lower.tail=F)

    LCL3[i,j] <- qnorm(spec_alpha/2,mean=alt_St3[(i-
1),j],sd=sqrt(C),lower.tail=T)

    UCL4[i,j] <- qnorm(spec_alpha/2,mean=alt_St4[(i-
1),j],sd=sqrt(C),lower.tail=F)

    LCL4[i,j] <- qnorm(spec_alpha/2,mean=alt_St4[(i-
1),j],sd=sqrt(C),lower.tail=T)

    UCL5[i,j] <- qnorm(spec_alpha/2,mean=alt_St5[(i-
1),j],sd=sqrt(C),lower.tail=F)

    LCL5[i,j] <- qnorm(spec_alpha/2,mean=alt_St5[(i-
1),j],sd=sqrt(C),lower.tail=T)

    UCL6[i,j] <- qnorm(spec_alpha/2,mean=alt_St6[(i-
1),j],sd=sqrt(C),lower.tail=F)

    LCL6[i,j] <- qnorm(spec_alpha/2,mean=alt_St6[(i-
1),j],sd=sqrt(C),lower.tail=T)

  }

}


## Calculat1ng Beta ##


b1 <- matrix(nrow=1000,ncol=length(gamma_1))

b2 <- matrix(nrow=1000,ncol=length(gamma_1))

b3 <- matrix(nrow=1000,ncol=length(gamma_1))
```

```
b4 <- matrix(nrow=1000,ncol=length(gamma_1))

b5 <- matrix(nrow=1000,ncol=length(gamma_1))

b6 <- matrix(nrow=1000,ncol=length(gamma_1))


for(j in 1:length(gamma_1)){

  b1[1,j] <- pnorm(UCL1[1,j],mean=(-
eps_parm1[j]),sd=sqrt(C0+CA*theta_parm[j]),lower.tail=T) -

                   pnorm(LCL1[1,j],mean=(-
eps_parm1[j]),sd=sqrt(C0+CA*theta_parm[j]),lower.tail=T)


  b2[1,j] <- pnorm(UCL2[1,j],mean=(-
eps_parm2[j]),sd=sqrt(C0+CA*theta_parm[j]),lower.tail=T) -

                   pnorm(LCL2[1,j],mean=(-
eps_parm2[j]),sd=sqrt(C0+CA*theta_parm[j]),lower.tail=T)


  b3[1,j] <- pnorm(UCL3[1,j],mean=(-
eps_parm3[j]),sd=sqrt(C0+CA*theta_parm[j]),lower.tail=T) -

                   pnorm(LCL3[1,j],mean=(-
eps_parm3[j]),sd=sqrt(C0+CA*theta_parm[j]),lower.tail=T)


  b4[1,j] <- pnorm(UCL4[1,j],mean=(-
eps_parm4[j]),sd=sqrt(C0+CA*theta_parm[j]),lower.tail=T) -

                   pnorm(LCL4[1,j],mean=(-
eps_parm4[j]),sd=sqrt(C0+CA*theta_parm[j]),lower.tail=T)


  b5[1,j] <- pnorm(UCL5[1,j],mean=(-
eps_parm5[j]),sd=sqrt(C0+CA*theta_parm[j]),lower.tail=T) -

                  pnorm(LCL5[1,j],mean=(-
eps_parm5[j]),sd=sqrt(C0+CA*theta_parm[j]),lower.tail=T)


  b6[1,j] <- pnorm(UCL6[1,j],mean=(-
eps_parm6[j]),sd=sqrt(C0+CA*theta_parm[j]),lower.tail=T) -

                   pnorm(LCL6[1,j],mean=(-
eps_parm6[j]),sd=sqrt(C0+CA*theta_parm[j]),lower.tail=T)}
```

```
for(i in 2:1000){

  for(j in 1:length(gamma_1)){

    b1[i,j] <- pnorm(UCL1[i,j],mean=(alt_St1[(i-1),j] -
eps_parm1[j]),sd=sqrt(C0+CA*theta_parm[j]),lower.tail=T) -

                      pnorm(LCL1[i,j],mean=(alt_St1[(i-1),j]
- eps_parm1[j]),sd=sqrt(C0+CA*theta_parm[j]),lower.tail=T)


    b2[i,j] <- pnorm(UCL2[i,j],mean=(alt_St2[(i-1),j] -
eps_parm2[j]),sd=sqrt(C0+CA*theta_parm[j]),lower.tail=T) -

                      pnorm(LCL2[i,j],mean=(alt_St2[(i-1),j]
- eps_parm2[j]),sd=sqrt(C0+CA*theta_parm[j]),lower.tail=T)


    b3[i,j] <- pnorm(UCL3[i,j],mean=(alt_St3[(i-1),j] -
eps_parm3[j]),sd=sqrt(C0+CA*theta_parm[j]),lower.tail=T) -

                      pnorm(LCL3[i,j],mean=(alt_St3[(i-1),j]
- eps_parm3[j]),sd=sqrt(C0+CA*theta_parm[j]),lower.tail=T)


    b4[i,j] <- pnorm(UCL4[i,j],mean=(alt_St4[(i-1),j] -
eps_parm4[j]),sd=sqrt(C0+CA*theta_parm[j]),lower.tail=T) -

                      pnorm(LCL4[i,j],mean=(alt_St4[(i-1),j]
- eps_parm4[j]),sd=sqrt(C0+CA*theta_parm[j]),lower.tail=T)


    b5[i,j] <- pnorm(UCL5[i,j],mean=(alt_St5[(i-1),j] -
eps_parm5[j]),sd=sqrt(C0+CA*theta_parm[j]),lower.tail=T) -

                      pnorm(LCL5[i,j],mean=(alt_St5[(i-1),j]
- eps_parm5[j]),sd=sqrt(C0+CA*theta_parm[j]),lower.tail=T)


    b6[i,j] <- pnorm(UCL6[i,j],mean=(alt_St6[(i-1),j] -
eps_parm6[j]),sd=sqrt(C0+CA*theta_parm[j]),lower.tail=T) -

                      pnorm(LCL6[i,j],mean=(alt_St6[(i-1),j]
-
eps_parm6[j]),sd=sqrt(C0+CA*theta_parm[j]),lower.tail=T)}}
```

```
b11 <- apply(b1,2,mean)
b21 <- apply(b2,2,mean)
b31 <- apply(b3,2,mean)
b41 <- apply(b4,2,mean)
b51 <- apply(b5,2,mean)
b61 <- apply(b6,2,mean)


colz <- c('n = 10' = 'red', 'n = 20' = 'blue', 'n = 30' =
'green', 'n = 40' = 'purple', 'n = 50' = 'pink',
          'n = 100' = 'black')


ggplot() +
  geom_line(aes(x = gamma_1, y = b11, col = 'n = 10')) +
  geom_line(aes(x = gamma_1, y = b21, col = 'n = 20')) +
  geom_line(aes(x = gamma_1, y = b31, col = 'n = 30')) +
  geom_line(aes(x = gamma_1, y = b41, col = 'n = 40')) +
  geom_line(aes(x = gamma_1, y = b51, col = 'n = 50')) +
  geom_line(aes(x = gamma_1, y = b61, col = 'n = 100'))+
  labs(x = expression(gamma), y = expression(beta)) +
  theme_classic() + ggtitle(bquote("C = 1," ~ C[A] == 1 ~",
and"~ alpha == 0.005)) +
  theme(plot.title = element_text(hjust=0.5)) +
  scale_color_manual(name = "Sample Size", values = colz,
                     limits = c('n = 10', 'n = 20', 'n =
30', 'n = 40', 'n = 50', 'n = 100'))
```

```
## Dissertation Simulation ##

## Estimating ARL1 for NEMT-CUSUM ##

library(foreach)
library(doParallel)

no_cores <- detectCores() - 1

cl <- makeCluster(no_cores)

registerDoParallel(cl)

## Setting Parameters ##

specified_alpha <- 0.0027

p0 <- 0.5

c <- 10
N <- 100
n <- N/c
big_sim_size <- 10000
```

```
EMT_function <-
function(o1,o2,o3,o4,o5,o6,o7,o8,o9,o10,n,p0){
  return(sum((o1-n*p0)/sqrt(n*p0*(1-p0)),
             (o2-n*p0)/sqrt(n*p0*(1-p0)),
             (o3-n*p0)/sqrt(n*p0*(1-p0)),
             (o4-n*p0)/sqrt(n*p0*(1-p0)),
             (o5-n*p0)/sqrt(n*p0*(1-p0)),
             (o6-n*p0)/sqrt(n*p0*(1-p0)),
             (o7-n*p0)/sqrt(n*p0*(1-p0)),
             (o8-n*p0)/sqrt(n*p0*(1-p0)),
             (o9-n*p0)/sqrt(n*p0*(1-p0)),
             (o10-n*p0)/sqrt(n*p0*(1-p0))))
}


## Estimating ARL1 Using Normal(1,1) ##


## Specifiy IC-Mean/Median ##


mu0 <- 1
```

```
## Apply Option Using doParallel ##


apply_function <- function(n,mu0,p0,delta){
    s1 <- rnorm(n,mean=1*delta,sd=1)
    s2 <- rnorm(n,mean=1*delta,sd=1)
    s3 <- rnorm(n,mean=1*delta,sd=1)
    s4 <- rnorm(n,mean=1*delta,sd=1)
    s5 <- rnorm(n,mean=1*delta,sd=1)
    s6 <- rnorm(n,mean=1,sd=1)
    s7 <- rnorm(n,mean=1,sd=1)
    s8 <- rnorm(n,mean=1,sd=1)
    s9 <- rnorm(n,mean=1,sd=1)
    s10 <- rnorm(n,mean=1,sd=1)


    o1 <- ifelse(is.na(table(s1 > mu0)[2]) ==
'TRUE',0,table(s1 > mu0)[2])
    o2 <- ifelse(is.na(table(s2 > mu0)[2]) ==
'TRUE',0,table(s2 > mu0)[2])
    o3 <- ifelse(is.na(table(s3 > mu0)[2]) ==
'TRUE',0,table(s3 > mu0)[2])
    o4 <- ifelse(is.na(table(s4 > mu0)[2]) ==
'TRUE',0,table(s4 > mu0)[2])
    o5 <- ifelse(is.na(table(s5 > mu0)[2]) ==
'TRUE',0,table(s5 > mu0)[2])
    o6 <- ifelse(is.na(table(s6 > mu0)[2]) ==
'TRUE',0,table(s6 > mu0)[2])
    o7 <- ifelse(is.na(table(s7 > mu0)[2]) ==
'TRUE',0,table(s7 > mu0)[2])
    o8 <- ifelse(is.na(table(s8 > mu0)[2]) ==
'TRUE',0,table(s8 > mu0)[2])
    o9 <- ifelse(is.na(table(s9 > mu0)[2]) ==
'TRUE',0,table(s9 > mu0)[2])
    o10 <- ifelse(is.na(table(s10 > mu0)[2]) ==
'TRUE',0,table(s10 > mu0)[2])
```

```
return(EMT_function(o1,o2,o3,o4,o5,o6,o7,o8,o9,o10,n,p0))
}

## Size of Shift to be Tested ##

delta <- 1

## While Looping ##

sim_time <- system.time({
arlz1 <- foreach(icount(big_sim_size),.combine = rbind)
%dopar% {
EMT <- c()
EMT[1] <- apply_function(n,mu0,p0,delta)
St <- c()
St[1] <- EMT[1]
UCL_t <- c()
LCL_t <- c()
cond_mu <- 0
UCL_t[1] <-
qnorm(specified_alpha/2,mean=cond_mu,sd=sqrt(c),lower.tail=
F)
LCL_t[1] <-
qnorm(specified_alpha/2,mean=cond_mu,sd=sqrt(c),lower.tail=
T)
i <- 1
```

```
while(St[i] < UCL_t[i] && St[i] > LCL_t[i]){
     EMT[i+1] <- apply_function(n,mu0,p0,delta)
     St[i+1]  <- sum(EMT[1:(i+1)])
     cond_mu  <- St[i]
     UCL_t[i+1] <-
qnorm(specified_alpha/2,mean=cond_mu,sd=sqrt(c),lower.tail=
F)
     LCL_t[i+1] <-
qnorm(specified_alpha/2,mean=cond_mu,sd=sqrt(c),lower.tail=
T)
     i <- i + 1
     }
i
}})


sim_time[3]
mean(arlz1)


## Estimating ARL1 Using UNIF(0,1) ##


## Specifiy IC-Mean/Median ##


mu0 <- 0.50


## Apply Option Using doParallel ##


apply_function <- function(n,mu0,p0,delta){
  s1 <- runif(n,min=0,max=1*delta)
  s2 <- runif(n,min=0,max=1*delta)
  s3 <- runif(n,min=0,max=1*delta)
  s4 <- runif(n,min=0,max=1*delta)
```

```
  s5 <- runif(n,min=0,max=1*delta)

  s6 <- runif(n,min=0,max=1)

  s7 <- runif(n,min=0,max=1)

  s8 <- runif(n,min=0,max=1)

  s9 <- runif(n,min=0,max=1)

  s10 <- runif(n,min=0,max=1)


  o1 <- ifelse(is.na(table(s1 > mu0)[2]) ==
'TRUE',0,table(s1 > mu0)[2])

  o2 <- ifelse(is.na(table(s2 > mu0)[2]) ==
'TRUE',0,table(s2 > mu0)[2])

  o3 <- ifelse(is.na(table(s3 > mu0)[2]) ==
'TRUE',0,table(s3 > mu0)[2])

  o4 <- ifelse(is.na(table(s4 > mu0)[2]) ==
'TRUE',0,table(s4 > mu0)[2])

  o5 <- ifelse(is.na(table(s5 > mu0)[2]) ==
'TRUE',0,table(s5 > mu0)[2])

  o6 <- ifelse(is.na(table(s6 > mu0)[2]) ==
'TRUE',0,table(s6 > mu0)[2])

  o7 <- ifelse(is.na(table(s7 > mu0)[2]) ==
'TRUE',0,table(s7 > mu0)[2])

  o8 <- ifelse(is.na(table(s8 > mu0)[2]) ==
'TRUE',0,table(s8 > mu0)[2])

  o9 <- ifelse(is.na(table(s9 > mu0)[2]) ==
'TRUE',0,table(s9 > mu0)[2])

  o10 <- ifelse(is.na(table(s10 > mu0)[2]) ==
'TRUE',0,table(s10 > mu0)[2])


  return(EMT_function(o1,o2,o3,o4,o5,o6,o7,o8,o9,o10,n,p0))

}
```

```
## Size of Shift to be Tested ##


delta <- 1


## While Looping ##


sim_time <- system.time({
  arlz1 <- foreach(icount(big_sim_size),.combine = rbind)
%dopar% {
    EMT <- c()
    EMT[1] <- apply_function(n,mu0,p0,delta)
    St <- c()
    St[1] <- EMT[1]
    UCL_t <- c()
    LCL_t <- c()
    cond_mu <- 0
    UCL_t[1] <-
qnorm(specified_alpha/2,mean=cond_mu,sd=sqrt(c),lower.tail=
F)
    LCL_t[1] <-
qnorm(specified_alpha/2,mean=cond_mu,sd=sqrt(c),lower.tail=
T)
    i <- 1
    while(St[i] < UCL_t[i] && St[i] > LCL_t[i]){
      EMT[i+1] <- apply_function(n,mu0,p0,delta)
      St[i+1]  <- sum(EMT[1:(i+1)])
      cond_mu  <- St[i]
      UCL_t[i+1] <-
qnorm(specified_alpha/2,mean=cond_mu,sd=sqrt(c),lower.tail=
F)
      LCL_t[i+1] <-
qnorm(specified_alpha/2,mean=cond_mu,sd=sqrt(c),lower.tail=
T)
```

```
      i <- i + 1
    }
    i
  }})

sim_time[3]
mean(arlz1)

## Estimating ARL1 Using Laplace(1,1) ##

library(rmutil)

## Specifiy IC-Mean/Median ##

mu0 <- 1

## Apply Option Using doParallel ##

apply_function <- function(n,mu0,p0,delta){
  s1 <- rlaplace(n,m=1*delta,s=1)
  s2 <- rlaplace(n,m=1*delta,s=1)
  s3 <- rlaplace(n,m=1*delta,s=1)
  s4 <- rlaplace(n,m=1*delta,s=1)
  s5 <- rlaplace(n,m=1*delta,s=1)
  s6 <- rlaplace(n,m=1,s=1)
  s7 <- rlaplace(n,m=1,s=1)
  s8 <- rlaplace(n,m=1,s=1)
  s9 <- rlaplace(n,m=1,s=1)
  s10 <- rlaplace(n,m=1,s=1)
```

```
  o1 <- ifelse(is.na(table(s1 > mu0)[2]) ==
'TRUE',0,table(s1 > mu0)[2])

  o2 <- ifelse(is.na(table(s2 > mu0)[2]) ==
'TRUE',0,table(s2 > mu0)[2])

  o3 <- ifelse(is.na(table(s3 > mu0)[2]) ==
'TRUE',0,table(s3 > mu0)[2])

  o4 <- ifelse(is.na(table(s4 > mu0)[2]) ==
'TRUE',0,table(s4 > mu0)[2])

  o5 <- ifelse(is.na(table(s5 > mu0)[2]) ==
'TRUE',0,table(s5 > mu0)[2])

  o6 <- ifelse(is.na(table(s6 > mu0)[2]) ==
'TRUE',0,table(s6 > mu0)[2])

  o7 <- ifelse(is.na(table(s7 > mu0)[2]) ==
'TRUE',0,table(s7 > mu0)[2])

  o8 <- ifelse(is.na(table(s8 > mu0)[2]) ==
'TRUE',0,table(s8 > mu0)[2])

  o9 <- ifelse(is.na(table(s9 > mu0)[2]) ==
'TRUE',0,table(s9 > mu0)[2])

  o10 <- ifelse(is.na(table(s10 > mu0)[2]) ==
'TRUE',0,table(s10 > mu0)[2])


  return(EMT_function(o1,o2,o3,o4,o5,o6,o7,o8,o9,o10,n,p0))
}


## Size of Shift to be Tested ##


delta <- 1
```

```
## While Looping ##


sim_time <- system.time({

  arlz1 <-
foreach(icount(big_sim_size),.packages=c("rmutil"),.combine
= rbind) %dopar% {

    EMT <- c()

    EMT[1] <- apply_function(n,mu0,p0,delta)

    St <- c()

    St[1] <- EMT[1]

    UCL_t <- c()

    LCL_t <- c()

    cond_mu <- 0

    UCL_t[1] <-
qnorm(specified_alpha/2,mean=cond_mu,sd=sqrt(c),lower.tail=
F)

    LCL_t[1] <-
qnorm(specified_alpha/2,mean=cond_mu,sd=sqrt(c),lower.tail=
T)

    i <- 1

    while(St[i] < UCL_t[i] && St[i] > LCL_t[i]){

      EMT[i+1] <- apply_function(n,mu0,p0,delta)

      St[i+1]  <- sum(EMT[1:(i+1)])

      cond_mu  <- St[i]

      UCL_t[i+1] <-
qnorm(specified_alpha/2,mean=cond_mu,sd=sqrt(c),lower.tail=
F)

      LCL_t[i+1] <-
qnorm(specified_alpha/2,mean=cond_mu,sd=sqrt(c),lower.tail=
T)

      i <- i + 1

    }

    i

  }})
```

```
sim_time[3]
mean(arlz1)

## Estimating ARL1 Using EXP(1) ##

## Specifiy IC-Mean/Median ##

mu0 <- 1
med <- mu0*log(2)

## Apply Option Using doParallel ##

apply_function <- function(n,mu0,p0,delta){
  s1 <- rexp(n,rate=mu0*delta)
  s2 <- rexp(n,rate=mu0*delta)
  s3 <- rexp(n,rate=mu0*delta)
  s4 <- rexp(n,rate=mu0*delta)
  s5 <- rexp(n,rate=mu0*delta)
  s6 <- rexp(n,rate=mu0)
  s7 <- rexp(n,rate=mu0)
  s8 <- rexp(n,rate=mu0)
  s9 <- rexp(n,rate=mu0)
  s10 <- rexp(n,rate=mu0)

  o1 <- ifelse(is.na(table(s1 > med)[2]) ==
'TRUE',0,table(s1 > med)[2])
  o2 <- ifelse(is.na(table(s2 > med)[2]) ==
'TRUE',0,table(s2 > med)[2])
  o3 <- ifelse(is.na(table(s3 > med)[2]) ==
'TRUE',0,table(s3 > med)[2])
```

```
  o4 <- ifelse(is.na(table(s4 > med)[2]) ==
'TRUE',0,table(s4 > med)[2])

  o5 <- ifelse(is.na(table(s5 > med)[2]) ==
'TRUE',0,table(s5 > med)[2])

  o6 <- ifelse(is.na(table(s6 > med)[2]) ==
'TRUE',0,table(s6 > med)[2])

  o7 <- ifelse(is.na(table(s7 > med)[2]) ==
'TRUE',0,table(s7 > med)[2])

  o8 <- ifelse(is.na(table(s8 > med)[2]) ==
'TRUE',0,table(s8 > med)[2])

  o9 <- ifelse(is.na(table(s9 > med)[2]) ==
'TRUE',0,table(s9 > med)[2])

  o10 <- ifelse(is.na(table(s10 > med)[2]) ==
'TRUE',0,table(s10 > med)[2])


  return(EMT_function(o1,o2,o3,o4,o5,o6,o7,o8,o9,o10,n,p0))
}


## Size of Shift to be Tested ##


delta <- 1
```

```
## While Looping ##

sim_time <- system.time({

  arlz1 <-
foreach(icount(big_sim_size),.packages=c("rmutil"),.combine
= rbind) %dopar% {

    EMT <- c()

    EMT[1] <- apply_function(n,mu0,p0,delta)

    St <- c()

    St[1] <- EMT[1]

    UCL_t <- c()

    LCL_t <- c()

    cond_mu <- 0

    UCL_t[1] <-
qnorm(specified_alpha/2,mean=cond_mu,sd=sqrt(c),lower.tail=
F)

    LCL_t[1] <-
qnorm(specified_alpha/2,mean=cond_mu,sd=sqrt(c),lower.tail=
T)

    i <- 1

    while(St[i] < UCL_t[i] && St[i] > LCL_t[i]){

      EMT[i+1] <- apply_function(n,mu0,p0,delta)

      St[i+1]  <- sum(EMT[1:(i+1)])

      cond_mu  <- St[i]

      UCL_t[i+1] <-
qnorm(specified_alpha/2,mean=cond_mu,sd=sqrt(c),lower.tail=
F)

      LCL_t[i+1] <-
qnorm(specified_alpha/2,mean=cond_mu,sd=sqrt(c),lower.tail=
T)

      i <- i + 1

    }

    i

  }})

mean(arlz1)
```

```
## Boyd's GCC ARL1 Estimation ##

## Estimating Control Limits from Preliminary Samples ##

## IC Distribution == N(1,1) ##

m <- 25
n <- 10
d2 <- 3.078
C <- 10
Ca <- 5
delta <- seq(0.25,3,by=0.25)

Big_ARL <- c()

mu0 <- 1

samplez <- matrix(nrow = n, ncol = m)

for(i in 1:m){
  samplez[,i] <- rnorm(n,mean=mu0,sd=1)
}

xdbar <- mean(apply(samplez,2,mean))
rbar <- mean(apply(samplez,1,FUN=function(x){max(x) -
min(x)}))

UCL <- xdbar + 3*rbar/(d2*sqrt(n))
LCL <- xdbar - 3*rbar/(d2*sqrt(n))
```

```
## Phase II ##

## Generating Data ##

for(t in 1:length(delta)){

sim_size <- 100000

boyd_dat <- matrix(ncol=C,nrow=sim_size)

max_min <- matrix(ncol=2,nrow=sim_size)

boyd_arl <- c()

for(i in 1:sim_size){

boyd_dat[i,1] <- mean(rnorm(n,mean=mu0*delta[t],sd=1))
boyd_dat[i,2] <- mean(rnorm(n,mean=mu0*delta[t],sd=1))
boyd_dat[i,3] <- mean(rnorm(n,mean=mu0*delta[t],sd=1))
boyd_dat[i,4] <- mean(rnorm(n,mean=mu0*delta[t],sd=1))
boyd_dat[i,5] <- mean(rnorm(n,mean=mu0*delta[t],sd=1))
boyd_dat[i,6] <- mean(rnorm(n,mean=mu0,sd=1))
boyd_dat[i,7] <- mean(rnorm(n,mean=mu0,sd=1))
boyd_dat[i,8] <- mean(rnorm(n,mean=mu0,sd=1))
boyd_dat[i,9] <- mean(rnorm(n,mean=mu0,sd=1))
boyd_dat[i,10] <- mean(rnorm(n,mean=mu0,sd=1))

max_min[i,1] <- max(boyd_dat[i,])
max_min[i,2] <- min(boyd_dat[i,])
```

```
boyd_arl[i] <- ifelse(max_min[i,1] > UCL | max_min[i,1] <
LCL |
                          max_min[i,2] > UCL | max_min[i,2] <
LCL, i, 0)


  }



Big_ARL[t] <- mean(diff(boyd_arl[which(boyd_arl != 0)]))


}


Big_ARL <- cbind(delta,Big_ARL)


write.csv(Big_ARL,'Boyd_Norm.csv',row.names=F)


rm(list=ls())


## IC Distribution == UNIF(0,1) ##


m <- 25
n <- 10
d2 <- 3.078
C <- 10
Ca <- 5
delta <- seq(0.25,3,by=0.25)


Big_ARL <- c()


mu0 <- 0.50
```

```
samplez <- matrix(nrow = n, ncol = m)


for(i in 1:m){
  samplez[,i] <- runif(n,min=0,max=1)
}


xdbar <- mean(apply(samplez,2,mean))
rbar <- mean(apply(samplez,1,FUN=function(x){max(x) -
min(x)}))


UCL <- xdbar + 3*rbar/(d2*sqrt(n))
LCL <- xdbar - 3*rbar/(d2*sqrt(n))


## Phase II ##


## Generating Data ##


for(t in 1:length(delta)){


  sim_size <- 100000


  boyd_dat <- matrix(ncol=C,nrow=sim_size)


  max_min <- matrix(ncol=2,nrow=sim_size)


  boyd_arl <- c()


  for(i in 1:sim_size){


    boyd_dat[i,1] <- mean(runif(n,min=0,max=1*delta[t]))
```

```
    boyd_dat[i,2] <- mean(runif(n,min=0,max=1*delta[t]))
    boyd_dat[i,3] <- mean(runif(n,min=0,max=1*delta[t]))
    boyd_dat[i,4] <- mean(runif(n,min=0,max=1*delta[t]))
    boyd_dat[i,5] <- mean(runif(n,min=0,max=1*delta[t]))
    boyd_dat[i,6] <- mean(runif(n,min=0,max=1))
    boyd_dat[i,7] <- mean(runif(n,min=0,max=1))
    boyd_dat[i,8] <- mean(runif(n,min=0,max=1))
    boyd_dat[i,9] <- mean(runif(n,min=0,max=1))
    boyd_dat[i,10] <- mean(runif(n,min=0,max=1))

    max_min[i,1] <- max(boyd_dat[i,])
    max_min[i,2] <- min(boyd_dat[i,])

    boyd_arl[i] <- ifelse(max_min[i,1] > UCL | max_min[i,1]
< LCL | max_min[i,2] > UCL | max_min[i,2] < LCL, i, 0)
    }

  Big_ARL[t] <- mean(diff(boyd_arl[which(boyd_arl != 0)]))

}

Big_ARL <- cbind(delta,Big_ARL)

write.csv(Big_ARL,'Boyd_Unif.csv',row.names=F)

rm(list=ls())
```

```
## IC Distribution == Laplace(1,1) ##


library(rmutil)


m <- 25

n <- 10

d2 <- 3.078

C <- 10

Ca <- 5

delta <- seq(0.25,3,by=0.25)


Big_ARL <- c()


mu0 <- 1


samplez <- matrix(nrow = n, ncol = m)


for(i in 1:m){

  samplez[,i] <- rlaplace(n,m=mu0,s=1)

}


xdbar <- mean(apply(samplez,2,mean))

rbar <- mean(apply(samplez,1,FUN=function(x){max(x) -
min(x)}))


UCL <- xdbar + 3*rbar/(d2*sqrt(n))

LCL <- xdbar - 3*rbar/(d2*sqrt(n))
```

```
## Phase II ##

## Generating Data ##

for(t in 1:length(delta)){

  sim_size <- 100000

  boyd_dat <- matrix(ncol=C,nrow=sim_size)

  max_min <- matrix(ncol=2,nrow=sim_size)

  boyd_arl <- c()

  for(i in 1:sim_size){

    boyd_dat[i,1] <- mean(rlaplace(n,m=mu0*delta[t],s=1))
    boyd_dat[i,2] <- mean(rlaplace(n,m=mu0*delta[t],s=1))
    boyd_dat[i,3] <- mean(rlaplace(n,m=mu0*delta[t],s=1))
    boyd_dat[i,4] <- mean(rlaplace(n,m=mu0*delta[t],s=1))
    boyd_dat[i,5] <- mean(rlaplace(n,m=mu0*delta[t],s=1))
    boyd_dat[i,6] <- mean(rlaplace(n,m=mu0,s=1))
    boyd_dat[i,7] <- mean(rlaplace(n,m=mu0,s=1))
    boyd_dat[i,8] <- mean(rlaplace(n,m=mu0,s=1))
    boyd_dat[i,9] <- mean(rlaplace(n,m=mu0,s=1))
    boyd_dat[i,10] <- mean(rlaplace(n,m=mu0,s=1))

    max_min[i,1] <- max(boyd_dat[i,])
    max_min[i,2] <- min(boyd_dat[i,])
```

```
    boyd_arl[i] <- ifelse(max_min[i,1] > UCL | max_min[i,1]
< LCL | max_min[i,2] > UCL | max_min[i,2] < LCL, i, 0)
    }

  Big_ARL[t] <- mean(diff(boyd_arl[which(boyd_arl != 0)]))

}

Big_ARL <- cbind(delta,Big_ARL)

write.csv(Big_ARL,'Boyd_Laplace.csv',row.names=F)

rm(list=ls())

## IC Distribution == EXP(1) ##

m <- 25
n <- 10
d2 <- 3.078
C <- 10
Ca <- 5
delta <- seq(0.25,3,by=0.25)

Big_ARL <- c()

mu0 <- 1

samplez <- matrix(nrow = n, ncol = m)
```

```
for(i in 1:m){
  samplez[,i] <- rexp(n,rate=1)
}

xdbar <- mean(apply(samplez,2,mean))
rbar <- mean(apply(samplez,1,FUN=function(x){max(x) -
min(x)}))

UCL <- xdbar + 3*rbar/(d2*sqrt(n))
LCL <- xdbar - 3*rbar/(d2*sqrt(n))

## Phase II ##

## Generating Data ##

for(t in 1:length(delta)){

  sim_size <- 100000

  boyd_dat <- matrix(ncol=C,nrow=sim_size)

  max_min <- matrix(ncol=2,nrow=sim_size)

  boyd_arl <- c()

  for(i in 1:sim_size){

    boyd_dat[i,1] <- mean(rexp(n,rate=1*delta[t]))
    boyd_dat[i,2] <- mean(rexp(n,rate=1*delta[t]))
    boyd_dat[i,3] <- mean(rexp(n,rate=1*delta[t]))
```

```
    boyd_dat[i,4] <- mean(rexp(n,rate=1*delta[t]))
    boyd_dat[i,5] <- mean(rexp(n,rate=1*delta[t]))
    boyd_dat[i,6] <- mean(rexp(n,rate=1))
    boyd_dat[i,7] <- mean(rexp(n,rate=1))
    boyd_dat[i,8] <- mean(rexp(n,rate=1))
    boyd_dat[i,9] <- mean(rexp(n,rate=1))
    boyd_dat[i,10] <- mean(rexp(n,rate=1))

    max_min[i,1] <- max(boyd_dat[i,])
    max_min[i,2] <- min(boyd_dat[i,])

    boyd_arl[i] <- ifelse(max_min[i,1] > UCL | max_min[i,1]
< LCL | max_min[i,2] > UCL | max_min[i,2] < LCL, i, 0)
    }

  Big_ARL[t] <- mean(diff(boyd_arl[which(boyd_arl != 0)]))

}

Big_ARL <- cbind(delta,Big_ARL)

write.csv(Big_ARL,'Boyd_Exp.csv',row.names=F)
```

```
## Mortell & Runger's Rt Shewhart Chart ##
##           ARL1 Estimation            ##

## IC Distribution == N(1,1) ##

bootz <- 100000
n <- 10
C <- 10
mu0 <- 1
delta <- seq(0.25,3,by=0.25)

mr_dat <- matrix(ncol=C,nrow=bootz)

for(i in 1:bootz){
mr_dat[i,1] <- mean(rnorm(n,mean=mu0,sd=1))
mr_dat[i,2] <- mean(rnorm(n,mean=mu0,sd=1))
mr_dat[i,3] <- mean(rnorm(n,mean=mu0,sd=1))
mr_dat[i,4] <- mean(rnorm(n,mean=mu0,sd=1))
mr_dat[i,5] <- mean(rnorm(n,mean=mu0,sd=1))
mr_dat[i,6] <- mean(rnorm(n,mean=mu0,sd=1))
mr_dat[i,7] <- mean(rnorm(n,mean=mu0,sd=1))
mr_dat[i,8] <- mean(rnorm(n,mean=mu0,sd=1))
mr_dat[i,9] <- mean(rnorm(n,mean=mu0,sd=1))
mr_dat[i,10] <- mean(rnorm(n,mean=mu0,sd=1))
}

initial_rangez <- apply(mr_dat,1,FUN=function(x){max(x)-
min(x)})

UCL <- quantile(initial_rangez, probs = c(0.99865))
```

```
LCL <- quantile(initial_rangez, probs = c(0.00135))

## Phase II ##

## Generating Data ##

Big_ARL <- c()

for(t in 1:length(delta)){

mr_dat1 <- matrix(ncol=C,nrow=bootz)
rt <- c()
rt_arl <- c()

for(i in 1:bootz){

  mr_dat1[i,1] <- mean(rnorm(n,mean=mu0*delta[t],sd=1))
  mr_dat1[i,2] <- mean(rnorm(n,mean=mu0*delta[t],sd=1))
  mr_dat1[i,3] <- mean(rnorm(n,mean=mu0*delta[t],sd=1))
  mr_dat1[i,4] <- mean(rnorm(n,mean=mu0*delta[t],sd=1))
  mr_dat1[i,5] <- mean(rnorm(n,mean=mu0*delta[t],sd=1))
  mr_dat1[i,6] <- mean(rnorm(n,mean=mu0,sd=1))
  mr_dat1[i,7] <- mean(rnorm(n,mean=mu0,sd=1))
  mr_dat1[i,8] <- mean(rnorm(n,mean=mu0,sd=1))
  mr_dat1[i,9] <- mean(rnorm(n,mean=mu0,sd=1))
  mr_dat1[i,10] <- mean(rnorm(n,mean=mu0,sd=1))

  rt[i] <- max(mr_dat1[i,]) - min(mr_dat1[i,])

  rt_arl[i] <- ifelse(rt[i] > UCL | rt[i] < LCL, i, 0)
```

```
  }

Big_ARL[t] <- mean(diff(rt_arl[which(rt_arl != 0)]))

}

Big_ARL <- cbind(delta,Big_ARL)

write.csv(Big_ARL,'MR_Norm.csv',row.names=F)

rm(list = ls())

## IC Distribution == UNIF(0,1) ##

bootz <- 100000
n <- 10
C <- 10
mu0 <- 0.5
delta <- seq(0.25,3,by=0.25)

mr_dat <- matrix(ncol=C,nrow=bootz)

for(i in 1:bootz){
  mr_dat[i,1] <- mean(runif(n,min=0,max=1))
  mr_dat[i,2] <- mean(runif(n,min=0,max=1))
  mr_dat[i,3] <- mean(runif(n,min=0,max=1))
  mr_dat[i,4] <- mean(runif(n,min=0,max=1))
  mr_dat[i,5] <- mean(runif(n,min=0,max=1))
  mr_dat[i,6] <- mean(runif(n,min=0,max=1))
```

```
  mr_dat[i,7] <- mean(runif(n,min=0,max=1))
  mr_dat[i,8] <- mean(runif(n,min=0,max=1))
  mr_dat[i,9] <- mean(runif(n,min=0,max=1))
  mr_dat[i,10] <- mean(runif(n,min=0,max=1))
}

initial_rangez <- apply(mr_dat,1,FUN=function(x){max(x)-
min(x)})

UCL <- quantile(initial_rangez, probs = c(0.99865))
LCL <- quantile(initial_rangez, probs = c(0.00135))

## Phase II ##

## Generating Data ##

Big_ARL <- c()

for(t in 1:length(delta)){

  mr_dat1 <- matrix(ncol=C,nrow=bootz)
  rt <- c()
  rt_arl <- c()

  for(i in 1:bootz){

    mr_dat1[i,1] <- mean(runif(n,min=0,max=1*delta[t]))
    mr_dat1[i,2] <- mean(runif(n,min=0,max=1*delta[t]))
    mr_dat1[i,3] <- mean(runif(n,min=0,max=1*delta[t]))
    mr_dat1[i,4] <- mean(runif(n,min=0,max=1*delta[t]))
```

```
    mr_dat1[i,5] <- mean(runif(n,min=0,max=1*delta[t]))
    mr_dat1[i,6] <- mean(runif(n,min=0,max=1))
    mr_dat1[i,7] <- mean(runif(n,min=0,max=1))
    mr_dat1[i,8] <- mean(runif(n,min=0,max=1))
    mr_dat1[i,9] <- mean(runif(n,min=0,max=1))
    mr_dat1[i,10] <- mean(runif(n,min=0,max=1))

    rt[i] <- max(mr_dat1[i,]) - min(mr_dat1[i,])

    rt_arl[i] <- ifelse(rt[i] > UCL | rt[i] < LCL, i, 0)

  }

  Big_ARL[t] <- mean(diff(rt_arl[which(rt_arl != 0)]))

}

Big_ARL <- cbind(delta,Big_ARL)

write.csv(Big_ARL,'MR_Unif.csv',row.names=F)

rm(list = ls())

## IC Distribution == Laplace(1,1) ##

library(rmutil)

bootz <- 100000
n <- 10
C <- 10
```

```
mu0 <- 1
delta <- seq(0.25,3,by=0.25)

mr_dat <- matrix(ncol=C,nrow=bootz)

for(i in 1:bootz){
  mr_dat[i,1] <- mean(rlaplace(n,m=1,s=1))
  mr_dat[i,2] <- mean(rlaplace(n,m=1,s=1))
  mr_dat[i,3] <- mean(rlaplace(n,m=1,s=1))
  mr_dat[i,4] <- mean(rlaplace(n,m=1,s=1))
  mr_dat[i,5] <- mean(rlaplace(n,m=1,s=1))
  mr_dat[i,6] <- mean(rlaplace(n,m=1,s=1))
  mr_dat[i,7] <- mean(rlaplace(n,m=1,s=1))
  mr_dat[i,8] <- mean(rlaplace(n,m=1,s=1))
  mr_dat[i,9] <- mean(rlaplace(n,m=1,s=1))
  mr_dat[i,10] <- mean(rlaplace(n,m=1,s=1))
}

initial_rangez <- apply(mr_dat,1,FUN=function(x){max(x)-
min(x)})

UCL <- quantile(initial_rangez, probs = c(0.99865))
LCL <- quantile(initial_rangez, probs = c(0.00135))

## Phase II ##

## Generating Data ##

Big_ARL <- c()
```

```
for(t in 1:length(delta)){

  mr_dat1 <- matrix(ncol=C,nrow=bootz)
  rt <- c()
  rt_arl <- c()

  for(i in 1:bootz){

    mr_dat1[i,1] <- mean(rlaplace(n,m=1*delta[t],s=1))
    mr_dat1[i,2] <- mean(rlaplace(n,m=1*delta[t],s=1))
    mr_dat1[i,3] <- mean(rlaplace(n,m=1*delta[t],s=1))
    mr_dat1[i,4] <- mean(rlaplace(n,m=1*delta[t],s=1))
    mr_dat1[i,5] <- mean(rlaplace(n,m=1*delta[t],s=1))
    mr_dat1[i,6] <- mean(rlaplace(n,m=1,s=1))
    mr_dat1[i,7] <- mean(rlaplace(n,m=1,s=1))
    mr_dat1[i,8] <- mean(rlaplace(n,m=1,s=1))
    mr_dat1[i,9] <- mean(rlaplace(n,m=1,s=1))
    mr_dat1[i,10] <- mean(rlaplace(n,m=1,s=1))

    rt[i] <- max(mr_dat1[i,]) - min(mr_dat1[i,])

    rt_arl[i] <- ifelse(rt[i] > UCL | rt[i] < LCL, i, 0)

  }

  Big_ARL[t] <- mean(diff(rt_arl[which(rt_arl != 0)]))

}

Big_ARL <- cbind(delta,Big_ARL)
```

```
write.csv(Big_ARL,'MR_Laplace.csv',row.names=F)

rm(list = ls())

## IC Distribution == EXP(1) ##

bootz <- 100000
n <- 10
C <- 10
mu0 <- 1
delta <- seq(0.25,3,by=0.25)

mr_dat <- matrix(ncol=C,nrow=bootz)

for(i in 1:bootz){
  mr_dat[i,1] <- mean(rexp(n,rate=1))
  mr_dat[i,2] <- mean(rexp(n,rate=1))
  mr_dat[i,3] <- mean(rexp(n,rate=1))
  mr_dat[i,4] <- mean(rexp(n,rate=1))
  mr_dat[i,5] <- mean(rexp(n,rate=1))
  mr_dat[i,6] <- mean(rexp(n,rate=1))
  mr_dat[i,7] <- mean(rexp(n,rate=1))
  mr_dat[i,8] <- mean(rexp(n,rate=1))
  mr_dat[i,9] <- mean(rexp(n,rate=1))
  mr_dat[i,10] <- mean(rexp(n,rate=1))
}

initial_rangez <- apply(mr_dat,1,FUN=function(x){max(x)-
min(x)})
```

```
UCL <- quantile(initial_rangez, probs = c(0.99865))
LCL <- quantile(initial_rangez, probs = c(0.00135))

## Phase II ##

## Generating Data ##

Big_ARL <- c()

for(t in 1:length(delta)){

  mr_dat1 <- matrix(ncol=C,nrow=bootz)
  rt <- c()
  rt_arl <- c()

  for(i in 1:bootz){

    mr_dat1[i,1] <- mean(rexp(n,rate=1*delta[t]))
    mr_dat1[i,2] <- mean(rexp(n,rate=1*delta[t]))
    mr_dat1[i,3] <- mean(rexp(n,rate=1*delta[t]))
    mr_dat1[i,4] <- mean(rexp(n,rate=1*delta[t]))
    mr_dat1[i,5] <- mean(rexp(n,rate=1*delta[t]))
    mr_dat1[i,6] <- mean(rexp(n,rate=1))
    mr_dat1[i,7] <- mean(rexp(n,rate=1))
    mr_dat1[i,8] <- mean(rexp(n,rate=1))
    mr_dat1[i,9] <- mean(rexp(n,rate=1))
    mr_dat1[i,10] <- mean(rexp(n,rate=1))

    rt[i] <- max(mr_dat1[i,]) - min(mr_dat1[i,])
```

```
    rt_arl[i] <- ifelse(rt[i] > UCL | rt[i] < LCL, i, 0)

  }

  Big_ARL[t] <- mean(diff(rt_arl[which(rt_arl != 0)]))

}

Big_ARL <- cbind(delta,Big_ARL)

write.csv(Big_ARL,'MR_Exp.csv',row.names=F)
```

```
## Meneces et al Chart-for-Every-Stream ##
##            ARL Estimation           ##

## Estimating Control Limits from Preliminary Samples ##

## IC Distribution == N(1,1) ##

m <- 25
n <- 10
c4 <- 0.975
C <- 10
Ca <- 5
L <- 3.33
delta <- seq(0.25,3,by=0.25)

Big_ARL <- c()

mu0 <- 1

samplez <- matrix(nrow = n, ncol = m)

for(i in 1:m){
  samplez[,i] <- rnorm(n,mean=mu0,sd=1)
}

xdbar <- mean(apply(samplez,2,mean))
sigma_hat <- mean(apply(samplez,1,FUN=function(x){sd(x)}))

UCL <- xdbar + L*sigma_hat/(c4*sqrt(n))
LCL <- xdbar - L*sigma_hat/(c4*sqrt(n))
```

```
## Phase II ##

## Generating Data ##

for(t in 1:length(delta)){

sim_size <- 100000

s1 <- matrix(nrow = sim_size, ncol = 1)
s2 <- matrix(nrow = sim_size, ncol = 1)
s3 <- matrix(nrow = sim_size, ncol = 1)
s4 <- matrix(nrow = sim_size, ncol = 1)
s5 <- matrix(nrow = sim_size, ncol = 1)
s6 <- matrix(nrow = sim_size, ncol = 1)
s7 <- matrix(nrow = sim_size, ncol = 1)
s8 <- matrix(nrow = sim_size, ncol = 1)
s9 <- matrix(nrow = sim_size, ncol = 1)
s10 <- matrix(nrow = sim_size, ncol = 1)

arl <- c()

for(i in 1:sim_size){
  s1[i] <- mean(rnorm(n,mean=mu0*delta[t],sd=1))
  s2[i] <- mean(rnorm(n,mean=mu0*delta[t],sd=1))
  s3[i] <- mean(rnorm(n,mean=mu0*delta[t],sd=1))
  s4[i] <- mean(rnorm(n,mean=mu0*delta[t],sd=1))
  s5[i] <- mean(rnorm(n,mean=mu0*delta[t],sd=1))
  s6[i] <- mean(rnorm(n,mean=mu0,sd=1))
  s7[i] <- mean(rnorm(n,mean=mu0,sd=1))
```

```
  s8[i] <- mean(rnorm(n,mean=mu0,sd=1))
  s9[i] <- mean(rnorm(n,mean=mu0,sd=1))
  s10[i] <- mean(rnorm(n,mean=mu0,sd=1))

  arl[i] <- ifelse(s1[i] > UCL | s1[i] < LCL |
                   s2[i] > UCL | s2[i] < LCL |
                   s3[i] > UCL | s3[i] < LCL |
                   s4[i] > UCL | s4[i] < LCL |
                   s5[i] > UCL | s5[i] < LCL |
                   s6[i] > UCL | s6[i] < LCL |
                   s7[i] > UCL | s7[i] < LCL |
                   s8[i] > UCL | s8[i] < LCL |
                   s9[i] > UCL | s9[i] < LCL |
                   s10[i] > UCL | s10[i] < LCL, i, 0)
}

Big_ARL[t] <- mean(diff(arl[which(arl != 0)]))

}

Big_ARL <- cbind(delta,Big_ARL)

write.csv(Big_ARL,"Meneces_Norm.csv",row.names=F)

rm(list = ls())

## IC Distribution == UNIF(0,1) ##

m <- 25
n <- 10
```

```
c4 <- 0.975
C <- 10
Ca <- 5
L <- 3.33
delta <- seq(0.25,3,by=0.25)

Big_ARL <- c()

mu0 <- 0.5

samplez <- matrix(nrow = n, ncol = m)

for(i in 1:m){
  samplez[,i] <- runif(n,min=0,max=1)
}

xdbar <- mean(apply(samplez,2,mean))
sigma_hat <- mean(apply(samplez,1,FUN=function(x){sd(x)}))

UCL <- xdbar + L*sigma_hat/(c4*sqrt(n))
LCL <- xdbar - L*sigma_hat/(c4*sqrt(n))

## Phase II ##

## Generating Data ##

for(t in 1:length(delta)){

  sim_size <- 100000
```

```
s1 <- matrix(nrow = sim_size, ncol = 1)
s2 <- matrix(nrow = sim_size, ncol = 1)
s3 <- matrix(nrow = sim_size, ncol = 1)
s4 <- matrix(nrow = sim_size, ncol = 1)
s5 <- matrix(nrow = sim_size, ncol = 1)
s6 <- matrix(nrow = sim_size, ncol = 1)
s7 <- matrix(nrow = sim_size, ncol = 1)
s8 <- matrix(nrow = sim_size, ncol = 1)
s9 <- matrix(nrow = sim_size, ncol = 1)
s10 <- matrix(nrow = sim_size, ncol = 1)

arl <- c()

for(i in 1:sim_size){
  s1[i] <- mean(runif(n,min=0,max=1*delta[t]))
  s2[i] <- mean(runif(n,min=0,max=1*delta[t]))
  s3[i] <- mean(runif(n,min=0,max=1*delta[t]))
  s4[i] <- mean(runif(n,min=0,max=1*delta[t]))
  s5[i] <- mean(runif(n,min=0,max=1*delta[t]))
  s6[i] <- mean(runif(n,min=0,max=1))
  s7[i] <- mean(runif(n,min=0,max=1))
  s8[i] <- mean(runif(n,min=0,max=1))
  s9[i] <- mean(runif(n,min=0,max=1))
  s10[i] <- mean(runif(n,min=0,max=1))

  arl[i] <- ifelse(s1[i] > UCL | s1[i] < LCL |
                     s2[i] > UCL | s2[i] < LCL |
                     s3[i] > UCL | s3[i] < LCL |
                     s4[i] > UCL | s4[i] < LCL |
                     s5[i] > UCL | s5[i] < LCL |
```

```
                        s6[i] > UCL | s6[i] < LCL |
                        s7[i] > UCL | s7[i] < LCL |
                        s8[i] > UCL | s8[i] < LCL |
                        s9[i] > UCL | s9[i] < LCL |
                        s10[i] > UCL | s10[i] < LCL, i, 0)
  }

  Big_ARL[t] <- mean(diff(arl[which(arl != 0)]))

}

Big_ARL <- cbind(delta,Big_ARL)

write.csv(Big_ARL,"Meneces_Unif.csv",row.names=F)

rm(list = ls())

## IC Distribution == Laplace(1,1) ##

library(rmutil)

m <- 25
n <- 10
c4 <- 0.975
C <- 10
Ca <- 5
L <- 3.33
delta <- seq(0.25,3,by=0.25)

Big_ARL <- c()
```

```
mu0 <- 1

samplez <- matrix(nrow = n, ncol = m)

for(i in 1:m){
  samplez[,i] <- rlaplace(n,m=mu0,s=1)
}

xdbar <- mean(apply(samplez,2,mean))
sigma_hat <- mean(apply(samplez,1,FUN=function(x){sd(x)}))

UCL <- xdbar + L*sigma_hat/(c4*sqrt(n))
LCL <- xdbar - L*sigma_hat/(c4*sqrt(n))

## Phase II ##

## Generating Data ##

for(t in 1:length(delta)){

  sim_size <- 100000

  s1 <- matrix(nrow = sim_size, ncol = 1)
  s2 <- matrix(nrow = sim_size, ncol = 1)
  s3 <- matrix(nrow = sim_size, ncol = 1)
  s4 <- matrix(nrow = sim_size, ncol = 1)
  s5 <- matrix(nrow = sim_size, ncol = 1)
  s6 <- matrix(nrow = sim_size, ncol = 1)
  s7 <- matrix(nrow = sim_size, ncol = 1)
```

```
s8 <- matrix(nrow = sim_size, ncol = 1)
s9 <- matrix(nrow = sim_size, ncol = 1)
s10 <- matrix(nrow = sim_size, ncol = 1)

arl <- c()

for(i in 1:sim_size){
  s1[i] <- mean(rlaplace(n,m=mu0*delta[t],s=1))
  s2[i] <- mean(rlaplace(n,m=mu0*delta[t],s=1))
  s3[i] <- mean(rlaplace(n,m=mu0*delta[t],s=1))
  s4[i] <- mean(rlaplace(n,m=mu0*delta[t],s=1))
  s5[i] <- mean(rlaplace(n,m=mu0*delta[t],s=1))
  s6[i] <- mean(rlaplace(n,m=mu0,s=1))
  s7[i] <- mean(rlaplace(n,m=mu0,s=1))
  s8[i] <- mean(rlaplace(n,m=mu0,s=1))
  s9[i] <- mean(rlaplace(n,m=mu0,s=1))
  s10[i] <- mean(rlaplace(n,m=mu0,s=1))

  arl[i] <- ifelse(s1[i] > UCL | s1[i] < LCL |
                     s2[i] > UCL | s2[i] < LCL |
                     s3[i] > UCL | s3[i] < LCL |
                     s4[i] > UCL | s4[i] < LCL |
                     s5[i] > UCL | s5[i] < LCL |
                     s6[i] > UCL | s6[i] < LCL |
                     s7[i] > UCL | s7[i] < LCL |
                     s8[i] > UCL | s8[i] < LCL |
                     s9[i] > UCL | s9[i] < LCL |
                     s10[i] > UCL | s10[i] < LCL, i, 0)
}
```

```
  Big_ARL[t] <- mean(diff(arl[which(arl != 0)]))

}

Big_ARL <- cbind(delta,Big_ARL)

write.csv(Big_ARL,"Meneces_Laplace.csv",row.names=F)

rm(list = ls())

## IC Distribution == EXP(1) ##

m <- 25
n <- 10
c4 <- 0.975
C <- 10
Ca <- 5
L <- 3.33
delta <- seq(0.25,3,by=0.25)

Big_ARL <- c()

mu0 <- 1

samplez <- matrix(nrow = n, ncol = m)


for(i in 1:m){
  samplez[,i] <- rexp(n,rate=mu0)
}
```

```
xdbar <- mean(apply(samplez,2,mean))
sigma_hat <- mean(apply(samplez,1,FUN=function(x){sd(x)}))

UCL <- xdbar + L*sigma_hat/(c4*sqrt(n))
LCL <- xdbar - L*sigma_hat/(c4*sqrt(n))

## Phase II ##

## Generating Data ##

for(t in 1:length(delta)){

  sim_size <- 100000

  s1 <- matrix(nrow = sim_size, ncol = 1)
  s2 <- matrix(nrow = sim_size, ncol = 1)
  s3 <- matrix(nrow = sim_size, ncol = 1)
  s4 <- matrix(nrow = sim_size, ncol = 1)
  s5 <- matrix(nrow = sim_size, ncol = 1)
  s6 <- matrix(nrow = sim_size, ncol = 1)
  s7 <- matrix(nrow = sim_size, ncol = 1)
  s8 <- matrix(nrow = sim_size, ncol = 1)
  s9 <- matrix(nrow = sim_size, ncol = 1)
  s10 <- matrix(nrow = sim_size, ncol = 1)

  arl <- c()
  for(i in 1:sim_size){
    s1[i] <- mean(rexp(n,rate=mu0*delta[t]))
    s2[i] <- mean(rexp(n,rate=mu0*delta[t]))
```

```
    s3[i] <- mean(rexp(n,rate=mu0*delta[t]))
    s4[i] <- mean(rexp(n,rate=mu0*delta[t]))
    s5[i] <- mean(rexp(n,rate=mu0*delta[t]))
    s6[i] <- mean(rexp(n,rate=mu0))
    s7[i] <- mean(rexp(n,rate=mu0))
    s8[i] <- mean(rexp(n,rate=mu0))
    s9[i] <- mean(rexp(n,rate=mu0))
    s10[i] <- mean(rexp(n,rate=mu0))

    arl[i] <- ifelse(s1[i] > UCL | s1[i] < LCL |
                       s2[i] > UCL | s2[i] < LCL |
                       s3[i] > UCL | s3[i] < LCL |
                       s4[i] > UCL | s4[i] < LCL |
                       s5[i] > UCL | s5[i] < LCL |
                       s6[i] > UCL | s6[i] < LCL |
                       s7[i] > UCL | s7[i] < LCL |
                       s8[i] > UCL | s8[i] < LCL |
                       s9[i] > UCL | s9[i] < LCL |
                       s10[i] > UCL | s10[i] < LCL, i, 0)
  }

  Big_ARL[t] <- mean(diff(arl[which(arl != 0)]))

}

Big_ARL <- cbind(delta,Big_ARL)
write.csv(Big_ARL,"Meneces_Exp.csv",row.names=F)
```